CHAPTER 32

DUCT DESIGN

COMMERCIAL, industrial, and residential air duct system design must consider (1) space availability, (2) space air diffusion, (3) noise levels, (4) duct leakage, (5) duct heat gains and losses, (6) balancing, (7) fire and smoke control, (8) initial investment cost, and (9) system operating cost.

Deficiencies in duct design can result in systems that operate incorrectly or are expensive to own and operate. Poor air distribution can cause discomfort; lack of sound attenuators may permit objectionable noise levels. Poorly designed ductwork can result in unbalanced systems. Faulty duct construction or lack of duct sealing produces inadequate airflow rates at the terminals. Proper duct insulation eliminates the problem caused by excessive heat gain or loss.

In this chapter, system design and the calculation of a system's frictional and dynamic resistance to airflow are considered. Chapter 16 of the 1996 *ASHRAE Handbook—Systems and Equipment* examines duct construction and presents construction standards for residential, commercial, and industrial heating, ventilating, air-conditioning, and exhaust systems.

BERNOULLI EQUATION

The Bernoulli equation can be developed by equating the forces on an element of a stream tube in a frictionless fluid flow to the rate of momentum change. On integrating this relationship for steady flow, the following expression (Osborne 1966) results:

$$\frac{v^2}{2g_c} + \int\frac{dP}{\rho} + \frac{gz}{g_c} = \text{constant, ft}\cdot\text{lb}_f/\text{lb}_m \tag{1}$$

where

v = streamline (local) velocity, fps
g_c = dimensional constant, 32.2 $\text{lb}_m\cdot\text{ft/lb}_f\cdot\text{s}^2$
P = absolute pressure, lb_f/ft^2
ρ = density, lb_m/ft^3
g = acceleration due to gravity, ft/s^2
z = elevation, ft

Assuming constant fluid density within the system, Equation (1) reduces to

$$\frac{v^2}{2g_c} + \frac{P}{\rho} + \frac{gz}{g_c} = \text{constant, ft}\cdot\text{lb}_f/\text{lb}_m \tag{2}$$

Although Equation (2) was derived for steady, ideal frictionless flow along a stream tube, it can be extended to analyze flow through ducts in real systems. In terms of pressure, the relationship for fluid resistance between two sections is

$$\frac{\rho_1 V_1^2}{2g_c} + P_1 + \frac{g}{g_c}\rho_1 z_1 = \frac{\rho_2 V_2^2}{2g_c} + P_2 + \frac{g}{g_c}\rho_2 z_2 + \Delta p_{t,1\text{-}2} \tag{3}$$

where

V = average duct velocity, fps
$\Delta p_{t,1\text{-}2}$ = total pressure loss due to friction and dynamic losses between sections 1 and 2, lb_f/ft^2

In Equation (3), V (section average velocity) replaces v (streamline velocity) because experimentally determined loss coefficients allow for errors in calculating $\rho v^2/2g_c$ (velocity pressure) across streamlines.

On the left side of Equation (3), add and subtract p_{z1}; on the right side, add and subtract p_{z2}, where p_{z1} and p_{z2} are the values of atmospheric air at heights z_1 and z_2. Thus,

$$\frac{\rho_1 V_1^2}{2g_c} + P_1 + (p_{z1} - p_{z1}) + \frac{g}{g_c}\rho_1 z_1$$
$$= \frac{\rho_2 V_2^2}{2g_c} + P_2 + (p_{z2} - p_{z2}) + \frac{g}{g_c}\rho_2 z_2 + \Delta p_{t,1\text{-}2} \tag{4}$$

The atmospheric pressure at any elevation (p_{z1} and p_{z2}) expressed in terms of the atmospheric pressure p_a at the same datum elevation is given by

$$p_{z1} = p_a - \frac{g}{g_c}\rho_a z_1 \tag{5}$$

$$p_{z2} = p_a - \frac{g}{g_c}\rho_a z_2 \tag{6}$$

Substituting Equations (5) and (6) into Equation (4) and simplifying yields the total pressure change between sections 1 and 2. Assume no change in temperature between sections 1 and 2 (no heat exchanger within the section); therefore, $\rho_1 = \rho_2$. When a heat exchanger is located within the section, the average of the inlet and outlet temperatures is generally used. Let $\rho = \rho_1 = \rho_2$. $(P_1 - p_{z1})$ and $(P_2 - p_{z2})$ are gage pressures at elevations z_1 and z_2.

$$\Delta p_{t,1\text{-}2} = \left(p_{s,1} + \frac{\rho V_1^2}{2g_c}\right) - \left(p_{s,2} + \frac{\rho V_2^2}{2g_c}\right) + \frac{g}{g_c}(\rho_a - \rho)(z_2 - z_1) \tag{7a}$$

$$\Delta p_{t,1\text{-}2} = \Delta p_t + \Delta p_{se} \tag{7b}$$

The preparation of this chapter is assigned to TC 5.2, Duct Design.

$$\Delta p_t = \Delta p_{t,1\text{-}2} - \Delta p_{se} \tag{7c}$$

where

$p_{s,1}$ = static pressure, gage at elevation z_1, lb_f/ft^2
$p_{s,2}$ = static pressure, gage at elevation z_2, lb_f/ft^2
V_1 = average velocity at section 1, fps
V_2 = average velocity at section 2, fps
ρ_a = density of ambient air, lb_m/ft^3
ρ = density of air or gas within duct, lb_m/ft^3
Δp_{se} = thermal gravity effect, lb_f/ft^2
Δp_t = total pressure change between sections 1 and 2, lb_f/ft^2
$\Delta p_{t,1-2}$ = total pressure loss due to friction and dynamic losses between sections 1 and 2, lb_f/ft^2

HEAD AND PRESSURE

The terms **head** and **pressure** are often used interchangeably; however, head is the height of a fluid column supported by fluid flow, while pressure is the normal force per unit area. For liquids, it is convenient to measure the head in terms of the flowing fluid. With a gas or air, however, it is customary to measure pressure on a column of liquid.

Static Pressure

The term $pg_c/\rho g$ is static head; p is static pressure.

Velocity Pressure

The term $V^2/2g$ refers to velocity head, and the term $\rho V^2/2g_c$ refers to velocity pressure. Although velocity head is independent of fluid density, velocity pressure, calculated by Equation (8), is not.

$$p_v = \rho\left(\frac{V}{1097}\right)^2 \tag{8}$$

where

p_v = velocity pressure, in. of water
V = fluid mean velocity, fpm

For air at standard conditions (0.075 lb_m/ft^3), Equation (8) becomes

$$p_v = \left(\frac{V}{4005}\right)^2 \tag{9}$$

Velocity is calculated by Equation (10) or (11).

$$V = 144Q/A \tag{10}$$

where

Q = airflow rate, cfm
A = cross-sectional area of duct, in^2

$$V = Q/A \tag{11}$$

where A = cross-sectional area of duct, ft^2.

Total Pressure

Total pressure is the sum of static pressure and velocity pressure:

$$p_t = p_s + \rho\left(\frac{V}{1097}\right)^2 \tag{12}$$

or

$$p_t = p_s + p_v \tag{13}$$

where

p_t = total pressure, in. of water
p_s = static pressure, in. of water

Pressure Measurement

The range, precision, and limitations of instruments for measuring pressure and velocity are discussed in Chapter 14. The manometer is a simple and useful means for measuring partial vacuum and low pressure. Static, velocity, and total pressures in a duct system relative to atmospheric pressure are measured with a pitot tube connected to a manometer. Pitot tube construction and locations for traversing round and rectangular ducts are presented in Chapter 14.

SYSTEM ANALYSIS

The total pressure change due to friction, fittings, equipment, and net **thermal gravity effect (stack effect)** for each section of a duct system is calculated by the following equation:

$$\Delta p_{t_i} = \Delta p_{f_i} + \sum_{j=1}^{m} \Delta p_{ij} + \sum_{k=1}^{n} \Delta p_{ik} - \sum_{r=1}^{\lambda} \Delta p_{se_{ir}} \tag{14}$$

$$\text{for } i = 1, 2, \ldots, n_{up} + n_{dn}$$

where

Δp_{t_i} = net total pressure change for i-section, in. of water
Δp_{f_i} = pressure loss due to friction for i-section, in. of water
Δp_{ij} = total pressure loss due to j-fittings, including fan system effect (FSE), for i-section, in. of water
Δp_{ik} = pressure loss due to k-equipment for i-section, in. of water
$\Delta p_{se_{ir}}$ = thermal gravity effect due to r-stacks for i-section, in. of water
m = number of fittings within i-section
n = number of equipment within i-section
λ = number of stacks within i-section
n_{up} = number of duct sections upstream of fan (exhaust/return air subsystems)
n_{dn} = number of duct sections downstream of fan (supply air subsystems)

From Equation (7), the thermal gravity effect for each nonhorizontal duct with a density other than that of ambient air is determined by the following equation:

$$\Delta p_{se} = 0.192(\rho_a - \rho)(z_2 - z_1) \tag{15}$$

where

Δp_{se} = thermal gravity effect, in. of water
z_1 and z_2 = elevation from datum in direction of airflow (Figure 1), ft
ρ_a = density of ambient air, lb_m/ft^3
ρ = density of air or gas within duct, lb_m/ft^3

Example 1. For Figure 1, calculate the thermal gravity effect for two cases: (a) air cooled to −30°F, and (b) air heated to 1000°F. The density of air at −30°F and 1000°F is 0.0924 lb_m/ft^3 and 0.0271 lb_m/ft^3, respectively. The density of the ambient air is 0.075 lb_m/ft^3. Stack height is 40 ft.

Solution:

$$\Delta p_{se} = 0.192(\rho_a - \rho)z$$

(a) For $\rho > \rho_a$ (Figure 1A),

$$\Delta p_{se} = 0.192(0.075 - 0.0924)40$$
$$= -0.13 \text{ in. of water}$$

(b) For $\rho < \rho_a$ (Figure 1B),

$$\Delta p_{se} = 0.192(0.075 - 0.0271)40$$
$$= +0.37 \text{ in. of water}$$

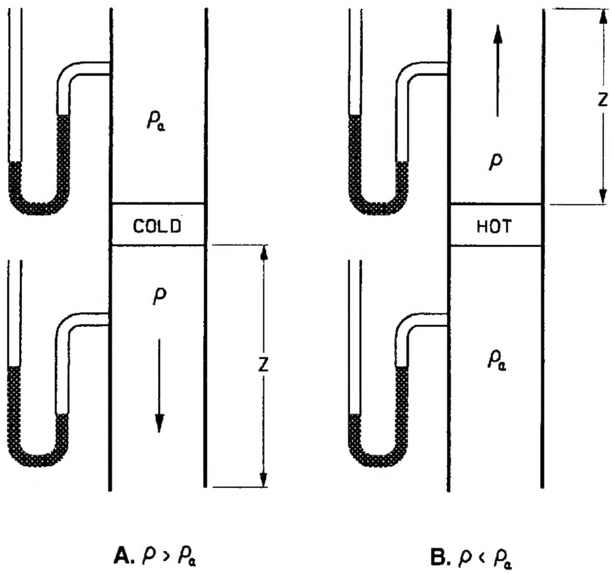

Fig. 1 Thermal Gravity Effect for Example 1

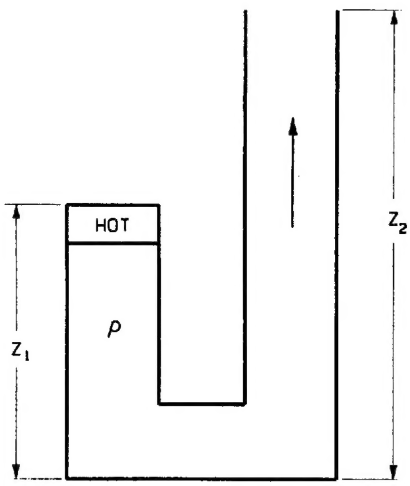

Fig. 2 Multiple Stacks for Example 2

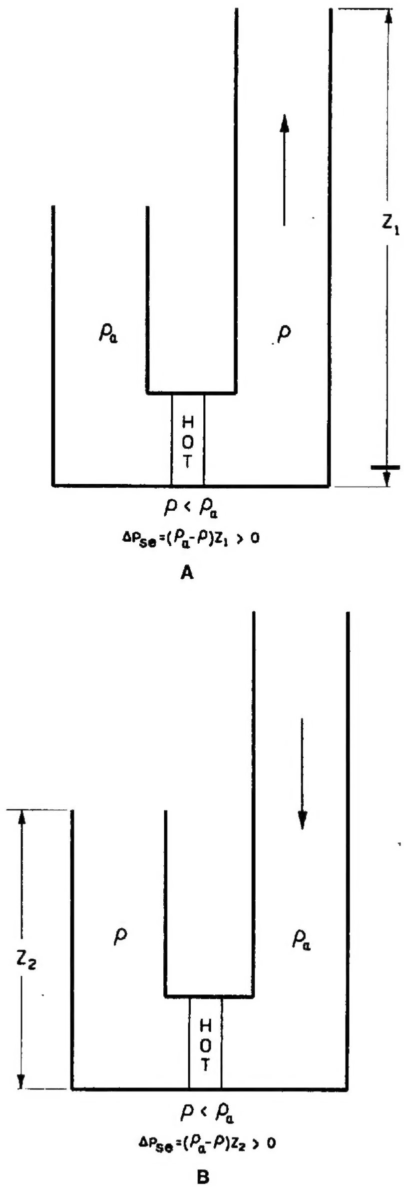

Fig. 3 Multiple Stack Analysis

Example 2. Calculate the thermal gravity effect for the two-stack system shown in Figure 2, where the air is 250°F and the stack heights are 50 and 100 ft. The density of 250°F air is 0.0558 lb_m/ft^3; ambient air is 0.075 lb_m/ft^3.

Solution:

$$\begin{aligned} \Delta p_{se} &= 0.192(0.075 - 0.0558)(100 - 50) \\ &= 0.18 \text{ in. of water} \end{aligned}$$

For the system shown in Figure 3, the direction of air movement created by the thermal gravity effect depends on the initiating force. The initiating force could be fans, wind, opening and closing doors, and turning equipment on and off. If for any reason air starts to enter the left stack (Figure 3A), it creates a buoyancy effect in the right stack. On the other hand, if flow starts to enter the right stack (Figure 3B), it creates a buoyancy effect in the left stack. In both cases the produced thermal gravity effect is stable and depends on the stack height and magnitude of heating. The starting direction of flow is important when using natural convection for ventilation.

To determine the fan total pressure requirement for a system, use the following equation:

$$P_t = \sum_{i \varepsilon F_{up}} \Delta p_{t_i} + \sum_{i \varepsilon F_{dn}} \Delta p_{t_i} \qquad \text{for } i = 1, 2, \ldots, n_{up} + n_{dn} \qquad (16)$$

where

F_{up} and F_{dn} = sets of duct sections upstream and downstream of a fan
P_t = fan total pressure, in. of water
ε = symbol that ties duct sections into system paths from the exhaust/return air terminals to the supply terminals

Figure 4 illustrates the use of Equation (16). This system has three supply and two return terminals consisting of nine sections connected in six paths: 1-3-4-9-7-5, 1-3-4-9-7-6, 1-3-4-9-8, 2-4-9-7-5, 2-4-9-7-6, and 2-4-9-8. Sections 1 and 3 are unequal area; thus, they are assigned separate numbers in accordance with the rules for

identifying sections (see Step 4 in the section on HVAC Duct Design Procedures). To determine the fan pressure requirement, the following six equations, derived from Equation (16), are applied. These equations must be satisfied to attain pressure balancing for design airflow. Relying entirely on dampers is not economical and may create objectionable flow-generated noise.

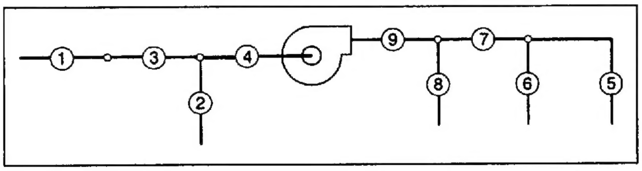

Fig. 4 Illustrative 6-Path, 9-Section System

$$\left\{\begin{array}{l} P_t = \Delta p_1 + \Delta p_3 + \Delta p_4 + \Delta p_9 + \Delta p_7 + \Delta p_5 \\ P_t = \Delta p_1 + \Delta p_3 + \Delta p_4 + \Delta p_9 + \Delta p_7 + \Delta p_6 \\ P_t = \Delta p_1 + \Delta p_3 + \Delta p_4 + \Delta p_9 + \Delta p_8 \\ P_t = \Delta p_2 + \Delta p_4 + \Delta p_9 + \Delta p_7 + \Delta p_5 \\ P_t = \Delta p_2 + \Delta p_4 + \Delta p_9 + \Delta p_7 + \Delta p_6 \\ P_t = \Delta p_2 + \Delta p_4 + \Delta p_9 + \Delta p_8 \end{array}\right. \tag{17}$$

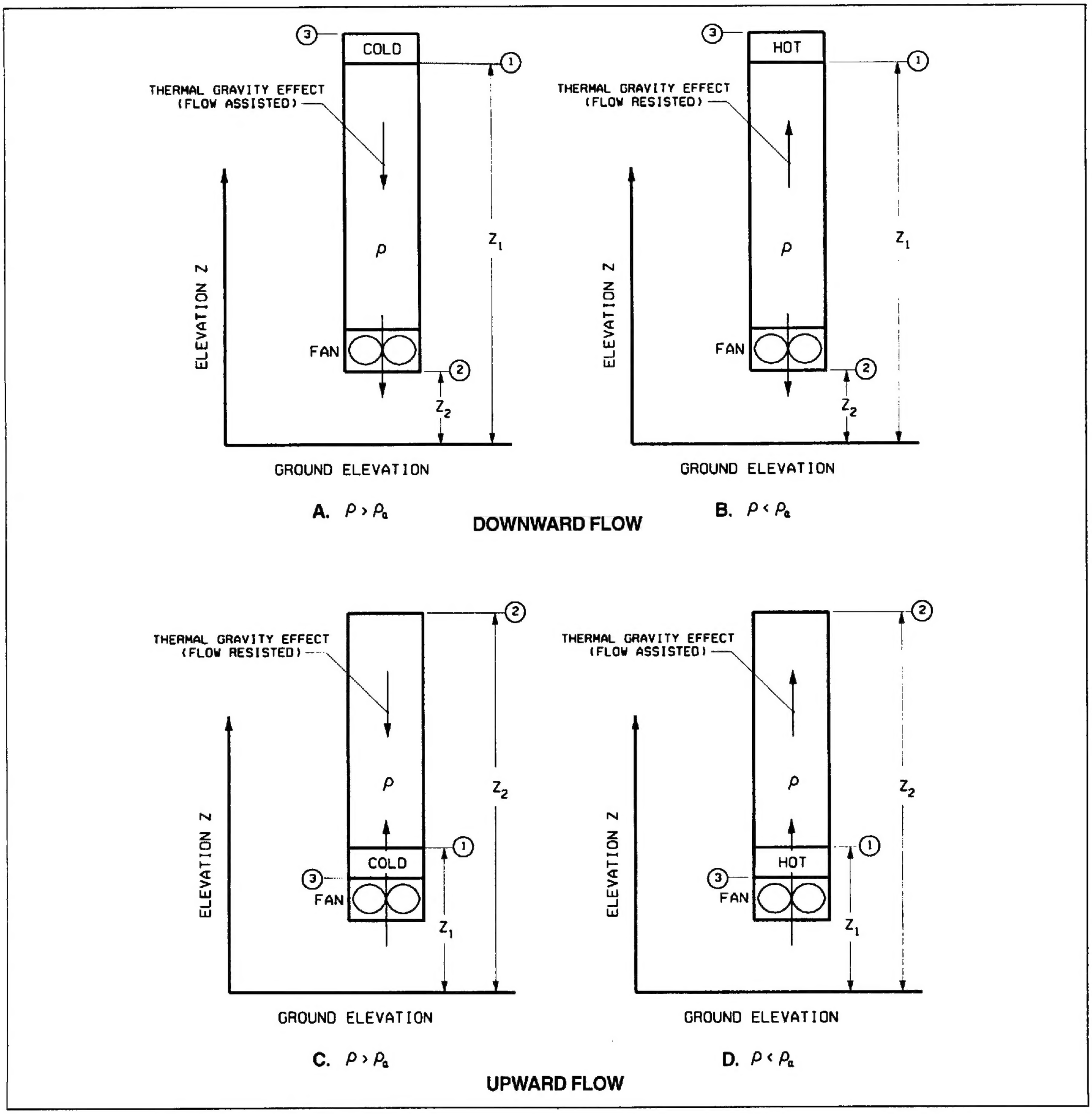

Fig. 5 Single Stack with Fan for Examples 3 and 4

Example 3. For Figures 5A and 5C, calculate the thermal gravity effect and fan total pressure required when the air is cooled to −30°F. The heat exchanger and ductwork (section 1 to 2) total pressure losses are 0.70 and 0.28 in. of water respectively. The density of −30°F air is 0.0924 lb_m/ft^3; ambient air is 0.075 lb_m/ft^3. Elevations are 70 ft and 10 ft as noted in the solutions below.

Solution:

(a) For Figure 5A (downward flow),

$$\begin{aligned}\Delta p_{se} &= 0.192(\rho_a - \rho)(z_2 - z_1)\\ &= 0.192(0.075 - 0.0924)(10 - 70)\\ &= 0.20 \text{ in. of water}\end{aligned}$$

$$\begin{aligned}P_t &= \Delta p_{t,3\text{-}2} - \Delta p_{se}\\ &= (0.70 + 0.28) - (0.20)\\ &= 0.78 \text{ in. of water}\end{aligned}$$

(b) For Figure 5C (upward flow),

$$\begin{aligned}\Delta p_{se} &= 0.192(\rho_a - \rho)(z_2 - z_1)\\ &= 0.192(0.075 - 0.0924)(70 - 10)\\ &= -0.20 \text{ in. of water}\end{aligned}$$

$$\begin{aligned}P_t &= \Delta p_{t,3\text{-}2} - \Delta p_{se}\\ &= (0.70 + 0.28) - (-0.20)\\ &= 1.18 \text{ in. of water}\end{aligned}$$

Example 4. For Figures 5B and 5D, calculate the thermal gravity effect and fan total pressure required when the air is heated to 250°F. The heat exchanger and ductwork (section 1 to 2) total pressure losses are 0.70 and 0.28 in. of water respectively. The density of 250°F air is 0.0558 lb_m/ft^3; ambient air is 0.075 lb_m/ft^3. Elevations are 70 ft and 10 ft as noted in the solutions below.

Solution:

(a) For Figure 5B (downward flow),

$$\begin{aligned}\Delta p_{se} &= 0.192(\rho_a - \rho)(z_2 - z_1)\\ &= 0.192(0.075 - 0.0558)(10 - 70)\\ &= -0.22 \text{ in. of water}\end{aligned}$$

$$\begin{aligned}P_t &= \Delta p_{t,3\text{-}2} - \Delta p_{se}\\ &= (0.70 + 0.28) - (-0.22)\\ &= 1.20 \text{ in. of water}\end{aligned}$$

(b) For Figure 5D (upward flow),

$$\begin{aligned}\Delta p_{se} &= 0.192(\rho_a - \rho)(z_2 - z_1)\\ &= 0.192(0.075 - 0.0558)(70 - 10)\\ &= 0.22 \text{ in. of water}\end{aligned}$$

$$\begin{aligned}P_t &= \Delta p_{t,3\text{-}2} - \Delta p_{se}\\ &= (0.70 + 0.28) - (0.22)\\ &= 0.76 \text{ in. of water}\end{aligned}$$

Example 5. Calculate the thermal gravity effect for each section of the system shown in Figure 6 and the net thermal gravity effect of the system. The density of ambient air is 0.075 lb_m/ft^3, and the lengths are as follows: z_1 = 50 ft, z_2 = 90 ft, z_4 = 95 ft, z_5 = 25 ft, and z_9 = 200 ft. The pressure required at section 3 is −0.1 in. of water. Write the equation to determine the fan total pressure requirement.

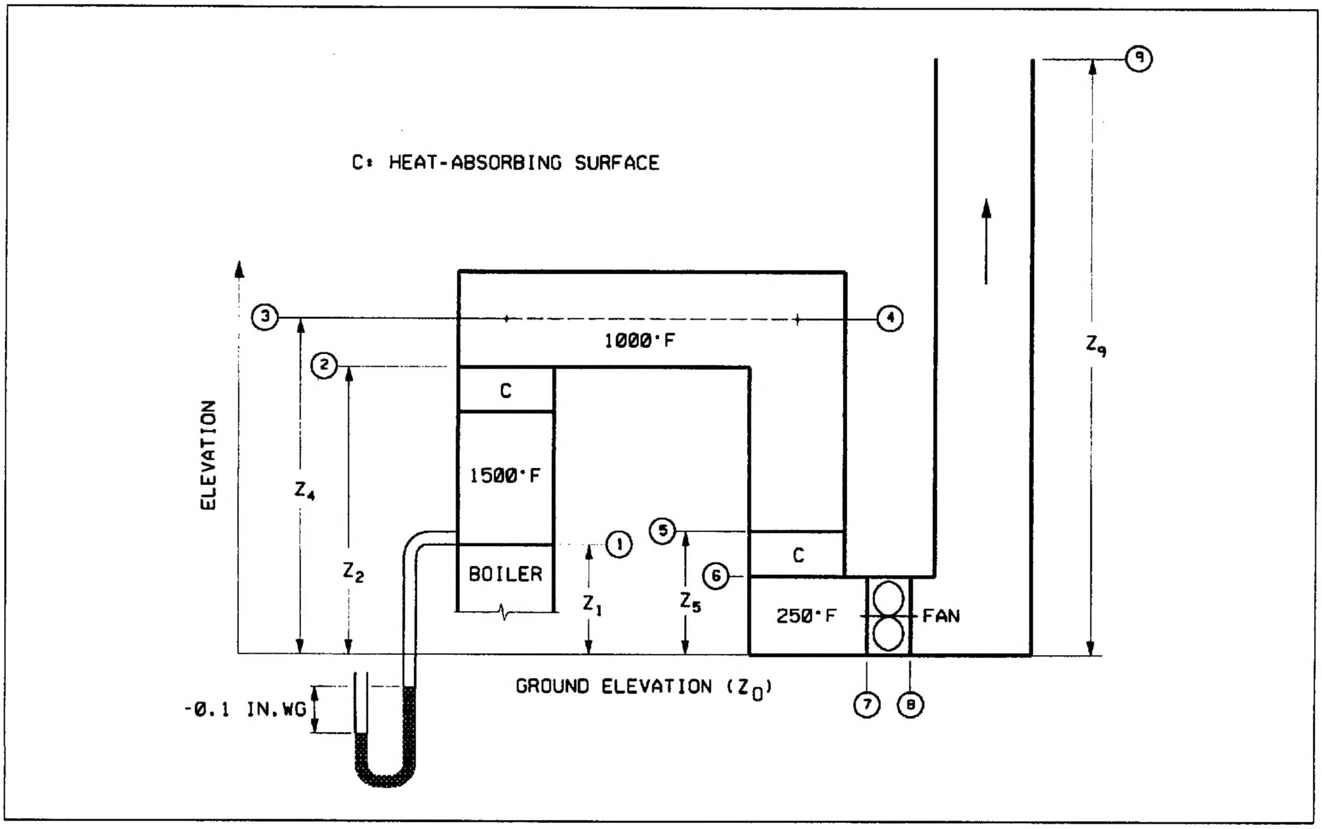

Fig. 6 Triple Stack System for Example 5

Solution: The following table summarizes the thermal gravity effect for each section of the system as calculated by Equation (15). The net thermal gravity effect for the system is 0.52 in. of water. To select a fan, use the following equation:

$$P_t = 0.1 + \Delta p_{t,1\text{-}7} + \Delta p_{t,8\text{-}9} - \Delta p_{se}$$
$$= 0.1 + \Delta p_{t,1\text{-}7} + \Delta p_{t,8\text{-}9} - 0.52$$
$$= \Delta p_{t,1\text{-}7} + \Delta p_{t,8\text{-}9} - 0.42$$

Path $(x\text{-}x')$	Temp., °F	ρ, lb_m/ft^3	Δz $(z_{x'} - z_x)$, ft	$\Delta\rho$ $(\rho_a - \rho_{x\text{-}x'})$, lb_m/ft^3	Δp_{se}, in. of water [Eq. (15)]
1-2	1500	0.0202	(90 – 50)	+0.0548	+0.42
3-4	1000	0.0271	0	+0.0479	0
4-5	1000	0.0271	(25 – 95)	+0.0479	–0.64
6-7	250	0.0558	0	+0.0192	0
8-9	250	0.0558	(200 – 0)	+0.0192	+0.74
Net Thermal Gravity Effect					0.52

PRESSURE CHANGES IN SYSTEM

Figure 7 shows total and static pressure changes in a fan/duct system consisting of a fan with both supply and return air ductwork. Also shown are the total and static pressure gradients referenced to atmospheric pressure.

For all constant-area sections, the total and static pressure losses are equal. At the diverging transitions, velocity pressure decreases, absolute total pressure decreases, and absolute static pressure can increase. The static pressure increase at these sections is known as **static regain**.

At the converging transitions, velocity pressure increases in the direction of airflow, and the absolute total and absolute static pressures decrease.

At the exit, the total pressure loss depends on the shape of the fitting and the flow characteristics. Exit loss coefficients C_o can be greater than, less than, or equal to one. The total and static pressure grade lines for the various coefficients are shown in Figure 3. Note that for a loss coefficient less than one, static pressure upstream of the exit is less than atmospheric pressure (negative). The static pressure just upstream of the discharge fitting can be calculated by subtracting the upstream velocity pressure from the upstream total pressure.

At section 1, the total pressure loss depends on the shape of the entry. The total pressure immediately downstream of the entrance equals the difference between the upstream pressure, which is zero (atmospheric pressure), and the loss through the fitting. The static pressure of the ambient air is zero; several diameters downstream, static pressure is negative, equal to the sum of the total pressure (negative) and the velocity pressure (always positive).

System resistance to airflow is noted by the total pressure grade line in Figure 7. Sections 3 and 4 include fan system effect pressure losses. To obtain the fan static pressure requirement for fan selection where the fan total pressure is known, use

$$P_s = P_t - p_{v,o} \tag{18}$$

where

P_s = fan static pressure, in. of water
P_t = fan total pressure, in. of water
$p_{v,o}$ = fan outlet velocity pressure, in. of water

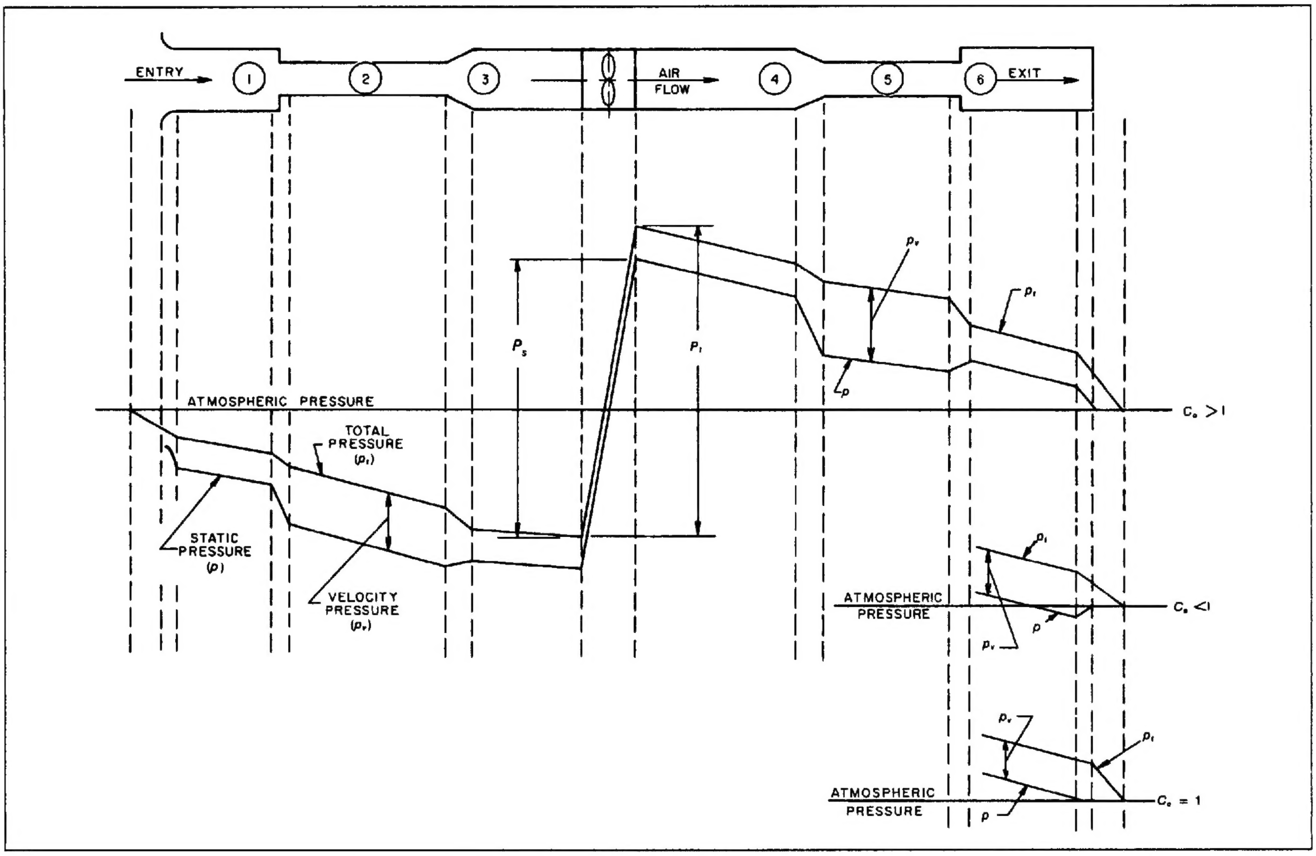

Fig. 7 Pressure Changes During Flow in Ducts

FLUID RESISTANCE

Duct system losses are the irreversible transformation of mechanical energy into heat. The two types of losses are (1) friction losses and (2) dynamic losses.

FRICTION LOSSES

Friction losses are due to fluid viscosity and are a result of momentum exchange between molecules in laminar flow and between individual particles of adjacent fluid layers moving at different velocities in turbulent flow. Friction losses occur along the entire duct length.

Darcy, Colebrook, and Altshul-Tsal Equations

For fluid flow in conduits, friction loss can be calculated by the Darcy equation:

$$\Delta p_f = \frac{12fL}{D_h}\rho\left(\frac{V}{1097}\right)^2 \quad (19)$$

where

Δp_f = friction losses in terms of total pressure, in. of water
f = friction factor, dimensionless
L = duct length, ft
D_h = hydraulic diameter [Equation (24)], in.
V = velocity, fpm
ρ = density, lb_m/ft^3

Within the region of laminar flow (Reynolds numbers less than 2000), the friction factor is a function of Reynolds number only.

For completely turbulent flow, the friction factor depends on Reynolds number, duct surface roughness, and internal protuberances such as joints. Between the bounding limits of hydraulically smooth behavior and fully rough behavior, is a transitional roughness zone where the friction factor depends on both roughness and Reynolds number. In this transitionally rough, turbulent zone the friction factor f is calculated by Colebrook's equation (Colebrook 1938-39). Colebrook's transition curve merges asymptotically into the curves representing laminar and completely turbulent flow. Because Colebrook's equation cannot be solved explicitly for f, use iterative techniques (Behls 1971).

$$\frac{1}{\sqrt{f}} = -2\log\left(\frac{12\varepsilon}{3.7D_h} + \frac{2.51}{\mathrm{Re}\sqrt{f}}\right) \quad (20)$$

where

ε = material absolute roughness factor, ft
Re = Reynolds number

A simplified formula for calculating friction factor, developed by Altshul (Altshul et al. 1975) and modified by Tsal, is

$$f' = 0.11\left(\frac{12\varepsilon}{D_h} + \frac{68}{\mathrm{Re}}\right)^{0.25} \quad (21)$$

If $f' \geq 0.018$: $f = f'$
If $f' < 0.018$: $f = 0.85f' + 0.0028$

Friction factors obtained from the Altshul-Tsal equation are within 1.6% of those obtained by Colebrook's equation.

Reynolds number (Re) may be calculated by using the following equation.

$$\mathrm{Re} = \frac{D_h V}{720\nu} \quad (22)$$

where ν = kinematic viscosity, ft^2/s.

For standard air, Re can be calculated by

$$\mathrm{Re} = 8.56 D_h V \quad (23)$$

Roughness Factors

The roughness factors ε listed in Table 1 are recommended for use with the Colebrook or Altshul-Tsal equation [Equations (20) and (21), respectively]. These values include not only material, but also duct construction, joint type, and joint spacing (Griggs and Khodabakhsh-Sharifabad 1992). Roughness factors for other materials are presented in Idelchik et al. (1986). Idelchik summarizes roughness factors for 80 materials including metal tubes; conduits made from concrete and cement; and wood, plywood, and glass tubes.

Swim (1978) conducted tests on duct liners of varying densities, surface treatments, transverse joints (workmanship), and methods of attachment to sheet metal ducts. As a result of these tests, Swim recommends for design 0.015 ft for spray-coated liners and 0.005 ft for liners with a facing material cemented onto the air side. In both cases, the roughness factor includes the resistance offered by mechanical fasteners and assumes good joints. Liners cut too short result in (1) loss of thermal performance, (2) possible condensation problems, (3) potential damage to the liner (erosion of the blanket or tearing away from the duct surface), and (4) the collection of dirt and debris and the initiation of biological problems. Liner density does not significantly influence flow resistance.

Manufacturers' data indicate that the absolute roughness for fully extended nonmetallic flexible ducts ranges from 0.0035 to 0.015 ft. For fully extended flexible metallic ducts, absolute roughness ranges from 0.0004 to 0.007 ft. This range covers flexible duct with the supporting wire exposed to flow or covered by the material. Figure 8 provides a pressure drop correction factor for straight flexible duct when less than fully extended.

Table 1 Duct Roughness Factors

Duct Material	Roughness Category	Absolute Roughness ε, ft
Uncoated carbon steel, clean (Moody 1944) (0.00015 ft)	Smooth	0.0001
PVC plastic pipe (Swim 1982) (0.00003 to 0.00015 ft)		
Aluminum (Hutchinson 1953) (0.000015 to 0.0002 ft)		
Galvanized steel, longitudinal seams, 4 ft joints (Griggs et al. 1987) (0.00016 to 0.00032 ft)	Medium smooth	0.0003
Galvanized steel, continuously rolled, spiral seams, 10 ft joints (Jones 1979) (0.0002 to 0.0004 ft)		
Galvanized steel, spiral seam with 1, 2, and 3 ribs, 12 ft joints (Griggs et al. 1987) (0.00029 to 0.00038 ft)		
Galvanized steel, longitudinal seams, 2.5 ft joints (Wright 1945) (0.0005 ft)	Average	0.0005
Fibrous glass duct, rigid	Medium rough	0.003
Fibrous glass duct liner, air side with facing material (Swim 1978) (0.005 ft)		
Fibrous glass duct liner, air side spray coated (Swim 1978) (0.015 ft)	Rough	0.01
Flexible duct, metallic (0.004 to 0.007 ft when fully extended)		
Flexible duct, all types of fabric and wire (0.0035 to 0.015 ft when fully extended)		
Concrete (Moody 1944) (0.001 to 0.01 ft)		

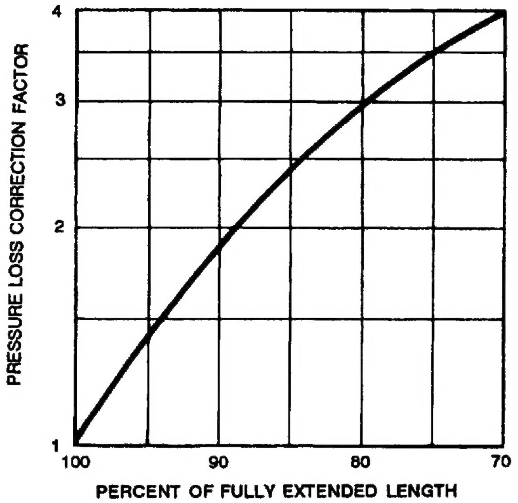

Fig. 8 Correction Factor for Unextended Flexible Duct

Friction Chart

Fluid resistance caused by friction in round ducts can be determined by the friction chart (Figure 9). This chart is based on standard air flowing through round galvanized ducts with beaded slip couplings on 48 in. centers, equivalent to an absolute roughness of 0.0003 ft.

Changes in barometric pressure, temperature, and humidity affect air density, air viscosity, and Reynolds number. No corrections to Figure 9 are needed for (1) duct materials with a medium smooth roughness factor, (2) temperature variations in the order of ±30°F from 70°F, (3) elevations to 1500 ft, and (4) duct pressures from −20 in. of water to +20 in. of water relative to the ambient pressure. These individual variations in temperature, elevation, and duct pressure result in duct losses within ±5% of the standard air friction chart.

For duct materials other than those categorized as medium smooth in Table 1, and for variations in temperature, barometric pressure (elevation), and duct pressures (outside the range listed), calculate the friction loss in a duct by the Altshul-Tsal and Darcy equations [Equations (21) and (19), respectively].

Noncircular Ducts

A momentum analysis can relate average wall shear stress to pressure drop per unit length for fully developed turbulent flow in a passage of arbitrary shape but uniform longitudinal cross-sectional area. This analysis leads to the definition of **hydraulic diameter**:

$$D_h = 4A/P \tag{24}$$

where

D_h = hydraulic diameter, in.
A = duct area, in^2
P = perimeter of cross section, in.

While the hydraulic diameter is often used to correlate noncircular data, exact solutions for laminar flow in noncircular passages show that such practice causes some inconsistencies. No exact solutions exist for turbulent flow. Tests over a limited range of turbulent flow indicated that fluid resistance is the same for equal lengths of duct for equal mean velocities of flow if the ducts have the same ratio of cross-sectional area to perimeter. From a series of experiments using round, square, and rectangular ducts having essentially the same hydraulic diameter, Huebscher (1948) found that each, for most purposes, had the same flow resistance at equal mean velocities. Tests by Griggs and Khodabakhsh-Sharifabad (1992) also indicated that experimental rectangular duct data for airflow over the range typical of HVAC systems can be correlated satisfactorily using Equation (20) together with hydraulic diameter, particularly when a realistic experimental uncertainty is accepted. These tests support using hydraulic diameter to correlate noncircular duct data.

Rectangular Ducts. Huebscher (1948) developed the relationship between rectangular and round ducts that is used to determine size equivalency based on equal flow, resistance, and length. This relationship, Equation (25), is the basis for Table 2.

$$D_e = \frac{1.30(ab)^{0.625}}{(a+b)^{0.250}} \tag{25}$$

where

D_e = circular equivalent of rectangular duct for equal length, fluid resistance, and airflow, in.
a = length of one side of duct, in.
b = length of adjacent side of duct, in.

To determine equivalent round duct diameter, use Table 2. Equations (21) or (20) and (19) must be used to determine pressure loss.

Flat Oval Ducts. To convert round ducts to spiral flat oval sizes, use Table 3. Table 3 is based on Equation (26) (Heyt and Diaz 1975), the circular equivalent of a flat oval duct for equal airflow, resistance, and length. Equations (21) or (20) and (19) must be used to determine friction loss.

$$D_e = \frac{1.55A^{0.625}}{P^{0.250}} \tag{26}$$

where A is the cross-sectional area of flat oval duct defined as

$$A = (\pi b^2/4) + b(a-b) \tag{27}$$

and the perimeter P is calculated by

$$P = \pi b + 2(a-b) \tag{28}$$

where

P = perimeter of flat oval duct, in.
a = major dimension of flat oval duct, in.
b = minor dimension of flat oval duct, in.

DYNAMIC LOSSES

Dynamic losses result from flow disturbances caused by duct-mounted equipment and fittings that change the airflow path's direction and/or area. These fittings include entries, exits, elbows, transitions, and junctions. Idelchik et al. (1986) discuss parameters affecting fluid resistance of fittings and presents local loss coefficients in three forms: tables, curves, and equations.

Local Loss Coefficients

The dimensionless coefficient C is used for fluid resistance, because this coefficient has the same value in dynamically similar streams (i.e., streams with geometrically similar stretches, equal Reynolds numbers, and equal values of other criteria necessary for dynamic similarity). The fluid resistance coefficient represents the ratio of total pressure loss to velocity pressure at the referenced cross section:

$$C = \frac{\Delta p_j}{\rho(V/1097)^2} = \frac{\Delta p_j}{p_v} \tag{29}$$

where

C = local loss coefficient, dimensionless
Δp_j = total pressure loss, in. of water
ρ = density, lb$_m$/ft^3
V = velocity, fpm
p_v = velocity pressure, in. of water

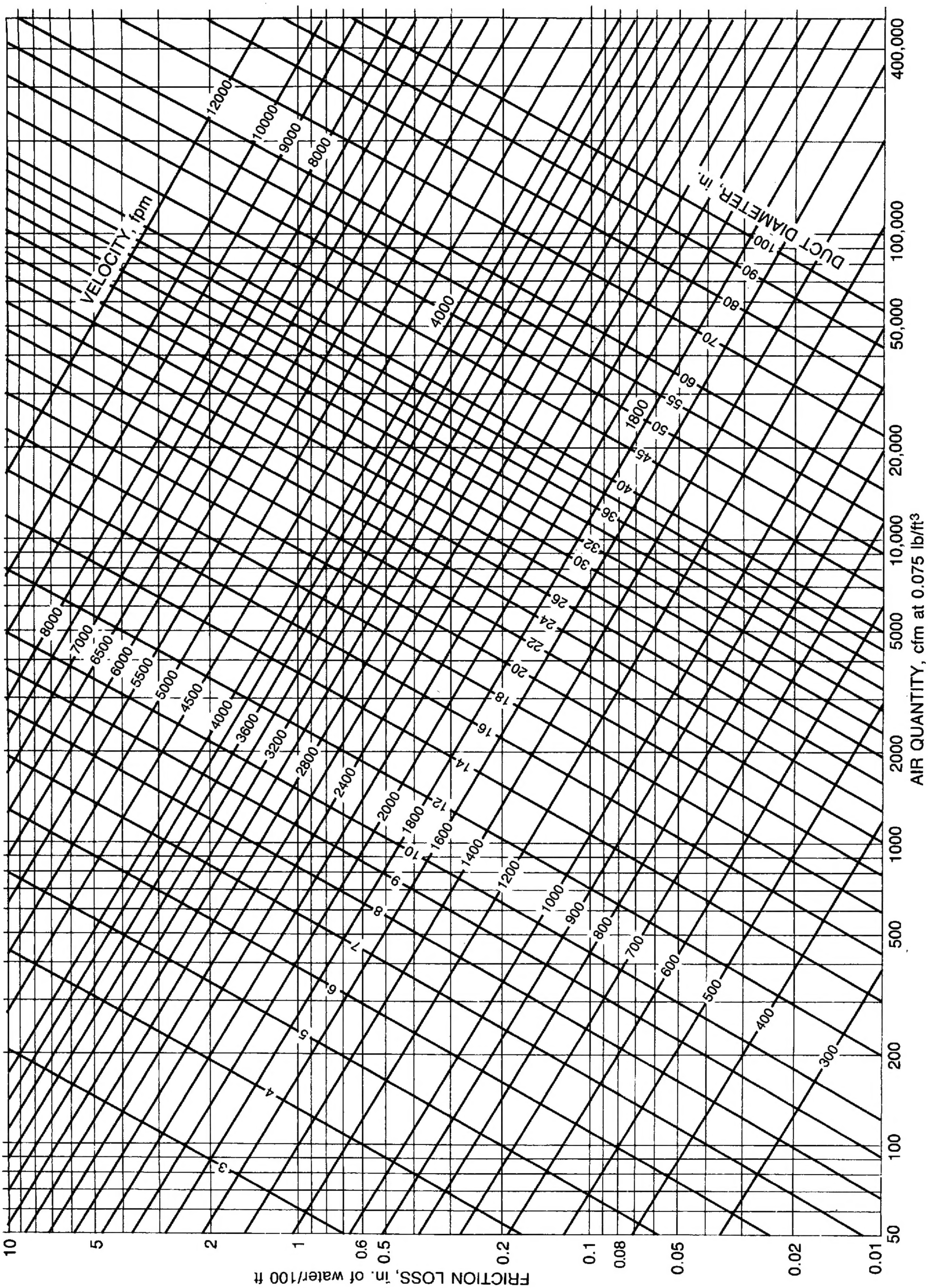

Fig. 9 Friction Chart for Round Duct ($\rho = 0.075\ lb_m/ft^3$ and $\varepsilon = 0.0003$ ft)

Table 2 Equivalent Rectangular Duct Dimension

Duct Diameter, in.		Aspect Ratio 1.00	1.25	1.50	1.75	2.00	2.25	2.50	2.75	3.00	3.50	4.00	5.00	6.00	7.00	8.00
		Rectangular Size, in.														
6	Width	—	6													
	Height	—	5													
7	Width	6	8													
	Height	6	6													
8	Width	7	9	9	11											
	Height	7	7	6	6											
9	Width	8	9	11	11	12	14									
	Height	8	7	7	6	6	6									
10	Width	9	10	12	12	14	14	15	17							
	Height	9	8	8	7	7	6	6	6							
11	Width	10	11	12	14	14	16	18	17	18	21					
	Height	10	9	8	8	7	7	7	6	6	6					
12	Width	11	13	14	14	16	16	18	19	21	21	24				
	Height	11	10	9	8	8	7	7	7	7	6	6				
13	Width	12	14	15	16	18	18	20	19	21	25	24	30			
	Height	12	11	10	9	9	8	8	7	7	7	6	6			
14	Width	13	14	17	18	18	20	20	22	24	25	28	30	36		
	Height	13	11	11	10	9	9	8	8	8	7	7	6	6		
15	Width	14	15	17	18	20	20	23	25	24	28	28	35	36	42	
	Height	14	12	11	10	10	9	9	9	8	8	7	7	6	6	
16	Width	15	16	18	19	20	23	23	25	27	28	32	35	42	42	48
	Height	15	13	12	11	10	10	9	9	9	8	8	7	7	6	6
17	Width	16	18	20	21	22	25	25	28	27	32	32	35	42	49	48
	Height	16	14	13	12	11	11	10	10	9	9	8	7	7	7	6
18	Width	16	19	21	23	24	25	28	28	30	32	36	40	42	49	56
	Height	16	15	14	13	12	11	11	10	10	9	9	8	7	7	7
19	Width	17	20	21	23	24	27	28	30	30	35	36	40	48	49	56
	Height	17	16	14	13	12	12	11	11	10	10	9	8	8	7	7
20	Width	18	20	23	25	26	27	30	30	33	35	40	45	48	56	56
	Height	18	16	15	14	13	12	12	11	11	10	10	9	8	8	7
21	Width	19	21	24	26	28	29	30	33	33	39	40	45	54	56	64
	Height	19	17	16	15	14	13	12	12	11	11	10	9	9	8	8
22	Width	20	23	26	26	28	32	33	36	36	39	44	50	54	56	64
	Height	20	18	17	15	14	14	13	13	12	11	11	10	9	8	8
23	Width	21	24	26	28	30	32	35	36	39	42	44	50	54	63	64
	Height	21	19	17	16	15	14	14	13	13	12	11	10	9	9	8
24	Width	22	25	27	30	32	34	35	39	39	42	48	55	60	63	72
	Height	22	20	18	17	16	15	14	14	13	12	12	11	10	9	9
25	Width	23	25	29	30	32	36	38	39	42	46	48	55	60	70	72
	Height	23	20	19	17	16	16	15	14	14	13	12	11	10	10	9
26	Width	24	26	30	32	34	36	38	41	42	46	52	55	66	70	72
	Height	24	21	20	18	17	16	15	15	14	13	13	11	11	10	9
27	Width	25	28	30	33	36	38	40	41	45	49	52	60	66	70	80
	Height	25	22	20	19	18	17	16	15	15	14	13	12	11	10	10
28	Width	26	29	32	35	36	38	43	44	45	49	56	60	66	77	80
	Height	26	23	21	20	18	17	17	16	15	14	14	12	11	11	10
29	Width	27	30	33	35	38	41	43	44	48	53	56	65	72	77	88
	Height	27	24	22	20	19	18	17	16	16	15	14	13	12	11	11
30	Width	27	31	35	37	40	43	45	47	48	53	60	65	72	77	88
	Height	27	25	23	21	20	19	18	17	16	15	15	13	12	11	11
31	Width	28	31	35	39	40	43	45	50	51	56	60	70	78	84	88
	Height	28	25	23	22	20	19	18	18	17	16	15	14	13	12	11
32	Width	29	33	36	39	42	45	48	50	54	56	60	70	78	84	96
	Height	29	26	24	22	21	20	19	18	18	16	15	14	13	12	12
33	Width	30	34	38	40	44	47	50	52	54	60	64	75	78	91	96
	Height	30	27	25	23	22	21	20	19	18	17	16	15	13	13	12
34	Width	31	35	39	42	44	47	50	52	57	60	64	75	84	91	96
	Height	31	28	26	24	22	21	20	19	19	17	16	15	14	13	12
35	Width	32	36	39	42	46	50	53	55	57	63	68	75	84	91	104
	Height	32	29	26	24	23	22	21	20	19	18	17	15	14	13	13
36	Width	33	36	41	44	48	50	53	55	60	63	68	80	90	98	104
	Height	33	29	27	25	24	22	21	20	20	18	17	16	15	14	13
38	Width	35	39	44	47	50	54	58	61	63	67	72	85	96	105	112
	Height	35	31	29	27	25	24	23	22	21	19	18	17	16	15	14

*Shaded area not recommended.

Table 2 Equivalent Rectangular Duct Dimension (*Continued*)

Duct Diameter, in.		Aspect Ratio 1.00	1.25	1.50	1.75	2.00	2.25	2.50	2.75	3.00	3.50	4.00	5.00	6.00	7.00	8.00
		Rectangular Size, in.														
40	Width	37	41	45	49	52	56	60	63	66	70	76	90	96	105	120
	Height	37	33	30	28	26	25	24	23	22	20	19	18	16	15	15
42	Width	38	43	48	51	56	59	63	66	69	74	80	90	102	112	120
	Height	38	34	32	29	28	26	25	24	23	21	20	18	17	16	15
44	Width	40	45	50	54	58	61	65	69	72	81	84	95	108	119	128
	Height	40	36	33	31	29	27	26	25	24	23	21	19	18	17	16
46	Width	42	48	53	56	60	65	68	72	75	84	88	100	114	126	136
	Height	42	38	35	32	30	29	27	26	25	24	22	20	19	18	17
48	Width	44	49	54	60	62	68	70	74	78	88	92	105	120	126	136
	Height	44	39	36	34	31	30	28	27	26	25	23	21	20	18	17
50	Width	46	51	57	61	66	70	75	77	81	91	96	110	120	133	144
	Height	46	41	38	35	33	31	30	28	27	26	24	22	20	19	18
52	Width	48	54	59	63	68	72	78	83	84	95	100	115	126	140	152
	Height	48	43	39	36	34	32	31	30	28	27	25	23	21	20	19
54	Width	49	55	62	67	70	77	80	85	90	98	104	120	132	147	160
	Height	49	44	41	38	35	34	32	31	30	28	26	24	22	21	20
56	Width	51	58	63	68	74	79	83	88	93	102	108	125	138	147	160
	Height	51	46	42	39	37	35	33	32	31	29	27	25	23	21	20
58	Width	53	60	66	70	76	81	85	91	96	105	112	130	144	154	168
	Height	53	48	44	40	38	36	34	33	32	30	28	26	24	22	21
60	Width	55	61	68	74	78	83	90	94	99	109	116	130	144	161	
	Height	55	49	45	42	39	37	36	34	33	31	29	26	24	23	
62	Width	57	64	71	75	82	88	93	96	102	112	120	135	150	168	
	Height	57	51	47	43	41	39	37	35	34	32	30	27	25	24	
64	Width	59	65	72	79	84	90	95	99	105	116	124	140	156		
	Height	59	52	48	45	42	40	38	36	35	33	31	28	26		
66	Width	60	68	75	81	86	92	98	105	108	119	128	145	162		
	Height	60	54	50	46	43	41	39	38	36	34	32	29	27		
68	Width	62	70	77	82	90	95	100	107	111	123	132	150	168		
	Height	62	56	51	47	45	42	40	39	37	35	33	30	28		
70	Width	64	71	80	86	92	99	105	110	114	126	136	155			
	Height	64	57	53	49	46	44	42	40	38	36	34	31			
72	Width	66	74	81	88	94	101	108	113	117	130	140	160			
	Height	66	59	54	50	47	45	43	41	39	37	35	32			
74	Width	68	76	84	91	98	104	110	116	123	133	144	165			
	Height	68	61	56	52	49	46	44	42	41	38	36	33			
76	Width	70	78	86	93	100	106	113	118	126	137	148	165			
	Height	70	62	57	53	50	47	45	43	42	39	37	33			
78	Width	71	80	89	95	102	110	115	121	129	140	152				
	Height	71	64	59	54	51	49	46	44	43	40	38				
80	Width	73	83	90	98	104	113	118	124	132	144	156				
	Height	73	66	60	56	52	50	47	45	44	41	39				
82	Width	75	84	93	100	108	115	123	129	135	147	160				
	Height	75	67	62	57	54	51	49	47	45	42	40				
84	Width	77	86	95	103	110	117	125	132	138	151	164				
	Height	77	69	63	59	55	52	50	48	46	43	41				
86	Width	79	88	98	105	112	119	128	135	141	154	168				
	Height	79	70	65	60	56	53	51	49	47	44	42				
88	Width	80	90	99	107	116	124	130	138	144	158					
	Height	80	72	66	61	58	55	52	50	48	45					
90	Width	82	93	102	110	118	126	133	140	147	161					
	Height	82	74	68	63	59	56	53	51	49	46					
92	Width	84	94	104	112	120	128	138	143	150	165					
	Height	84	75	69	64	60	57	55	52	50	47					
94	Width	86	96	107	116	124	131	140	146	153	168					
	Height	86	77	71	66	62	58	56	53	51	48					
96	Width	88	99	108	117	126	135	143	151	159						
	Height	88	79	72	67	63	60	57	55	53						
98	Width	90	100	111	119	128	137	145	154	162						
	Height	90	80	74	68	64	61	58	56	54						
100	Width	91	103	113	123	132	140	148	157	165						
	Height	91	82	75	70	66	62	59	57	55						
102	Width	93	105	116	124	134	142	153	160	168						
	Height	93	84	77	71	67	63	61	58	56						

*Shaded area not recommended.

Table 2 Equivalent Rectangular Duct Dimension (*Concluded*)

Duct Diameter, in.		Aspect Ratio 1.00	1.25	1.50	1.75	2.00	2.25	2.50	2.75	3.00	3.50	4.00	5.00	6.00	7.00	8.00
		Rectangular Size, in.														
104	Width	95	106	117	128	136	146	155	162							
	Height	95	85	78	73	68	65	62	59							
106	Width	97	109	120	130	140	149	158	165							
	Height	97	87	80	74	70	66	63	60							
108	Width	99	110	122	131	142	151	160	168							
	Height	99	88	81	75	71	67	64	61							
110	Width	101	113	125	135	144	153	163								
	Height	101	90	83	77	72	68	65								
112	Width	102	115	126	137	146	158	165								
	Height	102	92	84	78	73	70	66								
114	Width	104	116	129	140	150	160									
	Height	104	93	86	80	75	71									
116	Width	106	119	131	142	152	162									
	Height	106	95	87	81	76	72									
118	Width	108	121	134	144	154	164									
	Height	108	97	89	82	77	73									
120	Width	110	123	135	147	158										
	Height	110	98	90	84	79										

*Shaded area not recommended.

Table 3 Equivalent Spiral Flat Oval Duct Dimensions

Round Duct Diameter, in.	Minor Dimension (*b*), in. 3	4	5	6	7	8	9	10	11	12	14	16
	Major Dimension (*a*), in.											
5	8											
5.5	9	7										
6	11	9										
6.5	12	10	8									
7	15	12	10	8								
7.5	19	13	—	9								
8	22	15	11	—								
8.5		18	13	11	10							
9		20	14	12	—	10						
9.5		21	18	14	12	—						
10			19	15	13	11						
10.5			21	17	15	13	12					
11				19	16	14	—	12				
11.5				20	18	16	14	—				
12				23	20	17	15	13				
12.5				25	21	—	—	15	14			
13				28	23	19	17	16	—	14		
13.5				30	—	21	18	—	16	—		
14				33	—	22	20	18	17	15		
14.5				36	—	24	22	19	—	17		
15				39	—	27	23	21	19	18		
16				45	—	30	—	24	22	20	17	
17				52	—	35	—	27	24	21	19	
18				59	—	39	—	30	—	25	22	19

Round Duct Diameter, in.	Minor Dimension (*b*), in. 8	9	10	11	12	14	16	18	20	22	24
	Major Dimension (*a*), in.										
19	46	—	34	—	28	23	21				
20	50	—	38	—	31	27	24	21			
21	58	—	43	—	34	28	25	23			
22	65	—	48	—	37	31	29	26			
23	71	—	52	—	42	34	30	27			
24	77	—	57	—	45	38	33	29	26		
25			63	—	50	41	36	32	29		
26			70	—	56	45	38	34	31		
27			76	—	59	49	41	37	34		
28					65	52	46	40	36		
29					72	58	49	43	39	35	
30					78	61	54	46	40	38	
31					81	67	57	49	44	39	37
32						71	60	53	47	42	40
33						77	66	56	51	46	41
34							69	59	55	47	44
35							76	65	58	50	46
36							79	68	61	53	49
37								71	64	57	52
38								78	67	60	55
40									77	69	62
42										75	68
44										82	74

Dynamic losses occur along a duct length and cannot be separated from friction losses. For ease of calculation, dynamic losses are assumed to be concentrated at a section (local) and to exclude friction. Frictional losses must be considered only for relatively long fittings. Generally, fitting friction losses are accounted for by measuring duct lengths from the centerline of one fitting to that of the next fitting. For fittings closely coupled (less than six hydraulic diameters apart), the flow pattern entering subsequent fittings differs from the flow pattern used to determine loss coefficients. Adequate data for these situations are unavailable.

For all fittings, except junctions, calculate the total pressure loss Δp_j at a section by

$$\Delta p_j = C_o p_{v,o} \tag{30}$$

where the subscript o is the cross section at which the velocity pressure is referenced. The dynamic loss is based on the actual velocity in the duct, not the velocity in an equivalent noncircular duct. For the cross section to reference a fitting loss coefficient, refer to Step 4 in the section on HVAC Duct Design Procedures. Where necessary (unequal area fittings), convert a loss coefficient from section o to

section i using Equation (31), where V is the velocity at the respective sections.

$$C_i = \frac{C_o}{(V_i/V_o)^2} \tag{31}$$

For converging and diverging flow junctions, total pressure losses through the straight (main) section are calculated as

$$\Delta p_j = C_{c,s} p_{v,c} \tag{32}$$

For total pressure losses through the branch section,

$$\Delta p_j = C_{c,b} p_{v,c} \tag{33}$$

where $p_{v,c}$ is the velocity pressure at the common section c, and $C_{c,s}$ and $C_{c,b}$ are losses for the straight (main) and branch flow paths, respectively, each referenced to the velocity pressure at section c. To convert junction local loss coefficients referenced to straight and branch velocity pressures, use the following equation:

$$C_i = \frac{C_{c,i}}{(V_i/V_c)^2} \tag{34}$$

where

C_i = local loss coefficient referenced to section being calculated (see subscripts), dimensionless
$C_{c,i}$ = straight ($C_{c,s}$) or branch ($C_{c,b}$) local loss coefficient referenced to dynamic pressure at common section, dimensionless
V_i = velocity at section to which C_i is being referenced, fpm
V_c = velocity at common section, fpm

Subscripts:
b = branch
s = straight (main) section
c = common section

The junction of two parallel streams moving at different velocities is characterized by turbulent mixing of the streams, accompanied by pressure losses. In the course of this mixing, an exchange of momentum takes place between the particles moving at different velocities, finally resulting in the equalization of the velocity distributions in the common stream. The jet with higher velocity loses a part of its kinetic energy by transmitting it to the slower moving jet. The loss in total pressure before and after mixing is always large and positive for the higher velocity jet and increases with an increase in the amount of energy transmitted to the lower velocity jet. Consequently, the local loss coefficient, defined by Equation (29), will always be positive. The energy stored in the lower velocity jet increases as a result of mixing. The loss in total pressure and the local loss coefficient can, therefore, also have negative values for the lower velocity jet (Idelchik et al. 1986).

Duct Fitting Database

A duct fitting database, developed by ASHRAE (1994), which includes 228 round and rectangular fittings with the provision to include flat oval fittings, is available from ASHRAE in electronic form with the capability to be linked to duct design programs.

The fittings are numbered (coded) as shown in Table 4. Entries and converging junctions are only in the exhaust/return portion of systems. Exits and diverging junctions are only in supply systems. Equal-area elbows, obstructions, and duct-mounted equipment are common to both supply and exhaust systems. Transitions and unequal-area elbows can be either supply or exhaust fittings. Fitting ED5-1 (see the section on Fitting Loss Coefficients) is an **E**xhaust fitting with a round shape (**D**iameter). The number 5 indicates that the fitting is a junction, and 1 is its sequential number. Fittings SR3-1 and ER3-1 are **S**upply and **E**xhaust fittings, respectively. The R indicates that the fitting is **R**ectangular, and the 3 identifies the fitting as an elbow. Note that the cross-sectional areas at sections 0 and 1 are not equal (see the section on Fitting Loss Coefficients). Otherwise, the elbow would be a **C**ommon fitting such as CR3-6. Additional fittings are reproduced in the section on Fitting Loss Coefficients to support the example design problems (see Table 12 for Example 8; see Table 14 for Example 9).

Table 4 Duct Fitting Codes

Fitting Function	Geometry	Category	Sequential Number
S: Supply	D: round (Diameter)	1. Entries 2. Exits	1,2,3...n
E: Exhaust/Return	R: Rectangular	3. Elbows 4. Transitions	
C: Common (supply and return)	O: flat Oval	5. Junctions 6. Obstructions 7. Fan and system interactions 8. Duct-mounted equipment 9. Dampers 10. Hoods	

DUCTWORK SECTIONAL LOSSES

Darcy-Weisbach Equation

Total pressure loss in a duct section is calculated by combining Equations (19) and (29) in terms of Δp, where ΣC is the summation of local loss coefficients within the duct section. Each fitting loss coefficient must be referenced to that section's velocity pressure.

$$\Delta p = \left(\frac{12fL}{D_h} + \Sigma C\right)\rho\left(\frac{V}{1097}\right)^2 \tag{35}$$

FAN-SYSTEM INTERFACE

Fan Inlet and Outlet Conditions

Fan performance data measured in the field may show lower performance capacity than manufacturers' ratings. The most common causes of deficient performance of the fan/system combination are improper outlet connections, nonuniform inlet flow, and swirl at the fan inlet. These conditions alter the aerodynamic characteristics of the fan so that its full flow potential is not realized. One bad connection can reduce fan performance far below its rating. No data have been published that account for the effects of fan inlet and outlet flexible vibration connectors.

Normally, a fan is tested with open inlets and a section of straight duct attached to the outlet (ASHRAE *Standard* 51). This setup results in uniform flow into the fan and efficient static pressure recovery on the fan outlet. If good inlet and outlet conditions are not provided in the actual installation, the performance of the fan suffers. To select and apply the fan properly, these effects must be considered, and the pressure requirements of the fan, as calculated by standard duct design procedures, must be increased.

Figure 10 illustrates deficient fan/system performance. The system pressure losses have been determined accurately, and a fan has been selected for operation at Point 1. However, no allowance has been made for the effect of system connections to the fan on fan performance. To compensate, a fan system effect must be added to the calculated system pressure losses to determine the actual system curve. The point of intersection between the fan performance curve and the actual system curve is Point 4. The actual flow volume is, therefore, deficient by the difference from 1 to 4. To achieve design flow volume,

a fan system effect pressure loss equal to the pressure difference between Points 1 and 2 should be added to the calculated system pressure losses, and the fan should be selected to operate at Point 2.

Fan System Effect Coefficients

The system effect concept was formulated by Farquhar (1973) and Meyer (1973); the magnitudes of the system effect, called **system effect factors**, were determined experimentally in the laboratory of the Air Movement and Control Association (AMCA) (Brown 1973, Clarke et al. 1978) and published in their *Publication* 201 (AMCA 1990a). The system effect factors, converted to local loss coefficients, are in the *Duct Fitting Database* (ASHRAE 1994) for both centrifugal and axial fans. Fan system effect coefficients are only an approximation. Fans of different types and even fans of the same type, but supplied by different manufacturers, do not necessarily react to a system in the same way. Therefore, judgment based on experience must be applied to any design.

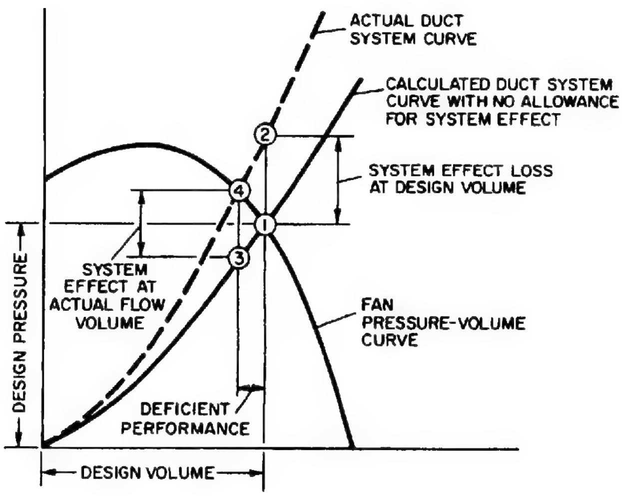

Fig. 10 Deficient System Performance with System Effect Ignored

Fan Outlet Conditions. Fans intended primarily for duct systems are usually tested with an outlet duct in place (ASHRAE *Standard* 51). Figure 11 shows the changes in velocity profiles at various distances from the fan outlet. For 100% recovery, the duct, including transition, must meet the requirements for 100% effective duct length [L_e (Figure 11)], which is calculated as follows:

For $V_o > 2500$ fpm,

$$L_e = \frac{V_o\sqrt{A_o}}{10{,}600} \tag{36}$$

For $V_o \le 2500$ fpm,

$$L_e = \frac{\sqrt{A_o}}{4.3} \tag{37}$$

where

V_o = duct velocity, fpm
L_e = effective duct length, ft
A_o = duct area, in^2

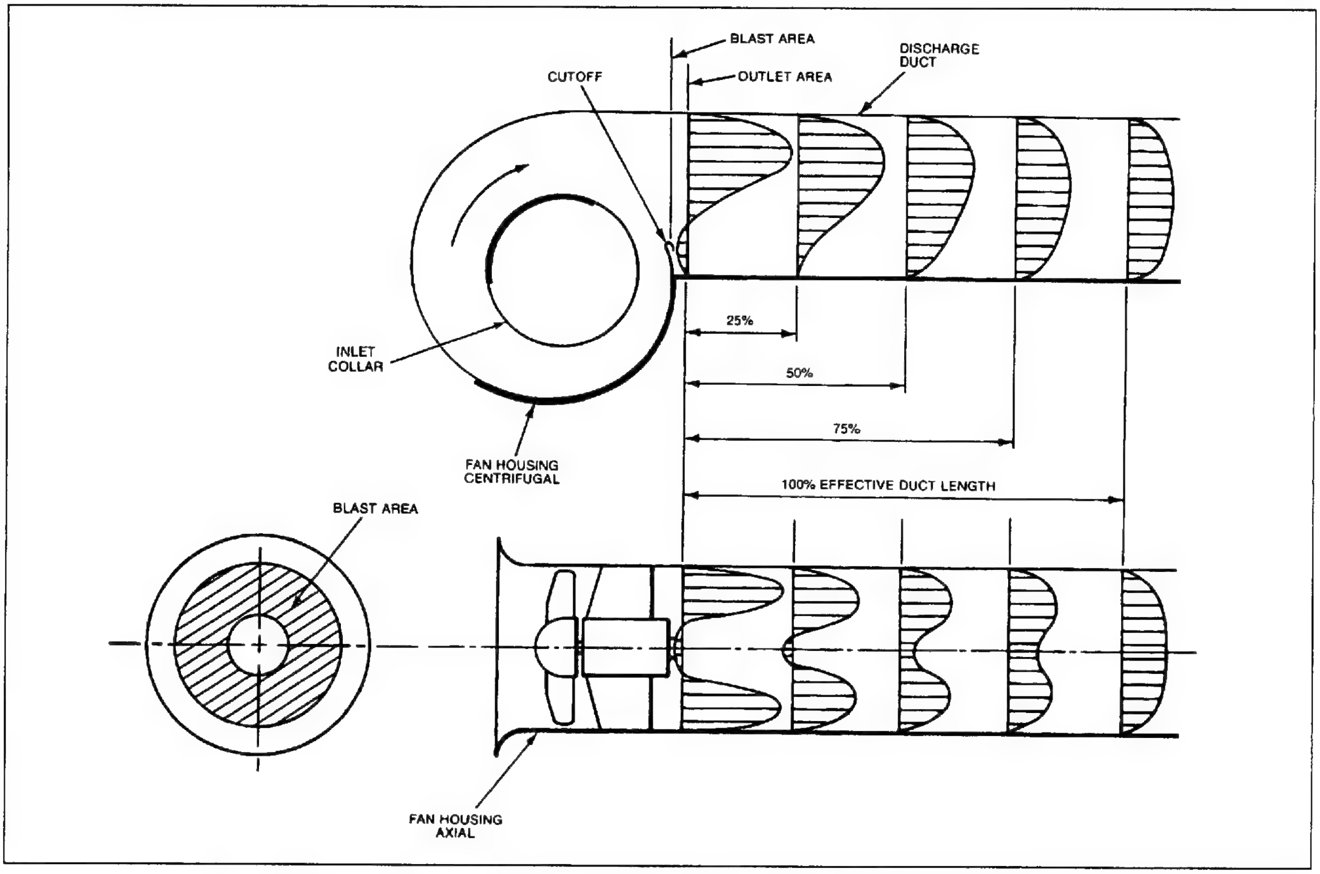

Fig. 11 Establishment of Uniform Velocity Profile in Straight Fan Outlet Duct
(Adapted by permission from AMCA *Publication* 201)

As illustrated by Fitting SR7-1 in the section on Fitting Loss Coefficients, centrifugal fans should not abruptly discharge to the atmosphere. A diffuser design should be selected from Fitting SR7-2 (see the section on Fitting Loss Coefficients) or SR7-3 (see ASHRAE 1994).

Fan Inlet Conditions. For rated performance, air must enter the fan uniformly over the inlet area in an axial direction without pre-rotation. Nonuniform flow into the inlet is the most common cause of reduced fan performance. Such inlet conditions are not equivalent to a simple increase in the system resistance; therefore, they cannot be treated as a percentage decrease in the flow and pressure from the fan. A poor inlet condition results in an entirely new fan performance. An elbow at the fan inlet, for example Fitting ED7-2 (see the section on Fitting Loss Coefficients), causes turbulence and uneven flow into the fan impeller. The losses due to the fan system effect can be eliminated by including an adequate length of straight duct between the elbow and the fan inlet.

The ideal inlet condition allows air to enter axially and uniformly without spin. A spin in the same direction as the impeller rotation reduces the pressure-volume curve by an amount dependent on the intensity of the vortex. A counterrotating vortex at the inlet slightly increases the pressure-volume curve, but the power is increased substantially.

Inlet spin may arise from a great variety of approach conditions, and sometimes the cause is not obvious. Inlet spin can be avoided by providing an adequate length of straight duct between the elbow and the fan inlet. Figure 12 illustrates some common duct connections that cause inlet spin and includes recommendations for correcting spin.

Fans within plenums and cabinets or next to walls should be located so that air may flow unobstructed into the inlets. Fan performance is reduced if the space between the fan inlet and the enclosure is too restrictive. The system effect coefficients for fans in an enclosure or adjacent to walls are listed under Fitting ED7-1 (see the section on Fitting Loss Coefficients). The manner in which the airstream enters an enclosure in relation to the fan inlets also affects fan performance. Plenum or enclosure inlets or walls that are not symmetrical with the fan inlets cause uneven flow and/or inlet spin.

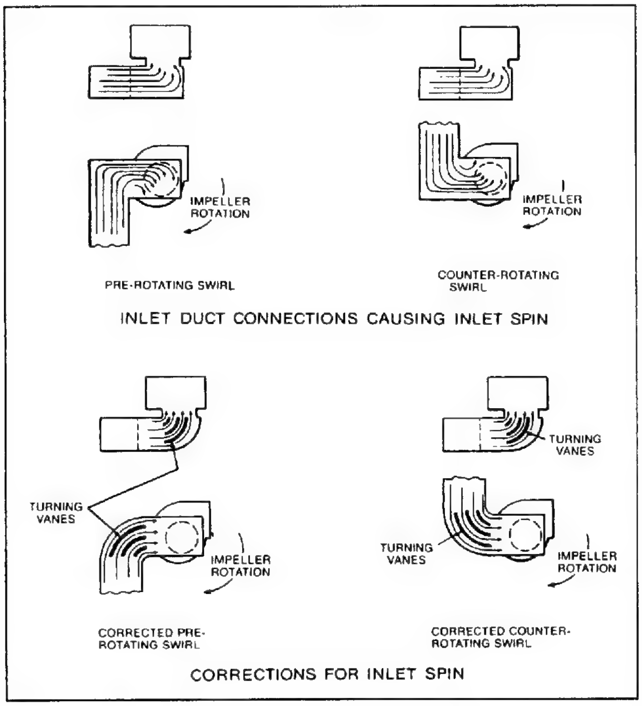

Fig. 12 Inlet Duct Connections Causing Inlet Spin and Corrections for Inlet Spin
(Adapted by permission from AMCA *Publication* 201)

Testing, Adjusting, and Balancing Considerations

Fan system effects (FSEs) are not only to be used in conjunction with the system resistance characteristics in the fan selection process, but are also applied in the calculations of the results of testing, adjusting, and balancing (TAB) field tests to allow direct comparison to design calculations and/or fan performance data. Fan inlet swirl and the effect on system performance of poor fan inlet and outlet ductwork connections cannot be measured directly. Poor inlet flow patterns affect fan performance within the impeller wheel (centrifugal fan) or wheel rotor impeller (axial fan), while the fan outlet system effect is flow instability and turbulence within the fan discharge ductwork.

The static pressure at the fan inlet and the static pressure at the fan outlet may be measured directly in some systems. In most cases, static pressure measurements for use in determining fan total (or static) pressure will not be made directly at the fan inlet and outlet, but at locations a relatively short distance from the fan inlet and downstream from the fan outlet. To calculate fan total pressure for this case from field measurements, use Equation (38), where $\Delta p_{x\text{-}y}$ is the summation of calculated total pressure losses between the fan inlet and outlet sections noted. Plane 3 is used to determine airflow rate. If necessary, use Equation (18) to calculate fan static pressure knowing fan total pressure. For locating measurement planes and calculation procedures, consult AMCA *Publication* 203 (AMCA 1990b).

$$\begin{aligned} P_t = {} & (p_{s,5} + p_{v,5}) + \Delta p_{2\text{-}5} + \mathrm{FSE}_2 \\ & + (p_{s,4} + p_{v,4}) + \Delta p_{4\text{-}1} + \mathrm{FSE}_1 + \mathrm{FSE}_{1,sw} \end{aligned} \tag{38}$$

where

P_t = fan total pressure, in. of water
p_s = static pressure, in. of water
p_v = velocity pressure, in. of water
FSE = fan system effect, in. of water
$\Delta p_{x\text{-}y}$ = summarization of total pressure losses between planes x and y, in. of water

Subscripts (numerical subscripts same as used by AMCA *Publication* 203):

1 = fan inlet
2 = fan outlet
3 = plane of airflow measurement
4 = plane of static pressure measurement upstream of fan
5 = plane of static pressure measurement downstream of fan
sw = swirl

DUCT SYSTEM DESIGN

DESIGN CONSIDERATIONS

Space Pressure Relationships

Space pressure is determined by fan location and duct system arrangement. For example, a supply fan that pumps air into a space increases space pressure; an exhaust fan reduces space pressure. If both supply and exhaust fans are used, space pressure depends on the relative capacity of the fans. Space pressure is positive if supply exceeds exhaust and negative if exhaust exceeds supply (Osborne 1966). System pressure variations due to wind can be minimized or eliminated by careful selection of intake air and exhaust vent locations (Chapter 15).

Fire and Smoke Management

Because duct systems can convey smoke, hot gases, and fire from one area to another and can accelerate a fire within the system, fire protection is an essential part of air-conditioning and ventilation system design. Generally, fire safety codes require compliance with the standards of national organizations. NFPA *Standard* 90A examines fire safety requirements for (1) ducts, connectors, and appurtenances; (2) plenums and corridors; (3) air outlets, air inlets, and fresh air intakes; (4) air filters; (5) fans; (6) electric wiring and equipment; (7) air-cooling and -heating equipment; (8) building construction, including protection of penetrations; and (9) controls, including smoke control.

Fire safety codes often refer to the testing and labeling practices of nationally recognized laboratories, such as Factory Mutual and Underwriters Laboratories (UL). The *Building Materials Directory* compiled by UL lists fire and smoke dampers that have been tested and meet the requirements of UL *Standards* 555 and 555S. This directory also summarizes maximum allowable sizes for individual dampers and assemblies of these dampers. Fire dampers are 1.5 h or 3 h fire-rated. Smoke dampers are classified by (1) temperature degradation [ambient air or high temperature (250°F minimum)] and (2) leakage at 1 and 4 in. of water pressure difference (8 and 12 in. of water classification optional). Smoke dampers are tested under conditions of maximum airflow. UL's *Fire Resistance Directory* lists the fire resistance of floor/roof and ceiling assemblies with and without ceiling fire dampers.

For a more detailed presentation of fire protection, see Chapter 48 of the 1995 *ASHRAE Handbook—Applications* and the NFPA *Fire Protection Handbook* (NFPA 1991).

Duct Insulation

In all new construction (except low-rise residential buildings), air-handling ducts and plenums installed as part of an HVAC air distribution system should be thermally insulated in accordance with Section 9.4 of ASHRAE *Standard* 90.1. Duct insulation for new low-rise residential buildings should be in compliance with ASHRAE *Standard* 90.2. Existing buildings should meet the requirements of ASHRAE *Standard* 100. The insulation thicknesses in these standards are minimum values. Economic considerations may justify higher insulation levels. Additional insulation, vapor retarders, or both may be required to limit vapor transmission and condensation.

Duct heat gains or losses must be known for the calculation of supply air quantities, supply air temperatures, and coil loads (see Chapter 28 of this volume and Chapter 2 of the 1996 *ASHRAE Handbook—Systems and Equipment*). To estimate duct heat transfer and entering or leaving air temperatures, use the following equations:

$$q_l = \frac{UPL}{12}\left[\left(\frac{t_e + t_l}{2}\right) - t_a\right] \tag{39}$$

$$t_e = \frac{t_l(y+1) - 2t_a}{(y-1)} \tag{40}$$

$$t_l = \frac{t_e(y-1) + 2t_a}{(y+1)} \tag{41}$$

where

q_l = heat loss/gain through duct walls, Btu/h (negative for heat gain)
U = overall heat transfer coefficient of duct wall, Btu/h·ft²·°F
P = perimeter of bare or insulated duct, in.
L = duct length, ft
t_e = temperature of air entering duct, °F

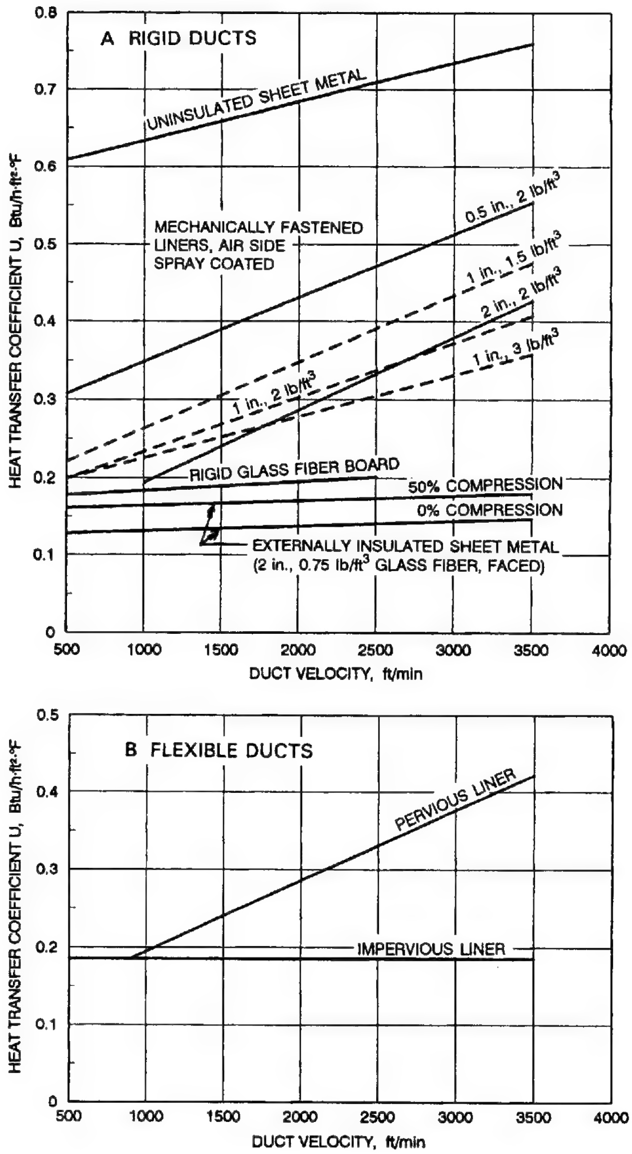

Fig. 13 Duct Heat Transfer Coefficients

t_l = temperature of air leaving duct, °F
t_a = temperature of air surrounding duct, °F
y = $10AV\rho c_p/UPL$ for rectangular ducts
= $2.5DV\rho c_p/UL$ for round ducts
A = cross-sectional area of duct, in²
V = average velocity, fpm
ρ = density of air, lb_m/ft^3
c_p = specific heat of air, $Btu/lb_m \cdot °F$
D = diameter of duct, in.

Use Figure 13A to determine U-factors for insulated and uninsulated ducts. Lauvray (1978) has shown the effects of (1) compressing insulation wrapped externally on sheet metal ducts and (2) insulated flexible ducts with air-porous liners. For a 2 in. thick, 0.75 lb_m/ft^3 fibrous glass blanket compressed 50% during installation, the heat transfer rate increases approximately 20% (see Figure 13A). Pervious flexible duct liners also influence heat transfer significantly (see Figure 13B). At 2500 fpm, the pervious liner U-factor is 0.33 Btu/h·ft²·°F; for an impervious liner, U = 0.19 Btu/h·ft²·°F.

Example 6. A 65 ft length of 24 in. by 36 in. uninsulated sheet metal duct, freely suspended, conveys heated air through a space maintained above freezing at 40°F. Based on heat loss calculations for the heated zone, 17,200 cfm of standard air (c_p = 0.24 Btu/lb$_m$·°F) at a supply air temperature of 122°F is required. The duct is connected directly to the heated zone. Determine the temperature of the air entering the duct and the duct heat loss.

Solution: Calculate duct velocity using Equation (10):

$$V = \frac{(144)(17{,}200\text{ cfm})}{(24\text{ in.})(36\text{ in.})} = 2900\text{ fpm}$$

Calculate entering air temperature using Equation (40):

$$U = 0.73\text{ Btu/h}\cdot\text{ft}^2\cdot{}^\circ\text{F (from Figure 13A)}$$

$$P = 2(24\text{ in.} + 36\text{ in.}) = 120\text{ in.}$$

$$y = \frac{(10)(24\text{ in.})(36\text{ in.})(2900\text{ fpm})(0.075\text{ lb}_m/\text{ft}^3)(0.24)}{(0.73\text{ Btu/h}\cdot\text{ft}^2\cdot{}^\circ\text{F})(120\text{ in.})(65\text{ ft})} = 79.2$$

$$t_e = \frac{122^\circ\text{F}(79.2+1)-(2\times 40^\circ\text{F})}{(79.2-1)} = 124.1^\circ\text{F}$$

Calculate duct heat loss using Equation (39):

$$q_l = \frac{(0.73\text{ Btu/h}\cdot\text{ft}^2\cdot{}^\circ\text{F})(120\text{ in.})(65\text{ ft})}{12} \times\left[\frac{124.1^\circ\text{F}+122^\circ\text{F}}{2} - 40^\circ\text{F}\right] = 39{,}400\text{ Btu/h}$$

Example 7. Same as Example 6, except the duct is insulated externally with 2 in. thick fibrous glass with a density of 0.75 lb$_m$/ft^3. The insulation is wrapped with 0% compression.

Solution: All values except U remain the same as in Example 6. From Figure 13A, U = 0.15 Btu/h·ft^2·°F at 2900 fpm. Therefore,

$$y = 385$$

$$t_e = 122.4^\circ\text{F}$$

$$q_l = 8014\text{ Btu/h}$$

Insulating this duct reduces heat loss to 20% of the uninsulated value.

Duct System Leakage

Leakage in all unsealed ducts varies considerably with the fabricating machinery used, the methods for assembly, and installation workmanship. For sealed ducts, a wide variety of sealing methods and products exists. Sealed and unsealed duct leakage tests (AISI/SMACNA 1972, ASHRAE/SMACNA/TIMA 1985, Swim and Griggs 1995) have confirmed that longitudinal seam, transverse joint, and assembled duct leakage can be represented by Equation (42) and that for the same construction, leakage is not significantly different in the negative and positive modes. A range of leakage rates for longitudinal seams commonly used in the construction of metal ducts is presented in Table 5. Longitudinal seam leakage for unsealed or unwelded metal ducts is about 10 to 15% of total duct leakage.

Table 5 Unsealed Longitudinal Seam Leakage, Metal Ducts

Type of Duct/Seam	Leakage, cfm per ft Seam Length[a] Range	Average
Rectangular		
Pittsburgh lock	0.01 to 0.56	0.16
Button punch snaplock	0.01 to 0.16	0.08
Round		
Snaplock	0.04 to 0.14	0.11
Grooved	0.11 to 0.18	0.12

[a]Leakage rate is at 1 in. of water static pressure.

$$Q = C\Delta p_s^{\,N} \tag{42}$$

where

Q = duct leakage rate, cfm
C = constant reflecting area characteristics of leakage path
Δp_s = static pressure differential from duct interior to exterior, in. of water
N = exponent relating turbulent or laminar flow in leakage path

Analysis of the AISI/ASHRAE/SMACNA/TIMA data resulted in the categorization of duct systems into **leakage classes** C_L based on Equation (43), where the exponent N is assumed to be 0.65. A selected series of leakage classes based on Equation (43) is shown in Figure 14.

$$C_L = Q/\Delta p_s^{\,0.65} \tag{43}$$

where

Q = leakage rate, cfm/100 ft^2 (surface area)
C_L = leakage class, cfm per 100 ft duct surface at 1 in. of water static pressure

Table 6 is a forecast of the leakage class attainable for commonly used duct construction and sealing practices. Connections of ducts to grilles, diffusers, and registers are not represented in the test data. Leakage classes listed are for a specific duct type, not a system with a variety of duct types, access doors, and other duct-mounted equipment. The designer is responsible for assigning acceptable system leakage rates. It is recommended that this be accomplished by using Table 7 as a guideline to specify a ductwork leakage class or by specifying a duct seal level as recommended by Table 8. The designer should take into account attainable leakage rates by duct type and the fact that casings of volume-controlling air terminal units may leak 2 to 5% of their maximum flow. The effects of such leakage should be anticipated, if allowed, and the ductwork should not be expected to compensate for equipment leakage. When a system leakage class is specified by a designer, it is a performance specification that should not be compromised by prescriptive sealing. A portion of a system may exceed its leakage class if the aggregate

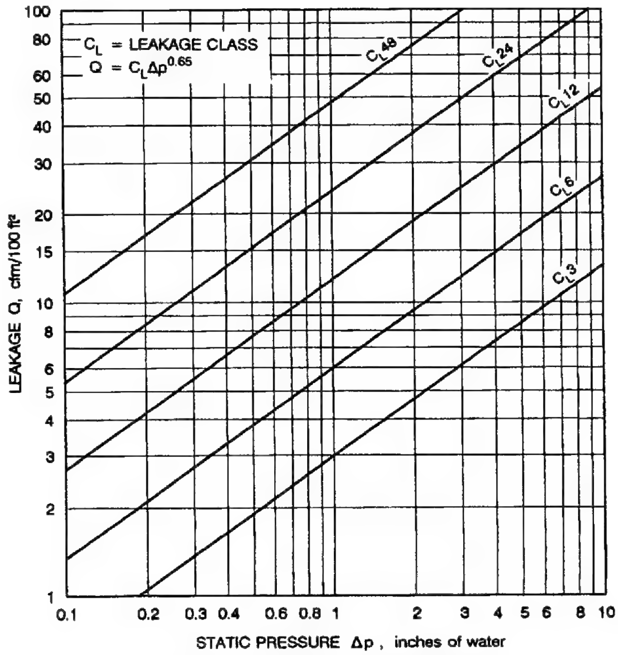

Fig. 14 Duct Leakage Classifications

system leakage meets the allowable rate. Table 9 can be used to estimate the system percent leakage based on the system design leakage class and system duct surface area. Table 9 is predicated on assessment at an average of upstream and downstream pressures because use of the highest pressure alone could indicate an artificially high rate. When several duct pressure classifications occur in a system, ductwork in each pressure class should be evaluated independently to arrive at an aggregate leakage for the system.

Leakage tests should be conducted in compliance with SMACNA's *HVAC Air Duct Leakage Test Manual* (1985) to verify the intent of the designer and the workmanship of the the installing contractor. Leakage tests used to confirm leakage class should be conducted at the pressure class for which the duct is constructed. Leakage testing is also addressed in ASHRAE *Standard* 90.1.

Pressure-sensitive tape should not be used as the primary sealant for sheet metal ducts designed to operate at static pressures in excess of 1 in. of water. UL *Standard* 181A rigid ducts may use UL *Standard* 181A listed pressure-sensitive tapes or other listed closure materials up to the pressure listing of the material. Soldered or

Table 6 Duct Leakage Classification[a]

Duct Type	Predicted Leakage Class C_L [Eq. (43)] Sealed[b,c]	Unsealed[c]
Metal (flexible excluded)		
Round and flat oval	3	30 (6 to 70)
Rectangular		
≤ 2 in. of water (both positive and negative pressures)	12	48 (12 to 110)
> 2 and ≤ 10 in. of water (both positive and negative pressures)	6	48 (12 to 110)
Flexible		
Metal, aluminum	8	30 (12 to 54)
Nonmetal	12	30 (4 to 54)
Fibrous glass		
Round	3	na
Rectangular	6	na

[a]The leakage classes listed in this table are averages based on tests conducted by AISI/SMACNA (1972), ASHRAE/SMACNA/TIMA (1985), and Swim and Griggs (1995).
[b]The leakage classes listed in the sealed category are based on the assumptions that for metal ducts, all transverse joints, seams, and openings in the duct wall are sealed at pressures over 3 in. of water, that transverse joints and longitudinal seams are sealed at 2 and 3 in. of water, and that transverse joints are sealed below 2 in. of water. Lower leakage classes are obtained by careful selection of joints and sealing methods.
[c]Leakage classes assigned anticipate about 25 joints per 100 linear feet of duct. For systems with a high fitting to straight duct ratio, greater leakage occurs in both the sealed and unsealed conditions.

Table 7 Recommended Ductwork Leakage Class by Duct Type

Duct Type	Leakage Class, cfm/100 ft² at 1 in. of water
Metal (flexible excluded)	
Round	3
Flat oval	3
Rectangular	6
Flexible	6
Fibrous glass	
Round	3
Rectangular	6

Table 8A Recommended Duct Seal Levels[a]

Duct Location	Supply ≤ 2 in. of water	Supply > 2 in. of water	Exhaust	Return
Outdoors	A	A	A	A
Unconditioned spaces	B	A	B	B
Conditioned spaces (concealed ductwork)	C	B	B	B
Conditioned spaces (exposed ductwork)				
Office-type spaces	A	A	B	B
Factory-type spaces	C	B	B	B

[a]See Table 8B for definition of seal level.

Table 8B Duct Seal Levels

Seal Level	Sealing Requirements[a]
A	All transverse joints, longitudinal seams, and duct wall penetrations
B	All transverse joints and longitudinal seams
C	Transverse joints only

[a]Transverse joints are connections of two duct or fitting elements oriented perpendicular to flow. Longitudinal seams are joints oriented in the direction of airflow. Duct wall penetrations are openings made by screws, non-self-sealing fasteners, pipe, tubing, rods, and wire. Round and flat oval spiral lock seams need not be sealed prior to assembly but may be coated after assembly to reduce leakage. All other connections are considered transverse joints, including but not limited to spin-ins, taps and other branch connections, access door frames, and duct connection to equipment.

Table 9 Leakage as Percentage of Airflow[a,b]

Leakage Class	System cfm per ft² Duct Surface	Static Pressure, in. of water 0.5	1	2	3	4	6
48	2	15	24	38	49	59	77
	2.5	12	19	30	39	47	62
	3	10	16	25	33	39	51
	4	7.7	12	19	25	30	38
	5	6.1	9.6	15	20	24	31
24	2	7.7	12	19	25	30	38
	2.5	6.1	9.6	15	20	24	31
	3	5.1	8.0	13	16	20	26
	4	3.8	6.0	9.4	12	15	19
	5	3.1	4.8	7.5	9.8	12	15
12	2	3.8	6	9.4	12	15	19
	2.5	3.1	4.8	7.5	9.8	12	15
	3	2.6	4.0	6.3	8.2	9.8	13
	4	1.9	3.0	4.7	6.1	7.4	9.6
	5	1.5	2.4	3.8	4.9	5.9	7.7
6	2	1.9	3	4.7	6.1	7.4	9.6
	2.5	1.5	2.4	3.8	4.9	5.9	7.7
	3	1.3	2.0	3.1	4.1	4.9	6.4
	4	1.0	1.5	2.4	3.1	3.7	4.8
	5	0.8	1.2	1.9	2.4	3.0	3.8
3	2	1.0	1.5	2.4	3.1	3.7	4.8
	2.5	0.8	1.2	1.9	2.4	3.0	3.8
	3	0.6	1.0	1.6	2.0	2.5	3.2
	4	0.5	0.8	1.3	1.6	2.0	2.6
	5	0.4	0.6	0.9	1.2	1.5	1.9

[a]Adapted with permission from HVAC *Air Duct Leakage Test Manual* (SMACNA 1985, Appendix A).
[b]Percentage applies to the airflow entering a section of duct operating at an assumed pressure equal to the average of the upstream and downstream pressures.
[c]The ratios in this column are typical of fan volumetric flow rate divided by total system surface. Portions of the systems may vary from these averages.

welded duct construction is necessary where sealants are not suitable. Sealants used on exterior ducts must be resistant to weather, temperature cycles, sunlight, and ozone.

Shaft and compartment pressure changes affect duct leakage and are important to health and safety in the design and operation of contaminant and smoke control systems. Shafts should not be used for supply, return, and/or exhaust air without accounting for their leakage rates. Airflow around buildings, building component leakage, and the distribution of inside and outside pressures over the height of a building, including shafts, are discussed in Chapters 15 and 24. Smoke management system design is covered in Chapter 48 of the 1995 *ASHRAE Handbook—Applications* and in Klote and Milke (1992).

System Component Design Velocities

Table 10 summarizes face velocities for HVAC components in built-up systems. In most cases, the values are abstracted from pertinent chapters in the 1996 *ASHRAE Handbook—Systems and Equipment*; final selection of the components should be based on data in these chapters or from manufacturers.

Louvers require special treatment since the blade shapes, angles, and spacing cause significant variations in louver-free area and performance (pressure drop and water penetration). Selection and analysis should be based on test data obtained in accordance with AMCA *Standard* 500. This standard presents both pressure drop and water penetration test procedures and a uniform method for calculating louver-free area. Tests are conducted on a 48 in. square louver with the frame mounted flush in the wall. For the water penetration tests, the rainfall is 4 in/h, no wind, and the water flow down the wall is 0.25 gpm per linear foot of louver width.

Use Figure 15 for preliminary sizing of air intake and exhaust louvers. For air quantities greater than 7000 cfm per louver, the air intake gross louver openings are based on 400 fpm; for exhaust louvers, 500 fpm is used for air quantities of 5000 cfm per louver and greater. For air quantities less than these, refer to Figure 15. These criteria are presented on a per louver basis (i.e., each louver in a bank of louvers) to include each louver frame. Representative production-run louvers were used in establishing Figure 15, and all data used in that analysis are based on AMCA standard tests. For louvers larger than 16 ft^2, the free areas are greater than 45%, while for louvers less than 16 ft^2, the free areas are less than 45%. Unless specific louver data are analyzed, no louver should have a face area less than 4 ft^2. If debris collection on the screen of an intake louver is possible, or if louvers are located at grade with adjacent pedestrian traffic, louver face velocity should not exceed 100 fpm.

Table 10 Typical Design Velocities for HVAC Components

Duct Element	Face Velocity, fpm
LOUVERS[a]	
Intake	
7000 cfm and greater	400
Less than 7000 cfm	See Figure 15
Exhaust	
5000 cfm and greater	500
Less than 5000 cfm	See Figure 15
FILTERS[b]	
Panel filters	
Viscous impingement	200 to 800
Dry-type, extended-surface	
Flat (low efficiency)	Duct velocity
Pleated media (intermediate efficiency)	Up to 750
HEPA	250
Renewable media filters	
Moving-curtain viscous impingement	500
Moving-curtain dry media	200
Electronic air cleaners	
Ionizing type	150 to 350
HEATING COILS[c]	
Steam and hot water	500 to 1000 200 min., 1500 max.
Electric	
Open wire	Refer to mfg. data
Finned tubular	Refer to mfg. data
DEHUMIDIFYING COILS[d]	400 to 500
AIR WASHERS[e]	
Spray type	300 to 600
Cell type	Refer to mfg. data
High-velocity spray type	1200 to 1800

[a]Based on assumptions presented in text.
[b]Abstracted from Chapter 24, 1996 *ASHRAE Handbook—Systems and Equipment*.
[c]Abstracted from Chapter 23, 1996 *ASHRAE Handbook—Systems and Equipment*.
[d]Abstracted from Chapter 21, 1996 *ASHRAE Handbook—Systems and Equipment*.
[e]Abstracted from Chapter 19, 1996 *ASHRAE Handbook—Systems and Equipment*.

System and Duct Noise

The major sources of noise from air-conditioning systems are diffusers, grilles, fans, ducts, fittings, and vibrations. Chapter 43 of the 1995 *ASHRAE Handbook—Applications* discusses sound control for each of these sources. Sound control for terminal devices consists of selecting devices that meet the design goal under all operating conditions and installing them properly so that no additional sound is generated. The sound power output of a fan is determined by the type of fan, airflow, and pressure. Sound control in the duct system requires proper duct layout, sizing, and provision for installing duct attenuators, if required. The noise generated by a system increases with both duct velocity and system pressure. Chapter 43 of the 1995 *ASHRAE Handbook—Applications* presents methods for calculating required sound attenuation.

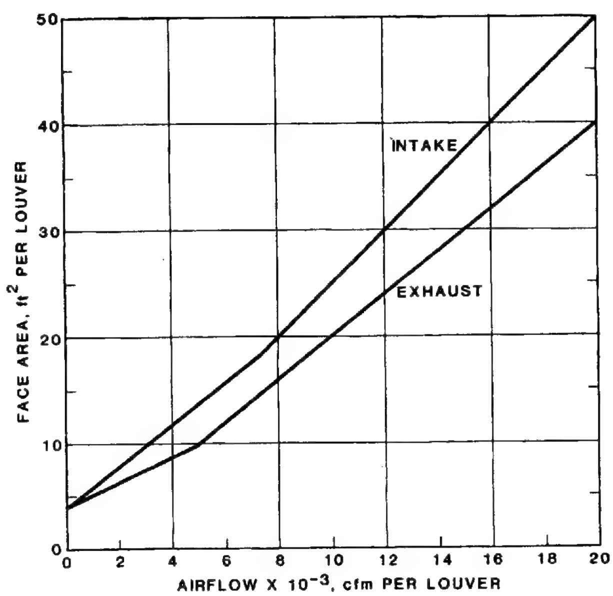

Parameters Used to Establish Figure	Intake Louver	Exhaust Louver
Minimum free area (48 in. square test section), %	45	45
Water penetration, oz/($ft^2 \cdot$0.25 h)	Negligible (less than 0.2)	na
Maximum static pressure drop, in. of water	0.15	0.25

Fig. 15 Criteria for Louver Sizing

Testing and Balancing

Each air duct system should be tested, adjusted, and balanced. Detailed procedures are given in Chapter 34 of the 1995 *ASHRAE Handbook—Applications*. To properly determine fan total (or static) pressure from field measurements taking into account fan system effect, refer to the section on Fan-System Interface. Equation (38) allows direct comparison of system resistance to design calculations and/or fan performance data. It is important that the system effect magnitudes be known prior to testing. If necessary, use Equation (18) to calculate fan static pressure knowing fan total pressure [Equation (38)]. For TAB calculation procedures of numerous fan/system configurations encountered in the field, refer to AMCA *Publication* 203 (AMCA 1990b).

DUCT DESIGN METHODS

Duct design methods for HVAC systems and for exhaust systems conveying vapors, gases, and smoke are the equal friction method, the static regain method, and the T-method. The section on Industrial Exhaust System Duct Design presents the design criteria and procedures for exhaust systems conveying particulates. Equal friction and static regain are nonoptimizing methods, while the T-method is a practical optimization method introduced by Tsal et al. (1988).

To ensure that system designs are acoustically acceptable, noise generation should be analyzed and sound attenuators and/or acoustically lined duct provided where necessary. Dampers must be installed throughout systems designed by equal friction, static regain, and the T-method because inaccuracies are introduced into these design methods by duct size round-off and the effect of close-coupled fittings on the total pressure loss calculations.

Equal Friction Method

In the equal friction method, ducts are sized for a constant pressure loss per unit length. The shaded area of the friction chart (Figure 9) is the suggested range of friction rate and air velocity. When energy cost is high and installed ductwork cost is low, a low friction rate design is more economical. For low energy cost and high duct cost, a higher friction rate is more economical. After initial sizing, calculate the total pressure loss for all duct sections, and then resize sections to balance pressure losses at each junction.

Static Regain Method

The objective of the static regain method is to obtain the same static pressure at diverging flow junctions by changing downstream duct sizes. This design objective can be developed by rearranging Equation (7a) and setting $p_{s,2}$ equal to $p_{s,1}$ (neglecting thermal gravity effect term). Thus,

$$p_{s,1} - p_{s,2} = \Delta p_{t,1\text{-}2} - \left[\frac{\rho V_1^2}{2g_c} - \frac{\rho V_2^2}{2g_c}\right] \tag{44}$$

and

$$\Delta p_{t,1\text{-}2} = \frac{\rho V_1^2}{2g_c} - \frac{\rho V_2^2}{2g_c} \tag{45}$$

where $\Delta p_{t,1\text{-}2}$ is the total pressure loss from upstream of junction 1 to upstream of junction 2, or the terminal of section 2. The immediate downstream duct size that satisfies Equation (45) is determined by iteration.

To start the design of a system, a maximum velocity is selected for the root section (duct section upstream and/or downstream of a fan). In Figure 17, section 6 is the root for the return air subsystem. Section 19 is the root for the supply air subsystem. The shaded area on the friction chart (Figure 9) is the suggested range of air velocity. When energy cost is high and installed ductwork cost is low, a lower initial velocity is more economical. For low energy cost and high duct cost, a higher velocity is more economical. All other sections, except terminal sections, are sized iteratively by Equation (45). In Figure 17, terminal sections are 1, 2, 4, 7, 8, 11, 12, 15, and 16. Knowing the terminal static pressure requirements, Equation (45) is used to calculate the duct size of terminal sections. If the terminal is an exit fitting rather than a register, diffuser, or terminal box, the static pressure at the exit of the terminal section is zero.

The classical static regain method (Carrier Corporation 1960, Chun-Lun 1983) is based on Equation (46), where R is the static pressure regain factor, and Δp_r is the static pressure regain between junctions.

$$\Delta p_r = R\left(\frac{\rho V_1^2}{2g_c} - \frac{\rho V_2^2}{2g_c}\right) \tag{46}$$

Typically R-values ranging from 0.5 to 0.95 have been used. Tsal and Behls (1988) show that this uncertainty exists because the splitting of mass at junctions and the dynamic (fitting) losses between junctions are ignored. The classical static regain method using an R-value should not be used because R is not predictable.

T-Method Optimization

T-method optimization (Tsal et al. 1988) is a dynamic programming procedure based on the tee-staging idea used by Bellman (1957), except that phase level vector tracing is eliminated by optimizing locally at each stage. This modification reduces the number of calculations but requires iteration.

Optimization Basis. The objective function, Equation (47), includes both initial system cost and the present worth of energy. Hours of operation, annual escalation and interest rates, and amortization period are also required for optimization.

$$E = E_p(\text{PWEF}) + E_s \tag{47}$$

where

E = present worth owning and operating cost
E_p = first year energy cost
E_s = initial cost
PWEF = present worth escalation factor (Smith 1968), dimensionless

Energy cost is determined by

$$E_p = Q_f\left[\frac{1.176 \times 10^4 (E_d + E_c T)}{\eta_f \eta_e}\right] P_t \tag{48}$$

where

Q_f = fan airflow rate, cfm
E_c = unit energy cost, cost/kWh
E_d = energy demand cost, cost/kW
T = system operating time, h/year
P_t = fan total pressure, in. of water
η_f = fan total efficiency, decimal
η_e = motor-drive efficiency, decimal

Energy cost depends on both applicable energy rates E_c and demand cost E_d. Since the difference in fan pressure between an optimized and a nonoptimized system is a small part of demand, it is usually neglected. Initial cost includes ducts and HVAC equipment, which is primarily the central handling unit. The cost of duct systems is given by the following equations:

Round $E_s = S_d \pi DL/12$ (49)

Rectangular $E_s = 2S_d(H + W)L/12$ (50)

where

S_d = unit ductwork cost/ft^2 (including material and labor)
H = duct height, in.
W = duct width, in.
L = duct length, ft

The cost of space required by ducts and equipment is another important factor of duct optimization. Including this cost reduces the size of ducts, thereby increasing energy consumption. Because the space available for ductwork is usually not used for anything else, its cost is ignored.

Both electrical energy rates and ductwork costs vary widely, by a factor of up to eight times for industrial users (DOE). Black iron rectangular ductwork can cost about 3.9 times that of spiral ductwork (Wendes 1989). Combining these ratios yields a factor of 30 to 1 based on locale and type of ductwork. Therefore, a great potential exists for reducing duct system life-cycle cost due to energy and ductwork cost variations.

The following constraints are necessary for duct optimization (Tsal and Adler 1987):

- *Continuity*. For each node, the flow in equals the flow out.
- *Pressure balancing*. The total pressure loss in each path must equal the fan total pressure; or, in effect, at any junction, the total pressure loss for all paths is the same.
- *Nominal duct size*. Ducts are constructed in discrete, nominal sizes. Each diameter of a round duct or height and width of a rectangular duct is rounded to the nearest increment, usually 1 or 2 in. If a lower nominal size is selected, the initial cost decreases, but the pressure loss increases and may exceed the fan pressure. If the higher nominal size is selected, the opposite is true—the initial cost increases, but the section pressure loss decreases. However, this lower pressure at one section may allow smaller ducts to be selected for sections that follow. Therefore, optimization must consider size rounding.
- *Air velocity restriction*. The maximum allowable velocity is an acoustic limitation (ductwork regenerated noise).
- *Construction restriction*. Architectural limits may restrict duct sizes. If air velocity or construction constraints are violated during an iteration, a duct size must be calculated. The pressure loss calculated for this preselected duct size is considered a fixed loss.

Calculation Procedure. The T-method comprises the following major procedures:

- *System condensing*. This procedure condenses a multiple-section duct system into a single imaginary duct section with identical hydraulic characteristics and the same owning cost as the entire system. By Equation (1.41) in Tsal et al. (1988), two or more converging or diverging sections and the common section at a junction can be replaced by one condensed section. By applying this equation from junction to junction in the direction to the root section (fan), the entire supply and return systems can be condensed into one section (a single resistance).
- *Fan selection*. From the condensed system, the ideal optimum fan total pressure P_t^{opt} is calculated and used to select a fan. If a fan with a different pressure is selected, its pressure P^{opt} is considered optimum.
- *System expansion*. The expansion process distributes the available fan pressure P^{opt} throughout the system. Unlike the condensing procedure, the expansion procedure starts at the root section and continues in the direction of the terminals.

Economic Analysis. Tsal et al. (1988) describe the calculation procedure and include an economic analysis of the T-method.

T-Method Simulation

T-method simulation, also developed by Tsal et al. (1990), determines the flow in each duct section of an existing system with a known operating fan performance curve. The simulation version of the T-method converges very efficiently. Usually three iterations are sufficient to obtain a solution with a high degree of accuracy.

Calculation procedure. The simulation version of the T-method includes the following major procedures:

- *System condensing*. This procedure condenses a branched tee system into a single imaginary duct section with identical hydraulic characteristics. Two or more converging or diverging sections and the common section at a junction can be replaced by one condensed section [by Equation (18) in Tsal et al. (1990)]. By applying this equation from junction to junction in the direction to the root section (fan), the entire system, including supply and return subsystems, can be condensed into one imaginary section (a single resistance).
- *Fan operating point*. This step determines the system flow and pressure by locating the intersection of the fan performance and system curves, where the system curve is represented by the imaginary section from the last step.
- *System expansion*. Knowing system flow and pressure, the previously condensed imaginary duct section is expanded into the original system with flow distributed in accordance with the ratio of pressure losses calculated in the system condensing step.

Simulation Applications. The need for duct system simulation appears in many HVAC problems. In addition to the following concerns that can be clarified by simulation, the T-method is an excellent design tool for simulating the flow distribution within a system with various modes of operation.

- Flow distribution in a variable air volume (VAV) system due to terminal box flow diversity
- Airflow redistribution due to HVAC system additions and/or modifications
- System airflow analysis for partially occupied buildings
- Necessity to replace fans and/or motors when retrofitting an air distribution system
- Multiple-fan system operating condition when one or more fans shut down
- Pressure differences between adjacent confined spaces within a nuclear facility when a design basis accident (DBA) occurs (Farajian et al. 1992)
- Smoke management system performance during a fire, when certain fire/smoke dampers close and others remain open

HVAC DUCT DESIGN PROCEDURES

The general procedure for HVAC system duct design is as follows:

1. Study the building plans, and arrange the supply and return outlets to provide proper distribution of air within each space. Adjust calculated air quantities for duct heat gains or losses and duct leakage. Also, adjust the supply, return, and/or exhaust air quantities to meet space pressurization requirements.
2. Select outlet sizes from manufacturers' data (see Chapter 31).
3. Sketch the duct system, connecting supply outlets and return intakes with the air-handling units/air conditioners. Space allocated for supply and return ducts often dictates system layout and ductwork shape. Use round ducts whenever feasible.
4. Divide the system into sections and number each section. A duct system should be divided at all points where flow, size, or shape changes. Assign fittings to the section toward the supply and return (or exhaust) terminals. The following examples are for the fittings identified for Example 6 (Figure 16), and system section numbers assigned (Figure 17). For converging flow fitting 3,

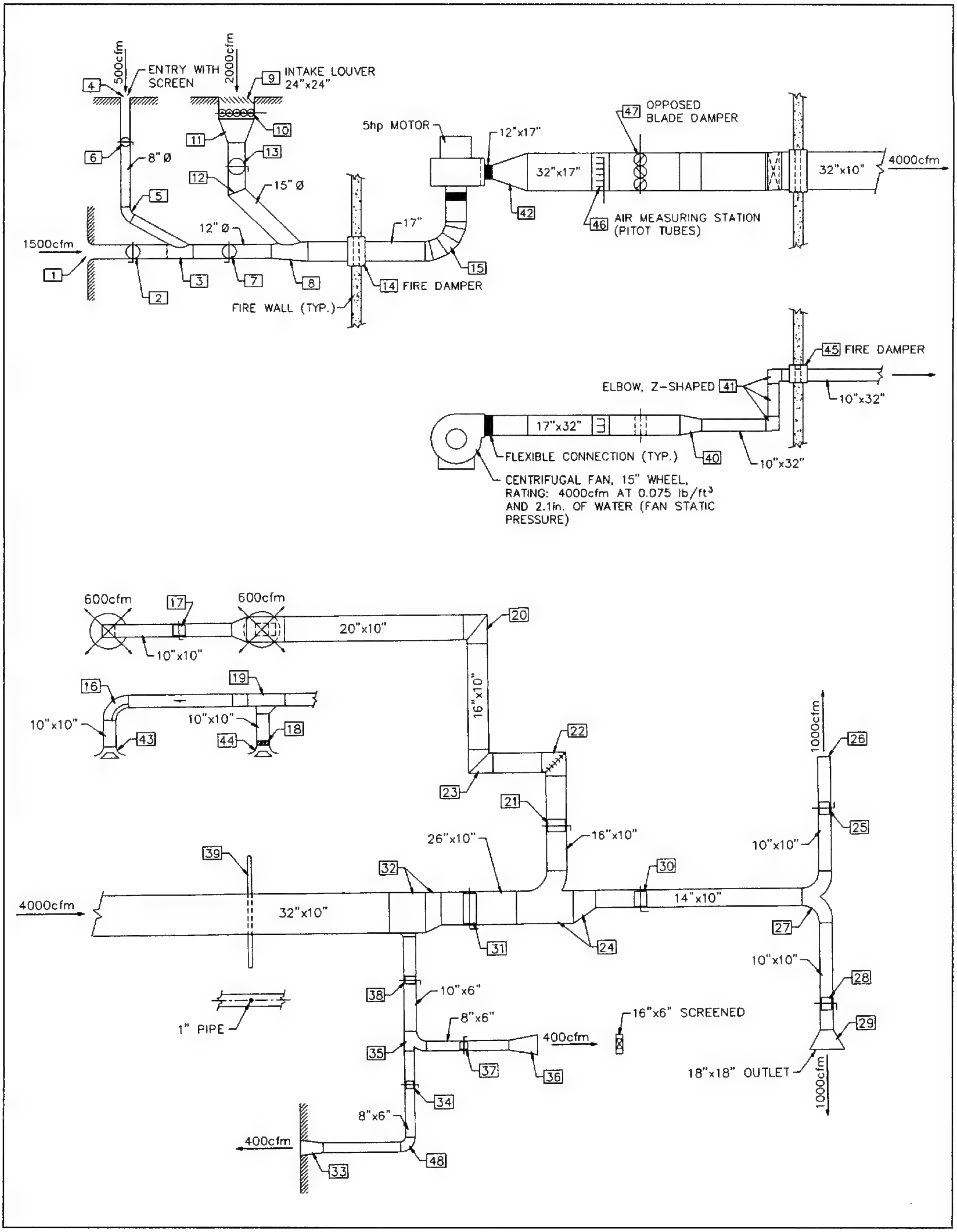

Fig. 16 Schematic for Example 8

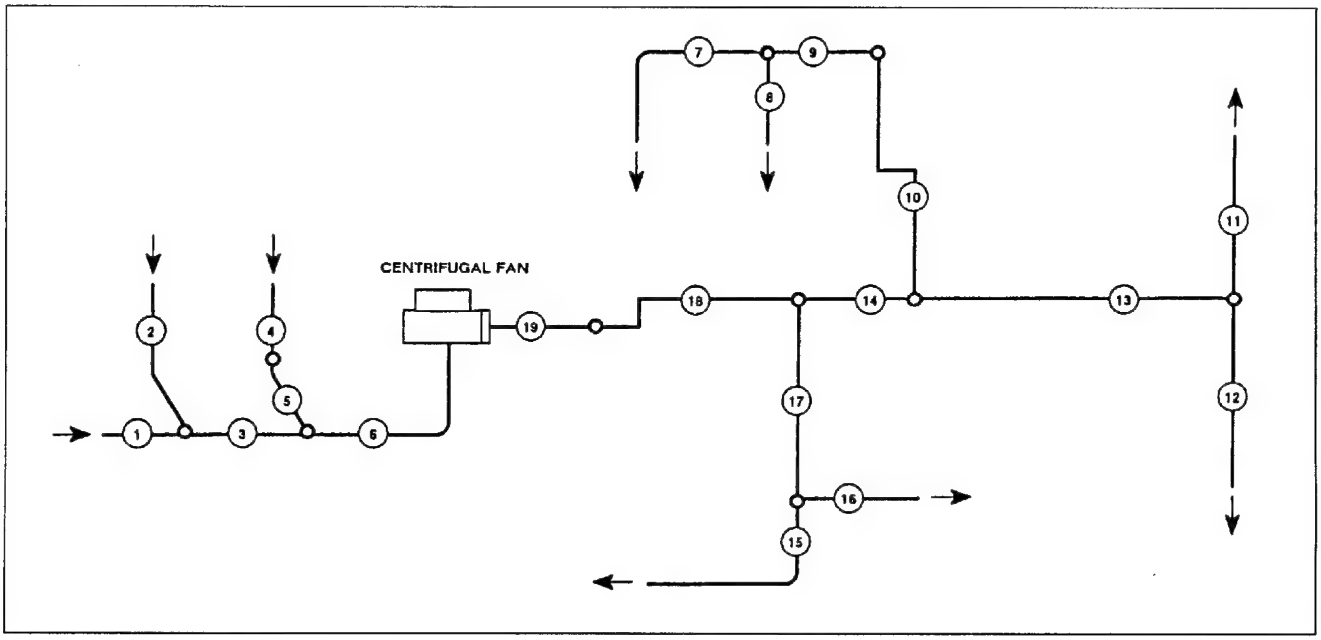

Fig. 17 System Schematic with Section Numbers for Example 8

assign the straight-through flow to section 1 (toward terminal 1), and the branch to section 2 (toward terminal 4). For diverging flow fitting 24, assign the straight-through flow to section 13 (toward terminals 26 and 29) and the branch to section 10 (toward terminals 43 and 44). For transition fitting 11, assign the fitting to upstream section 4 [toward terminal 9 (intake louver)]. For fitting 20, assign the unequal area elbow to downstream section 9 (toward diffusers 43 and 44). The fan outlet diffuser, fitting 42, is assigned to section 19 (again, toward the supply duct terminals).

5. Size ducts by the selected design method. Calculate system total pressure loss; then select the fan (refer to Chapter 18 of the 1996 *ASHRAE Handbook—Systems and Equipment*).
6. Lay out the system in detail. If duct routing and fittings vary significantly from the original design, recalculate the pressure losses. Reselect the fan if necessary.
7. Resize duct sections to approximately balance pressures at each junction.
8. Analyze the design for objectionable noise levels, and specify sound attenuators as necessary. Refer to the section on System and Duct Noise.

Example 8. For the system illustrated by Figures 16 and 17, size the ductwork by the equal friction method, and pressure balance the system by changing duct sizes (use 1 in. increments). Determine the system resistance and total pressure unbalance at the junctions. The airflow quantities are actual values adjusted for heat gains or losses, and ductwork is sealed (assume no leakage), galvanized steel ducts with transverse joints on 4 ft centers (ε = 0.0003 ft). Air is at standard conditions (0.075 lb_m/ft^3 density).

Because the primary purpose of Figure 16 is to illustrate calculation procedures, its duct layout is not typical of any real duct system. The layout includes fittings from the local loss coefficient tables, with emphasis on converging and diverging tees and various types of entries and discharges. The supply system is constructed of rectangular ductwork; the return system, round ductwork.

Solution: See Figure 17 for section numbers assigned to the system. The duct sections are sized within the suggested range of friction rate shown on the friction chart (Figure 9). Tables 11 and 12 give the total pressure loss calculations and the supporting summary of loss coefficients by sections. The straight duct friction factor and pressure loss

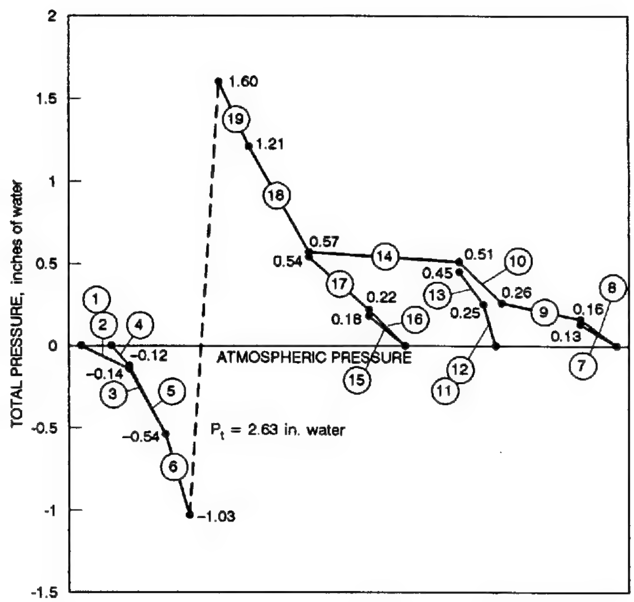

Fig. 18 Total Pressure Grade Line for Example 8

were calculated by Equations (19) and (20). The fitting loss coefficients are from the *Duct Fitting Database* (ASHRAE 1994). Loss coefficients were calculated automatically by the database program (not by manual interpolation). The pressure loss values in Table 11 for the diffusers (fittings 43 and 44), the louver (fitting 9), and the air-measuring station (fitting 46) are manufacturers' data.

The pressure unbalance at the junctions may be noted by referring to Figure 18, the total pressure grade line for the system. The system resistance P_t is 2.63 in. of water. Noise levels and the need for duct silencers were not evaluated. To calculate the fan static pressure, use Equation (18):

$$P_s = 2.63 - 0.50 = 2.1 \text{ in. of water}$$

where 0.50 in. of water is the fan outlet velocity pressure.

Table 11 Total Pressure Loss Calculations by Sections for Example 8

Duct Section[a]	Fitting No.[b]	Duct Element	Airflow, cfm	Duct Size (Equivalent Round)	Velocity, fpm	Velocity Pressure, in. of water	Duct Length,[c] ft	Summary of Fitting Loss Coefficients[d]	Duct Pressure Loss/100 ft,[e] in. of water	Total Pressure Loss, in. of water	Section Pressure Loss, in. of water
1	—	Duct	1500	12 in. ϕ	1910	—	15	—	0.40	0.06	
	—	Fittings	1500	—	1910	0.23	—	0.33	—	0.08	0.14
2	—	Duct	500	8 in. ϕ	1432	—	60	—	0.39	0.23	
	—	Fittings	500	—	1432	0.13	—	−0.71	—	−0.09	0.14
3	—	Duct	2000	12 in. ϕ	2546	—	20	—	0.67	0.13	
	—	Fittings	2000	—	2546	0.40	—	0.67	—	0.27	0.40
4	—	Duct	2000	24 in. × 24 in. (26.2)	500	—	5	—	0.01	0.00	
	—	Fittings	2000	—	500	0.02	—	1.11	—	0.02	
	9	Louver	2000	24 in. × 24 in.	—	—	—	—	—	0.10[f]	0.12
5	—	Duct	2000	15 in. ϕ	1630	—	55	—	0.23	0.13	
	—	Fittings	2000	—	1630	0.17	—	1.73	—	0.29	0.42
6	—	Duct	4000	17 in. ϕ	2538	—	30	—	0.45	0.14	
	—	Fittings	4000	—	2538	0.40	—	0.87	—	0.35	0.49
7	—	Duct	600	10 in. × 10 in. (10.9)	864	—	14	—	0.11	0.02	
	—	Fittings	600	—	864	0.05	—	0.26	—	0.01	
	43	Diffuser	600	10 in. × 10 in.	—	—	—	—	—	0.10[f]	0.13
8	—	Duct	600	10 in. × 10 in. (10.9)	864	—	4	—	0.11	0.00	
	—	Fittings	600	—	864	0.05	—	1.25	—	0.06	
	44	Diffuser	600	10 in. × 10 in.	—	—	—	—	—	0.10[f]	0.16
9	—	Duct	1200	20 in. × 10 in. (15.2)	864	—	25	—	0.08	0.02	
	—	Fittings	1200	—	864	0.05	—	1.67	—	0.08	0.10
10	—	Duct	1200	16 in. × 10 in. (13.7)	1080	—	45	—	0.13	0.06	
	—	Fittings	1200	—	1080	0.07	—	2.66	—	0.19	0.25
11	—	Duct	1000	10 in. × 10 in. (10.9)	1440	—	10	—	0.29	0.03	
	—	Fittings	1000	—	1440	0.13	—	1.68	—	0.22	0.25
12	—	Duct	1000	10 in. × 10 in. (10.9)	1440	—	22	—	0.29	0.06	
	—	Fittings	1000	—	1440	0.13	—	1.45	—	0.19	0.25
13	—	Duct	2000	14 in. × 10 in. (12.9)	2057	—	35	—	0.47	0.16	
	—	Fittings	2000	—	2057	0.26	—	0.16	—	0.04	0.20
14	—	Duct	3200	26 in. × 10 in. (17.1)	1772	—	15	—	0.27	0.04	
	—	Fittings	3200	—	1772	0.20	—	0.12	—	0.02	0.06
15	—	Duct	400	8 in. × 6 in. (7.6)	1200	—	40	—	0.32	0.13	
	—	Fittings	400	—	1200	0.09		0.58	—	0.05	0.18
16	—	Duct	400	8 in. × 6 in. (7.6)	1200	—	20	—	0.32	0.06	
	—	Fittings	400	—	1200	0.09	—	1.74	—	0.16	0.22
17	—	Duct	800	10 in. × 6 in. (8.4)	1920	—	22	—	0.70	0.15	
	—	Fittings	800	—	1920	0.23	—	0.76	—	0.17	0.32
18	—	Duct	4000	32 in. × 10 in. (18.8)	1800	—	23	—	0.25	0.06	
	—	Fittings	4000	—	1800	0.20		2.91	—	0.58	0.64
19	—	Duct	4000	32 in. × 17 in. (25.2)	1059	—	12	—	0.06	0.01	
	—	Fittings	4000	—	1059	0.07	—	4.71	—	0.33	
	46	Air-measuring station	4000	—	—	—	—	—	—	0.05[f]	0.39

[a]See Figure 17.
[b]See Figure 16.
[c]Duct lengths are to fitting centerlines.
[d]See Table 12.
[e]Duct pressure based on a 0.0003 ft absolute roughness factor.
[f]Pressure drop based on manufacturers' data.

Table 12 Loss Coefficient Summary by Sections for Example 8

Duct Section	Fitting Number	Type of Fitting	ASHRAE Fitting No.[a]	Parameters	Loss Coefficient
1	1	Entry	ED1-3	$r/D = 0.2$	0.03
	2	Damper	CD9-1	$\theta = 0°$	0.19
	3	Wye (30°), main	ED5-1	$A_s/A_c = 1.0$, $A_b/A_c = 0.444$, $Q_s/Q_c = 0.75$	0.11 (C_s)
	Summation of Section 1 loss coefficients				0.33
2	4	Entry	ED1-1	$L = 0$, $t = 0.064$ in. (16 gage)	0.50
	4	Screen	CD6-1	$n = 0.70$, $A_1/A_o = 1$	0.58
	5	Elbow	CD3-6	60°, $r/D = 1.5$, pleated	0.27
	6	Damper	CD9-1	$\theta = 0°$	0.19
	3	Wye (30°), branch	ED5-1	$A_s/A_c = 1.0$, $A_b/A_c = 0.444$, $Q_b/Q_c = 0.25$	−2.25 (C_b)
	Summation of Section 2 loss coefficients				−0.71
3	7	Damper	CD9-1	$\theta = 0°$	0.19
	8	Wye (45°), main	ED5-2	$A_s/A_c = 0.498$, $A_b/A_c = 0.779$, $Q_s/Q_c = 0.5$	0.48 (C_s)
	Summation of Section 3 loss coefficients				0.67

Table 12 Loss Coefficient Summary by Sections for Example 8 (*Concluded*)

Duct Section	Fitting Number	Type of Fitting	ASHRAE Fitting No.[a]	Parameters	Loss Coefficient
4	10	Damper	CR9-4	$\theta = 0°$, 5 blades (opposed), $L/R = 1.25$	0.52
	11	Transition	ER4-3	$L = 30$ in., $A_o/A_1 = 3.26$, $\theta = 17°$	0.59
		Summation of Section 4 loss coefficients			1.11
5	12	Elbow	CD3-17	45°, mitered	0.34
	13	Damper	CD9-1	$\theta = 0°$	0.19
	8	Wye (45°), branch	ED5-2	$Q_b/Q_c = 0.5$, $A_s/A_c = 0.498$, $A_b/A_c = 0.779$	1.20 (C_b)
		Summation of Section 5 loss coefficients			1.73
6	14	Fire damper	CD9-3	Curtain type, Type C	0.12
	15	Elbow	CD3-9	90°, 5 gore, $r/D = 1.5$	0.15
	—	Fan and system interaction	ED7-2	90° elbow, 5 gore, $r/D = 1.5$, $L = 34$ in.	0.60
		Summation of Section 6 loss coefficients			0.87
7	16	Elbow	CR3-3	90°, $r/W = 0.70$, 1 splitter vane	0.14
	17	Damper	CR9-1	$\theta = 0°$, $H/W = 1.0$	0.08
	19	Tee, main	SR5-13	$Q_s/Q_c = 0.5$, $A_s/A_c = 0.50$	0.04 (C_s)
		Summation of Section 7 loss coefficients			0.26
8	19	Tee, branch	SR5-13	$Q_b/Q_c = 0.5$, $A_b/A_c = 0.50$	0.73 (C_b)
	18	Damper	CR9-4	$\theta = 0°$, 3 blades (opposed), $L/R = 0.75$	0.52
		Summation of Section 8 loss coefficients			1.25
9	20	Elbow	SR3-1	90°, mitered, $H/W_1 = 0.625$, $W_o/W_1 = 1.25$	1.67
		Summation of Section 9 loss coefficients			1.67
10	21	Damper	CR9-1	$\theta = 0°$, $H/W = 0.625$	0.08
	22	Elbow	CR3-10	90°, single-thickness vanes, design 2	0.12
	23	Elbow	CR3-6	$\theta = 90°$, mitered, $H/W = 0.625$	1.25
	24	Tee, branch	SR5-1	$r/W_b = 1.0$, $Q_b/Q_c = 0.375$, $A_s/A_c = 0.538$, $A_b/A_c = 0.615$	1.21 (C_b)
		Summation of Section 10 loss coefficients			2.66
11	25	Damper	CR9-1	$\theta = 0°$, $H/W = 1.0$	0.08
	26	Exit	SR2-1	$H/W = 1.0$, Re = 122,500	1.00
	27	Wye, dovetail	SR5-14	$r/W_c = 1.5$, $Q_{b1}/Q_c = 0.5$, $A_{b1}/A_c = 0.714$	0.60 (C_b)
		Summation of Section 11 loss coefficients			1.68
12	28	Damper	CR9-1	$\theta = 0°$, $H/W = 1.0$	0.08
	29	Exit	SR2-5	$\theta = 19°$, $A_1/A_o = 3.24$, Re = 130,000	0.77
	27	Wye, dovetail	SR5-14	$r/W_c = 1.5$, $Q_{b2}/Q_c = 0.5$, $A_{b2}/A_c = 0.714$	0.60 (C_b)
		Summation of Section 12 loss coefficients			1.45
13	30	Damper	CR9-1	$\theta = 0°$, $H/W = 0.71$	0.08
	24	Tee, main	SR5-1	$r/W_b = 1.0$, $Q_s/Q_c = 0.625$, $A_s/A_c = 0.538$, $A_b/A_c = 0.615$	0.08 (C_s)
		Summation of Section 13 loss coefficients			0.16
14	31	Damper	CR9-1	$\theta = 0°$, $H/W = 0.38$	0.08
	32	Tee, main	SR5-13	$Q_s/Q_c = 0.8$, $A_s/A_c = 0.813$	0.04 (C_s)
		Summation of Section 14 loss coefficients			0.12
15	48	Elbow	CR3-1	$\theta = 90°$, $r/W = 1.5$, $H/W = 0.75$	0.19
	33	Exit	SR2-6	$L = 18$ in., $D_h = 6.86$	0.28
	34	Damper	CR9-1	$\theta = 0°$, $H/W = 0.75$	0.08
	35	Tee, main	SR5-1	$r/W_b = 1.0$, $Q_s/Q_c = 0.5$, $A_s/A_c = 0.80$, $A_b/A_c = 0.80$	0.03 (C_s)
		Summation of Section 15 loss coefficients			0.58
16	36	Exit	SR2-3	$\theta = 20°$, $A_1/A_o = 2.0$, Re = 70,000	0.63
	36	Screen	CR6-1	$n = 0.8$, $A_1/A_o = 2.0$	0.08
	37	Damper	CR9-1	$\theta = 0°$, $H/W = 0.75$	0.08
	35	Tee, branch	SR5-1	$r/W_b = 1.0$, $Q_b/Q_c = 0.5$, $A_s/A_c = 0.80$, $A_b/A_c = 0.80$	0.95 (C_b)
		Summation of Section 16 loss coefficients			1.74
17	38	Damper	CR9-1	$\theta = 0°$, $H/W = 0.6$	0.08
	32	Tee, branch	SR5-13	$Q_b/Q_c = 0.2$, $A_b/A_c = 0.187$	0.68 (C_b)
		Summation of Section 17 loss coefficients			0.76
18	39	Obstruction, pipe	CR6-4	Re = 15,000, $y = 0$, $d = 1$ in., $S_m/A_o = 0.1$, $y/H = 0$	0.17
	40	Transition	SR4-1	$\theta = 22°$, $A_o/A_1 = 0.588$, $L = 18$ in.	0.04
	41	Elbows, Z-shaped	CR3-17	$L = 42$ in., $L/W = 4.2$, $H/W = 3.2$, Re = 240,000	2.51
	45	Fire damper	CR9-6	Curtain type, Type B	0.19
		Summation of Section 18 loss coefficients			2.91
19	42	Diffuser, fan	SR7-17	$\theta_1 = 28°$, $L = 40$ in., $A_o/A_1 = 2.67$, $C_1 = 0.59$	4.19 (C_o)
	47	Damper	CR9-4	$\theta = 0°$, 8 blades (opposed), $L/R = 1.39$	0.52
		Summation of Section 19 loss coefficients			4.71

[a] *Duct Fitting Database* (ASHRAE 1994) data for fittings reprinted in the section on Fitting Loss Coefficients.

INDUSTRIAL EXHAUST SYSTEM DUCT DESIGN

Chapter 26 of the 1995 *ASHRAE Handbook—Applications* discusses design criteria, including hood design, for industrial exhaust systems. Exhaust systems conveying vapors, gases, and smoke can be designed by equal friction, static regain, or T-method. Systems conveying particulates are designed by the constant velocity method at duct velocities adequate to convey particles to the system air cleaner. For contaminant transport velocities, see Table 2 in Chapter 26 of the 1995 *ASHRAE Handbook—Applications*.

Two pressure-balancing methods can be considered when designing industrial exhaust systems. One method uses balancing devices (e.g., dampers, blast gates) to obtain design airflow through each hood. The other approach balances systems by adding resistance to ductwork sections (i.e., changing duct size, selecting different fittings, and increasing airflow). This self-balancing method is preferred, especially for systems conveying abrasive materials. Where potentially explosive or radioactive materials are conveyed, the prebalanced system is mandatory because contaminants could accumulate at the balancing devices. To balance systems by increasing airflow, use Equation (51), which assumes that all ductwork has the same diameter and that fitting loss coefficients, including main and branch tee coefficients, are constant.

$$Q_c = Q_d(P_h/P_l)^{0.5} \tag{51}$$

where

Q_c = airflow rate required to increase P_l to P_h, cfm
Q_d = total airflow rate through low-resistance duct run, cfm
P_h = absolute value of pressure loss in high-resistance ductwork section(s), in. of water
P_l = absolute value of pressure loss in low-resistance ductwork section(s), in. of water

For systems conveying particulates, use elbows with a large centerline radius-to-diameter ratio (r/D), greater than 1.5 whenever possible. If r/D is 1.5 or less, abrasion in dust-handling systems can reduce the life of elbows. Elbows are often made of seven or more gores, especially in large diameters. For converging flow fittings, a 30° entry angle is recommended to minimize energy losses and abrasion in dust-handling systems. For the entry loss coefficients of hoods and equipment for specific operations, refer to Chapter 26 of the 1995 *ASHRAE Handbook—Applications* and to ACGIH (1995).

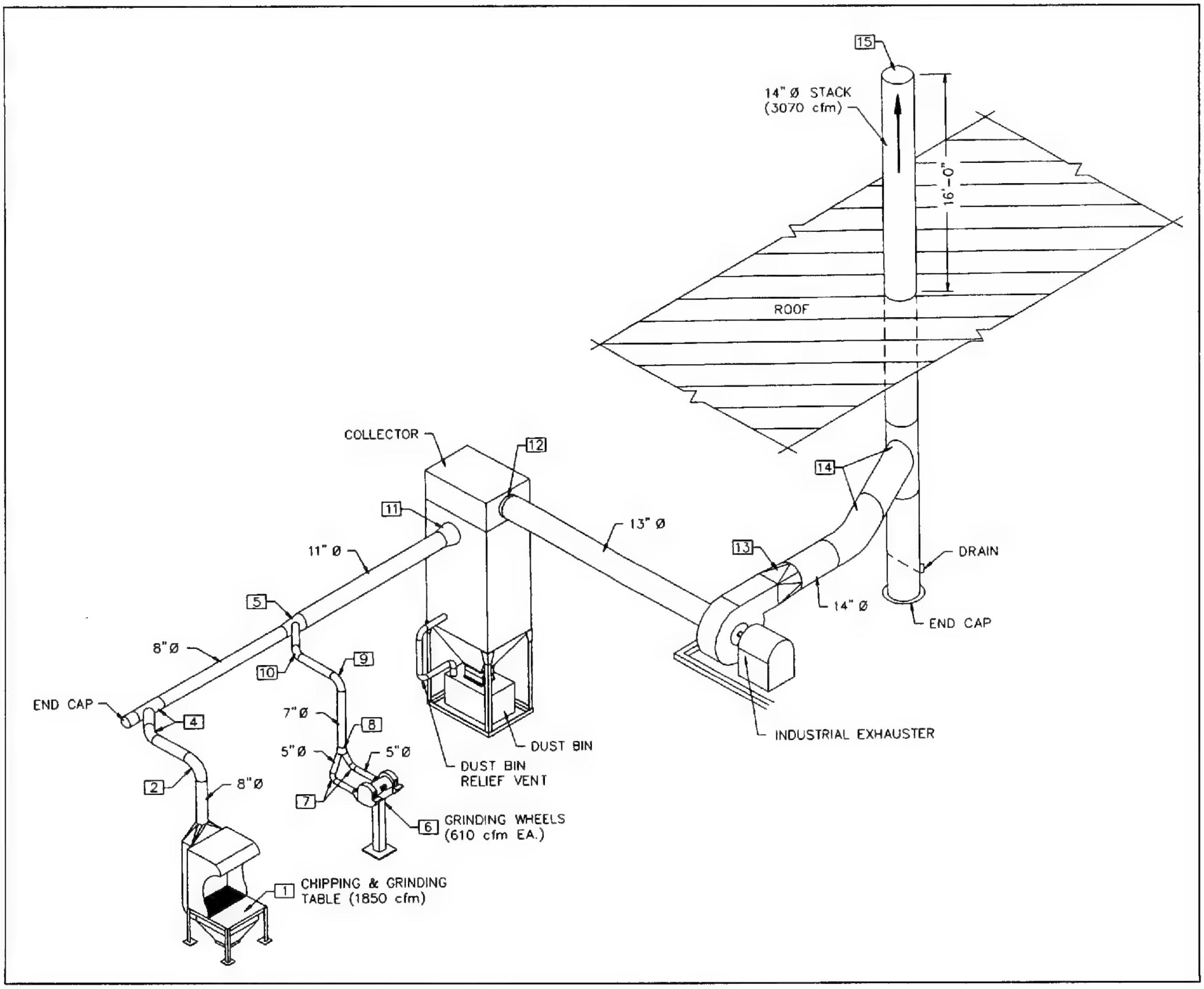

Fig. 19 Metalworking Exhaust System for Example 9

Example 9. For the metalworking exhaust system in Figures 19 and 20, size the ductwork and calculate the fan static pressure requirement for an industrial exhaust designed to convey granular materials. Pressure balance the system by changing duct sizes and adjusting airflow rates. The minimum particulate transport velocity for the chipping and grinding table ducts (sections 1 and 5, Figure 20) is 4000 fpm. For the ducts associated with the grinder wheels (sections 2, 3, 4, and 5), the minimum duct velocity is 4500 fpm. Ductwork is galvanized steel, with the absolute roughness being 0.0003 ft. Assume that air is standard and that duct and fittings are available in the following sizes: 3 in. through 9.5 in. diameters in 0.5 in. increments, 10 in. through 37 in. diameters in 1 in. diameter increments, and 38 in. through 90 in. diameters in 2 in. diameter increments.

The building is one story, and the design wind velocity is 20 mph. For the stack, use Design J shown in Figure 13 in Chapter 15 for complete rain protection. The stack height, determined by calculations from Chapter 15, is 16 ft above the roof. This stack height is based on minimized stack downwash; therefore, the stack discharge velocity must exceed 1.5 times the design wind velocity.

Solution: For the contaminated ducts upstream of the collector, initial duct sizes and transport velocities are summarized below. The 4474 fpm velocity in sections 2 and 3 is acceptable because the transport velocity is not significantly lower than 4500 fpm. For the next available duct size (4.5 in. diameter), the duct velocity is 5523 fpm, significantly higher than 4500 fpm.

Duct Section	Design Airflow, cfm	Transport Velocity, fpm	Duct Diameter, in.	Duct Velocity, fpm
1	1800	4000	9	4074
2,3	610 each	4500	5	4474
4	1220	4500	7	4565
5	3020	4500	11	4576

The following tabulation summarizes design calculations up through the junction after sections 1 and 4.

Design No.	D_1, in.	Δp_1, in. of water	Δp_{2+4}, in. of water	Imbalance, $\Delta p_1 - \Delta p_{2+4}$
1	9	1.46	3.09	−1.63
2	8.5	2.00	3.08	−1.08
3	8	2.79	3.00	−0.21
4	7.5	3.92	2.88	+1.04

Q_1 = 1800 cfm
Q_2 = 610 cfm; D_2 = 5 in. dia.
Q_3 = 610 cfm; D_3 = 5 in. dia.
Q_4 = 1220 cfm; D_4 = 7 in. dia.

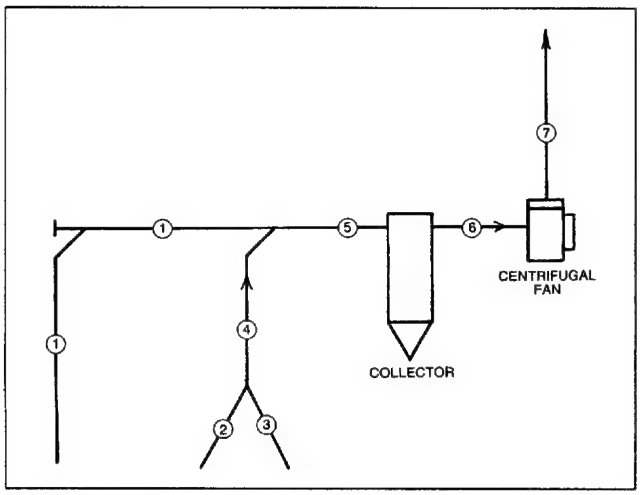

Fig. 20 System Schematic with Section Numbers for Example 9

For the initial design, Design 1, the imbalance between section 1 and section 2 (or 3) is 1.63 in. of water, with section 1 requiring additional resistance. Decreasing section 1 duct diameter by 0.5 in. increments results in the least imbalance, 0.21 in. of water, when the duct diameter is 8 in. (Design 3). Because section 1 requires additional resistance, estimate the new airflow rate using Equation (51):

$$Q_{c,1} = (1800)(3.00/2.79)^{0.5} = 1870 \text{ cfm}$$

At 1870 cfm flow in section 1, 0.13 in. of water imbalance remains at the junction of sections 1 and 4. By trial-and-error solution, balance is attained when the flow in section 1 is 1850 cfm. The duct between the collector and the fan inlet is 13 in. round to match the fan inlet (12.75 in. diameter). To minimize downwash, the stack discharge velocity must exceed 2640 fpm, 1.5 times the design wind velocity (20 mph) as stated in the problem definition. Therefore, the stack is 14 in. round, and the stack discharge velocity is 2872 fpm.

Table 13 summarizes the system losses by sections. The straight duct friction factor and pressure loss were calculated by Equations (19) and (20). Table 14 lists fitting loss coefficients and input parameters necessary to determine the loss coefficients. The fitting loss coefficients are from the *Duct Fitting Database* (ASHRAE 1994). The fitting loss coefficient tables are included in the section on Fitting Loss Coefficients for illustration but can not be obtained exactly by manual interpolation since the coefficients were calculated by the duct fitting database algorithms (more significant figures). For a pressure grade line of the system, see Figure 21. The fan total pressure, calculated by Equation (16), is 7.89 in. of water. To calculate the fan static pressure, use Equation (18):

$$P_s = 7.89 - 0.81 = 7.1 \text{ in. of water}$$

where 0.81 in. of water is the fan outlet velocity pressure. The fan airflow rate is 3070 cfm, and its outlet area is 0.853 ft^3 (10.125 in. by 12.125 in.). Therefore, the fan outlet velocity is 3600 fpm.

The hood suction for the chipping and grinding table hood is 2.2 in. of water, calculated by Equation (19) from Chapter 26 of the 1995 *ASHRAE Handbook—Applications* [$HS = (1 + 0.25)(1.74) = 2.2$ in. of water, where 0.25 is the hood entry loss coefficient C_o, and 1.74 is the duct velocity pressure P_v a few diameters downstream from the hood]. Similarly, the hood suction for each of the grinder wheels is 1.7 in. of water:

$$HS_{2,3} = (1 + 0.4)(1.24) = 1.7 \text{ in. of water}$$

where 0.4 is the hood entry loss coefficient, and 1.24 in. of water is the duct velocity pressure.

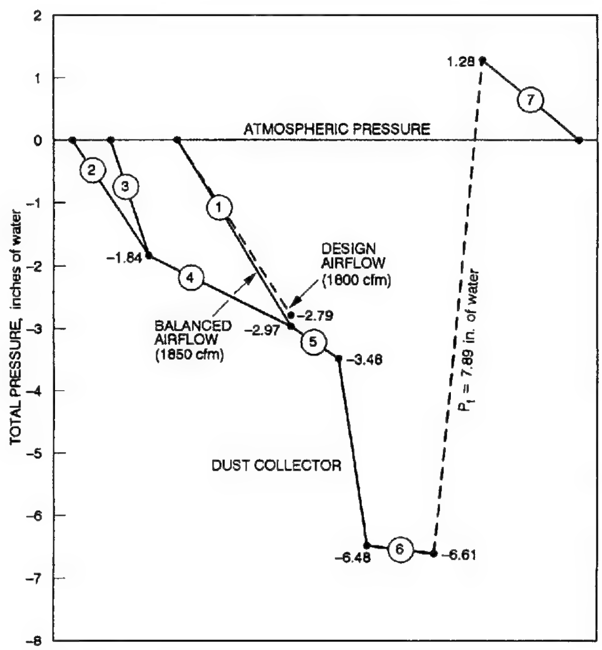

Fig. 21 Total Pressure Grade Line for Example 9

Table 13 Total Pressure Loss Calculations by Sections for Example 9

Duct Section[a]	Duct Element	Airflow, cfm	Duct Size	Velocity, fpm	Velocity Pressure, in. of water	Duct Length,[b] ft	Summary of Fitting Loss Coefficients[c]	Duct Pressure Loss/100 ft, in. of water[d]	Total Pressure Loss, in. of water	Section Pressure Loss, in. of water
1	Duct	1850	8 in. ϕ	5300	—	22.5	—	4.63	1.04	
	Fittings	1850		5300	1.75	—	1.10	—	1.93	2.97
2,3	Duct	610	5 in. ϕ	4474	—	9	—	5.94	0.53	
	Fittings	610		4474	1.24	—	1.06	—	1.31	1.84
4	Duct	1220	7 in. ϕ	4565	—	11.5	—	4.08	0.47	
	Fittings	1220		4565	1.30	—	0.51	—	0.66	1.13
5	Duct	3070	11 in. ϕ	4652	—	8.5	—	2.44	0.21	
	Fittings	3070		4652	1.35	—	0.22	—	0.30	0.51
—	Collector,[e] fabric	3070	—	—	—	—	—	—	3.0	3.0
6	Duct	3070	13 in. ϕ	3331	—	12	—	1.05	0.13	
	Fittings	3070		3331	0.69	—	0.00	—	0.00	0.13
7	Duct	3070	14 in. ϕ	2872	—	29	—	0.72	0.21	
	Fittings	3070		2872	0.51	—	2.09	—	1.07	1.28

[a]See Figure 20.
[b]Duct lengths are to fitting centerlines.
[c]See Table 14.
[d]Duct pressure based on a 0.0003 ft absolute roughness factor.
[e]Collector manufacturers set the fabric bag cleaning mechanism to actuate at a pressure difference of 3.0 in. of water between the inlet and outlet plenums. The pressure difference across the clean media is approximately 1.5 in. of water.

Table 14 Loss Coefficient Summary by Sections for Example 9

Duct Section	Fitting Number	Type of Fitting	ASHRAE Fitting No.[a]	Parameters	Loss Coefficient
1	1	Hood[b]	—	Hood face area: 3 ft by 4 ft	0.25
	2	Elbow	CD3-10	90°, 7 gore, $r/D = 2.5$	0.11
	4	Capped wye (45°), with 45° elbow	ED5-6	$A_b/A_c = 1$	0.64 (C_b)
	5	Wye (30°), main	ED5-1	$Q_s/Q_c = 0.60$, $A_s/A_c = 0.529$, $A_b/A_c = 0.405$	0.10 (C_s)
Summation of Section 1 loss coefficients					1.10
2,3	6	Hood[c]	—	Type hood: For double wheels, dia. = 22 in. each, wheel width = 4 in. each; type takeoff: tapered	0.40
	7	Elbow	CD3-12	90°, 3 gore, $r/D = 1.5$	0.34
	8	Symmetrical wye (60°)	ED5-9	$Q_b/Q_c = 0.5$, $A_b/A_c = 0.51$	0.32 (C_b)
Summation of Sections 2 and 3 loss coefficients					1.06
4	9	Elbow	CD3-10	90°, 7 gore, $r/D = 2.5$	0.11
	10	Elbow	CD3-13	60°, 3 gore, $r/D = 1.5$	0.19
	5	Wye (30°), branch	ED5-1	$Q_b/Q_c = 0.40$, $A_s/A_c = 0.529$, $A_b/A_c = 0.405$	0.21 (C_b)
Summation of Section 4 loss coefficients					0.51
5	11	Exit, conical diffuser to collector	ED2-1	$L = 24$ in., $L/D_o = 2.18$, $A_1/A_o \approx 16$	0.22
Summation of Section 5 loss coefficients					0.22
6	12	Entry, bellmouth from collector	ER2-1	$r/D_1 = 0.20$	0.00 (C_1)
Summation of Section 6 loss coefficients					0.00
7	13	Diffuser, fan outlet[d]	SR7-17	Fan outlet size: 10.125 in. by 12.125 in., $A_o/A_1 = 1.596$ (assume 14 in. by 14 in. outlet rather than 16 in. round), $L = 18$ in.	0.45 (C_o)
	14	Capped wye (45°), with 45° elbow	ED5-6	$A_b/A_c = 1$	0.64 (C_b)
	15	Stackhead	SD2-6	$D_e/D = 1$	1.0
Summation of Section 7 loss coefficients					2.09

[a]*Duct Fitting Database* (ASHRAE 1994) data for fittings reprinted in the section on Fitting Loss Coefficients.
[b]From *Industrial Ventilation* (ACGIH 1995, Figure VS-80-19).
[c]From *Industrial Ventilation* (ACGIH 1995, Figure VS-80-11).
[d]Fan specified: Industrial exhauster for granular materials: 21 in. wheel diameter, 12.75 in. inlet diameter, 10.125 in. by 12.125 in. outlet, 7.5 hp motor.

REFERENCES

ACGIH. 1995. *Industrial ventilation: A manual of recommended practice*, 22nd ed. American Conference of Governmental Industrial Hygienists, Lansing, MI.

AISI/SMACNA. 1972. Measurement and analysis of leakage rates from seams and joints of air handling systems.

Altshul, A.D., L.C. Zhivotovckiy, and L.P. Ivanov. 1987. *Hydraulics and aerodynamics*. Stroisdat Publishing House, Moscow.

AMCA. 1989. Test methods for louvers, dampers and shutters. *Standard* 500. Air Movement and Control Association, Arlington Heights, IL.

AMCA. 1990a. Fans and systems. *Publication* 201.

AMCA. 1990b. Field performance measurement of fan systems. *Publication* 203.

ASHRAE. 1985. Laboratory methods of testing fans for rating. ANSI/ASHRAE *Standard* 51-1985. Also AMCA *Standard* 210-85.

ASHRAE. 1989. Energy efficient design of new buildings except low-rise residential buildings. ASHRAE/IESNA *Standard* 90.1-1989.

ASHRAE. 1993. Energy-efficient design of new low-rise residential buildings. ASHRAE *Standard* 90.2-1993.
ASHRAE. 1994. *Duct fitting database*.
ASHRAE. 1995. Energy conservation in existing buildings. ASHRAE/IESNA *Standard* 100-1995. Addendum 1-1996.
ASHRAE/SMACNA/TIMA. 1985. Investigation of duct leakage. ASHRAE *Research Project* 308.
Behls, H.F. 1971. Computerized calculation of duct friction. *Building Science Series* 39, p. 363. National Institute of Standards and Technology, Gaithersburg, MD.
Bellman, R.E. 1957. *Dynamic programming*. Princeton University Press, New York.
Brown, R.B. 1973. Experimental determinations of fan system effect factors. In *Fans and systems*, ASHRAE Symposium Bulletin LO-73-1, Louisville, KY (June).
Carrier Corporation. 1960. Air duct design. Chapter 2 in *System design manual*, Part 2: Air distribution. pp.17-63. Syracuse, NY.
Chun-Lun, S. 1983. Simplified static-regain duct design procedure. *ASHRAE Transactions* 89(2A):78.
Clarke, M.S., J.T. Barnhart, F.J. Bubsey, and E. Neitzel. 1978. The effects of system connections on fan performance. *ASHRAE Transactions* 84(2): 227-63.
Colebrook, C.F. 1938-39. Turbulent flow in pipes, with particular reference to the transition region between the smooth and rough pipe laws. *Journal of the Institution of Civil Engineers* 11:133. London.
DOE. *Electrical sales and revenue*, latest edition. Department of Energy, Washington, D.C. (To purchase, call Energy Information Administration 202-512-1800.)
Farajian, T., G. Grewal, and R.J. Tsal. 1992. Post-accident air leakage analysis in a nuclear facility via T-method airflow simulation. 22nd DOE/NRC Nuclear Air Cleaning and Treatment Conference, Denver, CO, October.
Farquhar, H.F. 1973. System effect values for fans. In *Fans and systems*, ASHRAE Symposium Bulletin LO-73-1, Louisville, KY (June).
Griggs, E.I. and F. Khodabakhsh-Sharifabad. 1992. Flow characteristics in rectangular ducts. *ASHRAE Transactions* 98(1).
Griggs, E.I., W.B. Swim, and G.H. Henderson. 1987. Resistance to flow of round galvanized ducts. *ASHRAE Transactions* 93(1):3-16.
Heyt, J.W. and M.J. Diaz. 1975. Pressure drop in flat-oval spiral air duct. *ASHRAE Transactions* 81(2):221-32.
Huebscher, R.G. 1948. Friction equivalents for round, square and rectangular ducts. *ASHVE Transactions* 54:101-18.
Hutchinson, F.W. 1953. Friction losses in round aluminum ducts. *ASHVE Transactions* 59:127-38.
Idelchik, I.E., G.R. Malyavskaya, O.G. Martynenko, and E. Fried. 1986. *Handbook of hydraulic resistance*, 2nd ed. Hemisphere Publishing Corp., subsidiary of Harper & Row, New York.
Jones, C.D. 1979. Friction factor and roughness of United Sheet Metal Company spiral duct. United Sheet Metal, Division of United McGill Corp., Westerville, OH (August). Based on data contained in Friction loss tests, United Sheet Metal Company Spiral Duct, Ohio State University Engineering Experiment Station, File No. T-1011, September, 1958.
Klote, J.H. and J. Milke. 1992. *Design of smoke management systems*. ASHRAE, Atlanta.
Lauvray, T.L. 1978. Experimental heat transmission coefficients for operating air duct systems. *ASHRAE Journal* (June):69.
Meyer, M.L. 1973. A new concept: The fan system effect factor. In *Fans and systems*, ASHRAE Symposium Bulletin LO-73-1, Louisville, KY (June).
Moody, L.F. 1944. Friction factors for pipe flow. *ASME Transactions* 66:671.
NFPA. 1991. *Fire protection handbook*, 17th ed. National Fire Protection Association, Quincy, MA.
NFPA. 1993. Installation of air conditioning and ventilating systems. ANSI/NFPA *Standard* 90A-93.
Osborne, W.C. 1966. *Fans*. Pergamon Press Ltd., London.
SMACNA. 1985. *HVAC air duct leakage manual*. Sheet Metal and Air Conditioning Contractors' National Association, Chantilly, VA.
Smith, G.W. 1968. *Engineering economy: Analysis of capital expenditures*. The Iowa State University Press, Ames, IA.
Swim, W.B. 1978. Flow losses in rectangular ducts lined with fiberglass. *ASHRAE Transactions* 84(2):216.
Swim, W.B. 1982. Friction factor and roughness for airflow in plastic pipe. *ASHRAE Transactions* 88(1):269.
Swim, W.B. and E.I. Griggs. 1995. Duct leakage measurement and analysis. *ASHRAE Transactions* 101(1).
Tsal, R.J. and M.S. Adler. 1987. Evaluation of numerical methods for ductwork and pipeline optimization. *ASHRAE Transactions* 93(1):17-34.
Tsal, R.J. and H.F. Behls. 1988. Fallacy of the static regain duct design method. *ASHRAE Transactions* 94(2):76-89.
Tsal, R.J., H.F. Behls, and R. Mangel. 1988. T-method duct design, Part I: Optimization theory; Part II: Calculation procedure and economic analysis. *ASHRAE Transactions* 94(2):90-111.
Tsal, R.J., H.F. Behls, and R. Mangel. 1990. T-method duct design, Part III: Simulation. *ASHRAE Transactions* 96(2).
UL. Published annually. *Building materials directory*. Underwriters Laboratories, Northbrook, IL.
UL. Published annually. *Fire resistance directory*.
UL. 1991. Closure systems for use with rigid air ducts and air connectors. *Standard* 181A-91.
UL. 1995. Fire dampers, 5th ed. *Standard* 555-95.
UL. 1995. Leakage rated dampers for use in smoke control systems, 2nd ed. *Standard* 555S-95.
Wendes, H.C. 1989. *Sheet metal estimating*. Wendes Mechanical Consulting Services, Elk Grove Village, IL.
Wright, D.K., Jr. 1945. A new friction chart for round ducts. *ASHVE Transactions* 51:303-16.

BIBLIOGRAPHY

SMACNA. 1987. Duct research destroys design myths. Videotape (VHS). Sheet Metal and Air Conditioning Contractors' National Association, Chantilly, VA.

FITTING LOSS COEFFICIENTS

Fittings to support Examples 8 and 9 reprinted here. For the complete fitting database see the *Duct Fitting Database* (ASHRAE 1984).

ROUND FITTINGS

CD3-6 Elbow, Pleated, 60 Degree, $r/D = 1.5$

D, in.	4	6	8	10	12	14	16
C_o	0.45	0.34	0.27	0.23	0.20	0.19	0.19

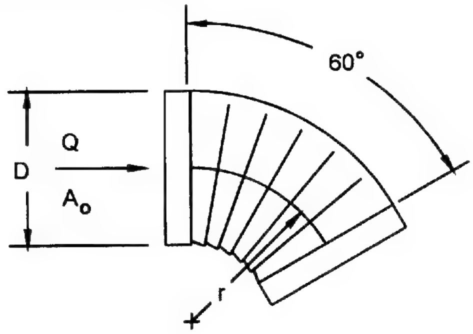

CD3-9 Elbow, 5 Gore, 90 Degree, $r/D = 1.5$

D, in.	3	6	9	12	15	18	21	24	27	30	60
C_o	0.51	0.28	0.21	0.18	0.16	0.15	0.14	0.13	0.12	0.12	0.12

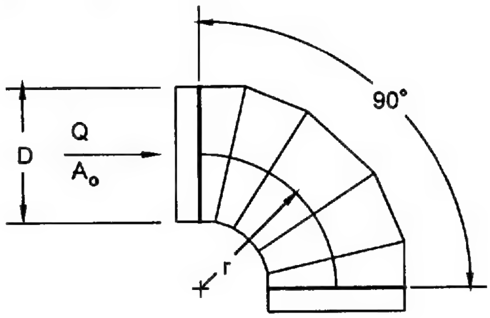

CD3-10 Elbow, 7 Gore, 90 Degree, $r/D = 2.5$

D, in.	3	6	9	12	15	18	27	60
C_o	0.16	0.12	0.10	0.08	0.07	0.06	0.05	0.03

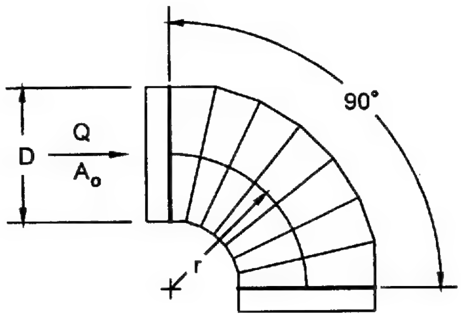

CD3-12 Elbow, 3 Gore, 90 Degree, $r/D = 0.75$ to 2.0

r/D	0.75	1.00	1.50	2.00
C_o	0.54	0.42	0.34	0.33

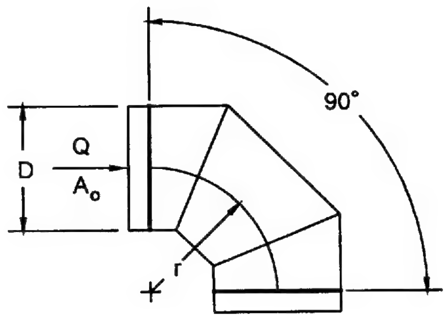

CD3-13 Elbow, 3 Gore, 60 Degree, $r/D = 1.5$

D, in.	3	6	9	12	15	18	21	24	27	30	60
C_o	0.40	0.21	0.16	0.14	0.12	0.12	0.11	0.10	0.09	0.09	0.09

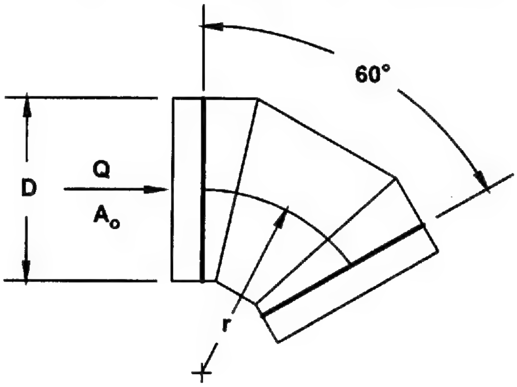

CD3-17 Elbow, Mitered, 45 Degree

D, in.	3	6	9	12	15	18	21	24	27	60
C_o	0.34	0.34	0.34	0.34	0.34	0.34	0.34	0.34	0.34	0.34

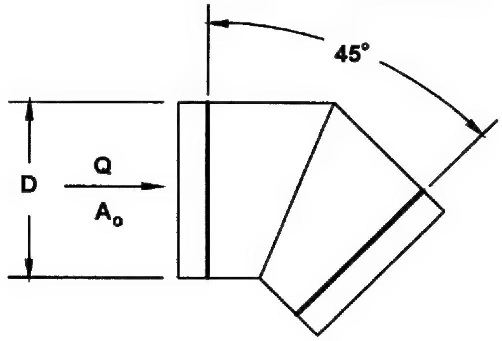

CD6-1 Screen (Only)

	C_o Values												
	n												
A_1/A_o	0.30	0.35	0.40	0.45	0.50	0.55	0.60	0.65	0.70	0.75	0.80	0.90	1.00
0.2	155.00	102.50	75.00	55.00	41.25	31.50	24.25	18.75	14.50	11.00	8.00	3.50	0.00
0.3	68.89	45.56	33.33	24.44	18.33	14.00	10.78	8.33	6.44	4.89	3.56	1.56	0.00
0.4	38.75	25.63	18.75	13.75	10.31	7.88	6.06	4.69	3.63	2.75	2.00	0.88	0.00
0.5	24.80	16.40	12.00	8.80	6.60	5.04	3.88	3.00	2.32	1.76	1.28	0.56	0.00
0.6	17.22	11.39	8.33	6.11	4.58	3.50	2.69	2.08	1.61	1.22	0.89	0.39	0.00
0.7	12.65	8.37	6.12	4.49	3.37	2.57	1.98	1.53	1.18	0.90	0.65	0.29	0.00
0.8	9.69	6.40	4.69	3.44	2.58	1.97	1.52	1.17	0.91	0.69	0.50	0.22	0.00
0.9	7.65	5.06	3.70	2.72	2.04	1.56	1.20	0.93	0.72	0.54	0.40	0.17	0.00
1.0	6.20	4.10	3.00	2.20	1.65	1.26	0.97	0.75	0.58	0.44	0.32	0.14	0.00
1.2	4.31	2.85	2.08	1.53	1.15	0.88	0.67	0.52	0.40	0.31	0.22	0.10	0.00
1.4	3.16	2.09	1.53	1.12	0.84	0.64	0.49	0.38	0.30	0.22	0.16	0.07	0.00
1.6	2.42	1.60	1.17	0.86	0.64	0.49	0.38	0.29	0.23	0.17	0.13	0.05	0.00
1.8	1.91	1.27	0.93	0.68	0.51	0.39	0.30	0.23	0.18	0.14	0.10	0.04	0.00
2.0	1.55	1.03	0.75	0.55	0.41	0.32	0.24	0.19	0.15	0.11	0.08	0.04	0.00
2.5	0.99	0.66	0.48	0.35	0.26	0.20	0.16	0.12	0.09	0.07	0.05	0.02	0.00
3.0	0.69	0.46	0.33	0.24	0.18	0.14	0.11	0.08	0.06	0.05	0.04	0.02	0.00
4.0	0.39	0.26	0.19	0.14	0.10	0.08	0.06	0.05	0.04	0.03	0.02	0.01	0.00
6.0	0.17	0.11	0.08	0.06	0.05	0.04	0.03	0.02	0.02	0.01	0.01	0.00	0.00

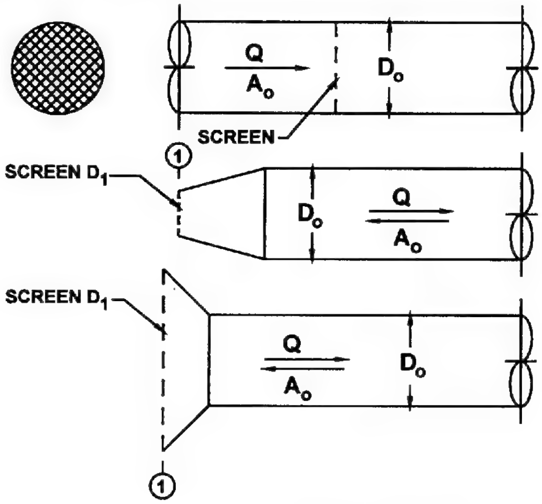

n = free area ratio of screen
A_o = area of duct
A_1 = cross-sectional area of duct or fitting where screen is located

CD9-1 Damper, Butterfly

	C_o Values											
	θ											
D/D_o	0	10	20	30	40	50	60	70	75	80	85	90
0.5	0.19	0.27	0.37	0.49	0.61	0.74	0.86	0.96	0.99	1.02	1.04	1.04
0.6	0.19	0.32	0.48	0.69	0.94	1.21	1.48	1.72	1.82	1.89	1.93	2.00
0.7	0.19	0.37	0.64	1.01	1.51	2.12	2.81	3.46	3.73	3.94	4.08	6.00
0.8	0.19	0.45	0.87	1.55	2.60	4.13	6.14	8.38	9.40	10.30	10.80	15.00
0.9	0.19	0.54	1.22	2.51	4.97	9.57	17.80	30.50	38.00	45.00	50.10	100.00
1.0	0.19	0.67	1.76	4.38	11.20	32.00	113.00	619.00	2010.00	10350.00	99999.00	99999.00

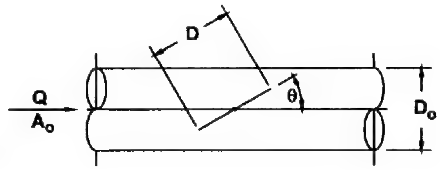

CD9-3 Fire Damper, Curtain Type, Type C

$C_o = 0.12$

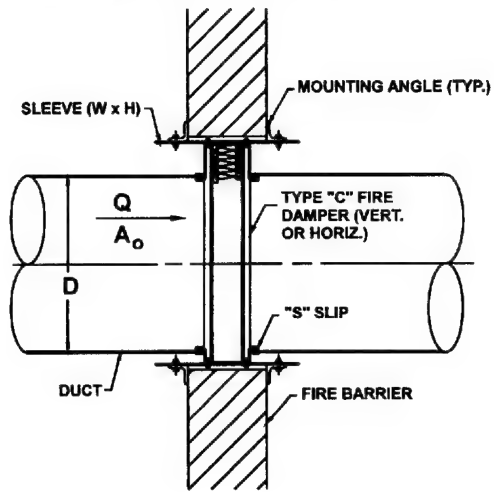

ED1-1 Duct Mounted in Wall

	C_o Values								
	L/D								
t/D	0.00	0.002	0.01	0.05	0.10	0.20	0.30	0.50	10.00
0.00	0.50	0.57	0.68	0.80	0.86	0.92	0.97	1.00	1.00
0.02	0.50	0.51	0.52	0.55	0.60	0.66	0.69	0.72	0.72
0.05	0.50	0.50	0.50	0.50	0.50	0.50	0.50	0.50	0.50
10.00	0.50	0.50	0.50	0.50	0.50	0.50	0.50	0.50	0.50

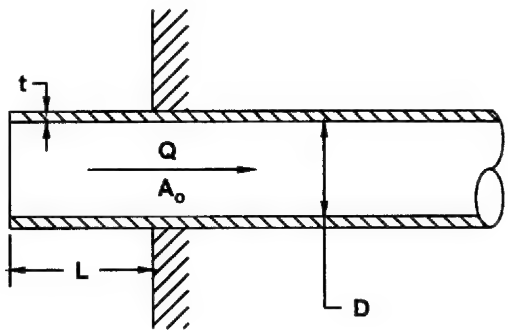

ED1-3 Bellmouth, with Wall

r/D	0.00	0.01	0.02	0.03	0.04	0.05	0.06	0.08	0.10	0.12	0.16	0.20	10.00
C_o	0.50	0.44	0.37	0.31	0.26	0.22	0.20	0.15	0.12	0.09	0.06	0.03	0.03

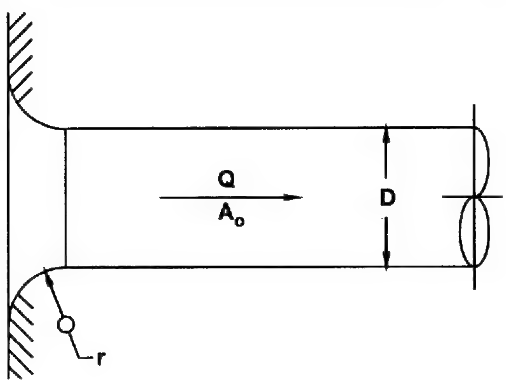

ED2-1 Conical Diffuser, Round to Plenum, Exhaust/Return Systems

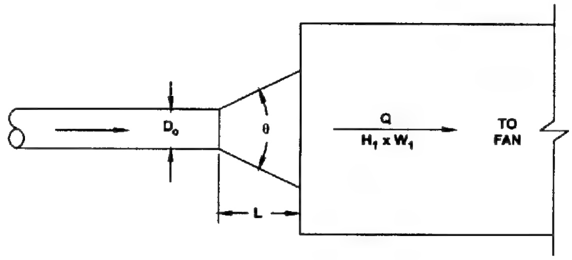

	C_o Values										
	L/D_o										
A_1/A_o	0.5	1.0	2.0	3.0	4.0	5.0	6.0	8.0	10.0	12.0	14.0
1.5	0.03	0.02	0.03	0.03	0.04	0.05	0.06	0.08	0.10	0.11	0.13
2.0	0.08	0.06	0.04	0.04	0.04	0.05	0.05	0.06	0.08	0.09	0.10
2.5	0.13	0.09	0.06	0.06	0.06	0.06	0.06	0.06	0.07	0.08	0.09
3.0	0.17	0.12	0.09	0.07	0.07	0.06	0.06	0.07	0.07	0.08	0.08
4.0	0.23	0.17	0.12	0.10	0.09	0.08	0.08	0.08	0.08	0.08	0.08
6.0	0.30	0.22	0.16	0.13	0.12	0.10	0.10	0.09	0.09	0.09	0.08
8.0	0.34	0.26	0.18	0.15	0.13	0.12	0.11	0.10	0.09	0.09	0.09
10.0	0.36	0.28	0.20	0.16	0.14	0.13	0.12	0.11	0.10	0.09	0.09
14.0	0.39	0.30	0.22	0.18	0.16	0.14	0.13	0.12	0.10	0.10	0.10
20.0	0.41	0.32	0.24	0.20	0.17	0.15	0.14	0.12	0.11	0.11	0.10

	Optimum Angle θ										
A_1/A_o	0.5	1.0	2.0	3.0	4.0	5.0	6.0	8.0	10.0	12.0	14.0
1.5	34	20	13	9	7	6	4	3	2	2	2
2.0	42	28	17	12	10	9	8	6	5	4	3
2.5	50	32	20	15	12	11	10	8	7	6	5
3.0	54	34	22	17	14	12	11	10	8	8	6
4.0	58	40	26	20	16	14	13	12	10	10	9
6.0	62	42	28	22	19	16	15	12	11	10	9
8.0	64	44	30	24	20	18	16	13	12	11	10
10.0	66	46	30	24	22	19	17	14	12	11	10
14.0	66	48	32	26	22	19	17	14	13	11	11
20.0	68	48	32	26	22	20	18	15	13	12	11

ED5-1 Wye, 30 Degree, Converging

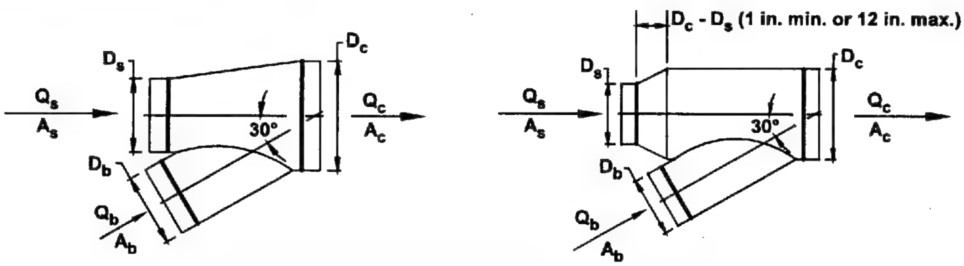

		C_b Values								
		Q_b/Q_c								
A_s/A_c	A_b/A_c	0.1	0.2	0.3	0.4	0.5	0.6	0.7	0.8	0.9
0.2	0.2	−24.17	−3.78	−0.60	0.30	0.64	0.77	0.83	0.88	0.98
	0.3	−55.88	−9.77	−2.57	−0.50	0.25	0.55	0.67	0.70	0.71
	0.4	−99.93	−17.94	−5.13	−1.45	−0.11	0.42	0.62	0.68	0.68
	0.5	−156.51	−28.40	−8.37	−2.62	−0.52	0.30	0.62	0.71	0.69
	0.6	−225.62	−41.13	−12.30	−4.01	−0.99	0.20	0.66	0.78	0.75
	0.7	−307.26	−56.14	−16.90	−5.61	−1.51	0.11	0.73	0.90	0.86
	0.8	−401.44	−73.44	−22.18	−7.44	−2.08	0.04	0.84	1.06	1.01
	0.9	−508.15	−93.02	−28.15	−9.49	−2.71	−0.03	0.99	1.27	1.20
	1.0	−627.39	−114.89	−34.80	−11.77	−3.39	−0.08	1.18	1.52	1.43
0.3	0.2	−13.97	−1.77	0.08	0.59	0.77	0.84	0.88	0.92	1.06
	0.3	−33.06	−5.33	−1.09	0.10	0.51	0.66	0.71	0.72	0.74
	0.4	−59.43	−10.08	−2.52	−0.41	0.32	0.59	0.67	0.68	0.66
	0.5	−93.24	−16.11	−4.30	−1.00	0.14	0.56	0.69	0.70	0.66
	0.6	−134.51	−23.45	−6.44	−1.68	−0.03	0.57	0.76	0.77	0.70
	0.7	−183.25	−32.08	−8.93	−2.45	−0.21	0.61	0.87	0.88	0.79
	0.8	−239.47	−42.01	−11.77	−3.32	−0.38	0.69	1.02	1.03	0.91
	0.9	−303.16	−53.25	−14.97	−4.27	−0.56	0.80	1.21	1.23	1.07
	1.0	−374.32	−65.79	−18.53	−5.32	−0.73	0.94	1.45	1.47	1.27
0.4	0.2	−9.20	−0.85	0.39	0.71	0.82	0.87	0.90	0.94	1.09
	0.3	−22.31	−3.24	−0.38	0.39	0.64	0.73	0.76	0.78	0.85
	0.4	−40.52	−6.48	−1.37	0.02	0.48	0.64	0.67	0.66	0.65
	0.5	−63.71	−10.50	−2.50	−0.33	0.40	0.63	0.69	0.67	0.63
	0.6	−92.00	−15.37	−3.84	−0.71	0.33	0.67	0.75	0.71	0.65
	0.7	−125.40	−21.08	−5.40	−1.13	0.28	0.75	0.85	0.80	0.70
	0.8	−163.90	−27.65	−7.16	−1.59	0.25	0.86	1.00	0.93	0.80
	0.9	−207.52	−35.07	−9.14	−2.09	0.25	1.02	1.18	1.10	0.93
	1.0	−256.25	−43.35	−11.33	−2.63	0.26	1.21	1.42	1.31	1.09

ED5-1 Wye, 30 Degree, Converging (*Continued*)

		C_b Values (*Concluded*)								
		Q_b/Q_c								
A_s/A_c	A_b/A_c	0.1	0.2	0.3	0.4	0.5	0.6	0.7	0.8	0.9
0.5	0.2	−6.62	−0.36	0.54	0.77	0.85	0.88	0.90	0.95	1.11
	0.3	−16.42	−2.11	−0.01	0.54	0.72	0.78	0.80	0.83	0.96
	0.4	−30.26	−4.59	−0.79	0.22	0.54	0.64	0.66	0.64	0.64
	0.5	−47.68	−7.55	−1.61	−0.02	0.48	0.63	0.65	0.62	0.59
	0.6	−68.93	−11.13	−2.56	−0.28	0.45	0.67	0.69	0.65	0.58
	0.7	−94.00	−15.31	−3.65	−0.55	0.44	0.74	0.77	0.71	0.61
	0.8	−122.90	−20.12	−4.88	−0.83	0.46	0.85	0.90	0.81	0.68
	0.9	−155.63	−25.54	−6.25	−1.12	0.51	1.00	1.06	0.94	0.77
	1.0	−192.18	−31.58	−7.77	−1.43	0.59	1.19	1.26	1.12	0.90
0.6	0.2	−5.12	−0.10	0.62	0.79	0.85	0.87	0.90	0.95	1.11
	0.3	−13.00	−1.49	0.18	0.61	0.75	0.79	0.82	0.86	1.02
	0.4	−24.31	−3.55	−0.50	0.30	0.55	0.62	0.63	0.62	0.63
	0.5	−38.41	−5.94	−1.16	0.09	0.48	0.59	0.60	0.57	0.55
	0.6	−55.58	−8.80	−1.92	−0.12	0.45	0.61	0.62	0.57	0.52
	0.7	−75.83	−12.16	−2.79	−0.33	0.44	0.66	0.67	0.60	0.52
	0.8	−99.17	−16.00	−3.76	−0.54	0.46	0.74	0.76	0.67	0.56
	0.9	−125.60	−20.33	−4.83	−0.76	0.51	0.86	0.88	0.77	0.62
	1.0	−155.12	−25.14	−6.02	−0.99	0.58	1.02	1.04	0.90	0.71
0.7	0.2	−4.24	0.05	0.65	0.80	0.85	0.87	0.89	0.94	1.12
	0.3	−11.00	−1.15	0.27	0.63	0.75	0.79	0.82	0.87	1.06
	0.4	−20.82	−3.00	−0.38	0.31	0.52	0.59	0.60	0.59	0.61
	0.5	−32.99	−5.09	−0.98	0.10	0.43	0.53	0.54	0.52	0.51
	0.6	−47.78	−7.58	−1.67	−0.11	0.38	0.52	0.53	0.49	0.45
	0.7	−65.22	−10.50	−2.44	−0.32	0.34	0.53	0.54	0.49	0.43
	0.8	−85.32	−13.83	−3.30	−0.53	0.33	0.58	0.59	0.52	0.43
	0.9	−108.07	−17.58	−4.26	−0.75	0.34	0.66	0.67	0.58	0.46
	1.0	−133.48	−21.76	−5.30	−0.97	0.38	0.76	0.78	0.67	0.51
0.8	0.2	−3.75	0.11	0.65	0.79	0.84	0.86	0.88	0.94	1.12
	0.3	−9.88	−0.99	0.29	0.63	0.74	0.78	0.81	0.87	1.09
	0.4	−18.88	−2.75	−0.36	0.28	0.48	0.55	0.56	0.57	0.61
	0.5	−29.98	−4.71	−0.96	0.04	0.36	0.46	0.47	0.46	0.47
	0.6	−43.46	−7.05	−1.64	−0.20	0.26	0.41	0.43	0.41	0.39
	0.7	−59.34	−9.77	−2.40	−0.44	0.19	0.38	0.41	0.38	0.34
	0.8	−77.64	−12.88	−3.26	−0.69	0.13	0.38	0.42	0.37	0.31
	0.9	−98.35	−16.38	−4.20	−0.95	0.09	0.40	0.45	0.39	0.30
	1.0	−121.48	−20.27	−5.24	−1.23	0.06	0.45	0.51	0.43	0.31
0.9	0.2	−3.52	0.12	0.64	0.78	0.82	0.85	0.88	0.93	1.12
	0.3	−9.34	−0.95	0.28	0.60	0.71	0.76	0.80	0.87	1.10
	0.4	−17.96	−2.70	−0.40	0.22	0.43	0.50	0.53	0.54	0.60
	0.5	−28.58	−4.65	−1.05	−0.07	0.26	0.37	0.40	0.41	0.42
	0.6	−41.45	−6.97	−1.77	−0.35	0.12	0.28	0.32	0.32	0.32
	0.7	−56.61	−9.66	−2.58	−0.65	0.00	0.21	0.27	0.26	0.24
	0.8	−74.08	−12.74	−3.49	−0.97	−0.12	0.16	0.23	0.22	0.18
	0.9	−93.84	−16.21	−4.50	−1.30	−0.23	0.13	0.21	0.19	0.14
	1.0	−115.92	−20.06	−5.61	−1.66	−0.34	0.11	0.21	0.18	0.11
1.0	0.2	−3.48	0.10	0.62	0.76	0.81	0.84	0.87	0.92	1.11
	0.3	−9.22	−1.00	0.23	0.56	0.68	0.74	0.78	0.86	1.11
	0.4	−17.76	−2.79	−0.50	0.14	0.37	0.45	0.49	0.52	0.60
	0.5	−28.31	−4.82	−1.21	−0.20	0.15	0.28	0.33	0.35	0.38
	0.6	−41.06	−7.21	−2.01	−0.55	−0.04	0.15	0.22	0.23	0.25
	0.7	−56.09	−9.99	−2.91	−0.92	−0.23	0.03	0.12	0.14	0.15
	0.8	−73.39	−13.17	−3.92	−1.32	−0.41	−0.07	0.04	0.06	0.06
	0.9	−92.98	−16.75	−5.04	−1.75	−0.60	−0.17	−0.03	−0.01	−0.02
	1.0	−114.85	−20.74	−6.28	−2.21	−0.79	−0.26	−0.09	−0.07	−0.09

		C_s Values								
		Q_s/Q_c								
A_s/A_c	A_b/A_c	0.1	0.2	0.3	0.4	0.5	0.6	0.7	0.8	0.9
0.2	0.2	−16.02	−3.15	−0.80	0.04	0.45	0.69	0.86	0.99	1.10
	0.3	−11.65	−1.94	−0.26	0.32	0.60	0.77	0.90	1.01	1.10
	0.4	−8.56	−1.20	0.05	0.47	0.68	0.82	0.92	1.02	1.11
	0.5	−6.41	−0.71	0.25	0.57	0.73	0.84	0.93	1.02	1.11
	0.6	−4.85	−0.36	0.38	0.63	0.76	0.86	0.94	1.02	1.11
	0.7	−3.68	−0.10	0.48	0.68	0.79	0.87	0.95	1.03	1.11
	0.8	−2.77	0.10	0.56	0.71	0.81	0.88	0.95	1.03	1.11
	0.9	−2.04	0.26	0.62	0.74	0.82	0.89	0.95	1.03	1.11
	1.0	−1.45	0.38	0.66	0.76	0.83	0.89	0.96	1.03	1.11

ED5-1 Wye, 30 Degree, Converging (*Concluded*)

		C_s Values (*Concluded*)								
		Q_s/Q_c								
A_s/A_c	A_b/A_c	0.1	0.2	0.3	0.4	0.5	0.6	0.7	0.8	0.9
0.3	0.2	−36.37	−7.59	−2.48	−0.79	−0.06	0.29	0.47	0.57	0.61
	0.3	−26.79	−5.07	−1.42	−0.27	0.21	0.42	0.53	0.59	0.61
	0.4	−19.94	−3.49	−0.80	0.02	0.35	0.49	0.56	0.60	0.62
	0.5	−15.18	−2.44	−0.41	0.20	0.43	0.54	0.58	0.61	0.62
	0.6	−11.73	−1.70	−0.13	0.32	0.49	0.56	0.60	0.61	0.62
	0.7	−9.13	−1.14	0.07	0.41	0.53	0.58	0.60	0.61	0.62
	0.8	−7.11	−0.72	0.23	0.48	0.57	0.60	0.61	0.62	0.62
	0.9	−5.49	−0.38	0.35	0.53	0.59	0.61	0.62	0.62	0.62
	1.0	−4.17	−0.11	0.45	0.58	0.61	0.62	0.62	0.62	0.62
0.4	0.2	−64.82	−13.76	−4.74	−1.81	−0.59	−0.02	0.24	0.36	0.39
	0.3	−47.92	−9.38	−2.93	−0.94	−0.16	0.19	0.34	0.39	0.40
	0.4	−35.81	−6.62	−1.88	−0.46	0.07	0.30	0.38	0.41	0.40
	0.5	−27.39	−4.78	−1.20	−0.16	0.22	0.36	0.41	0.42	0.41
	0.6	−21.28	−3.48	−0.73	0.04	0.31	0.41	0.43	0.43	0.41
	0.7	−16.68	−2.51	−0.38	0.20	0.38	0.44	0.45	0.43	0.41
	0.8	−13.10	−1.77	−0.12	0.31	0.44	0.46	0.46	0.44	0.41
	0.9	−10.24	−1.18	0.09	0.40	0.48	0.48	0.46	0.44	0.41
	1.0	−7.90	−0.69	0.26	0.47	0.51	0.50	0.47	0.44	0.41
0.5	0.2	−101.39	−21.64	−7.61	−3.07	−1.19	−0.34	0.05	0.22	0.26
	0.3	−75.05	−14.87	−4.83	−1.75	−0.54	−0.03	0.19	0.26	0.27
	0.4	−56.18	−10.59	−3.21	−1.02	−0.20	0.13	0.26	0.29	0.27
	0.5	−43.04	−7.74	−2.16	−0.56	0.02	0.23	0.30	0.30	0.27
	0.6	−33.51	−5.72	−1.43	−0.24	0.16	0.30	0.33	0.31	0.28
	0.7	−26.34	−4.22	−0.90	−0.01	0.27	0.35	0.35	0.32	0.28
	0.8	−20.75	−3.06	−0.49	0.16	0.35	0.39	0.37	0.33	0.28
	0.9	−16.29	−2.14	−0.17	0.30	0.41	0.41	0.38	0.33	0.28
	1.0	−12.64	−1.39	0.10	0.41	0.46	0.44	0.39	0.33	0.28
0.6	0.2	−146.06	−31.26	−11.09	−4.56	−1.89	−0.68	−0.12	0.10	0.16
	0.3	−108.19	−21.55	−7.12	−2.69	−0.97	−0.24	0.07	0.17	0.17
	0.4	−81.04	−15.40	−4.80	−1.65	−0.48	−0.01	0.17	0.20	0.18
	0.5	−62.13	−11.31	−3.30	−0.99	−0.17	0.13	0.22	0.22	0.18
	0.6	−48.43	−8.41	−2.25	−0.54	0.03	0.22	0.26	0.24	0.18
	0.7	−38.10	−6.25	−1.49	−0.22	0.18	0.29	0.29	0.25	0.19
	0.8	−30.07	−4.59	−0.90	0.03	0.30	0.34	0.31	0.25	0.19
	0.9	−23.64	−3.27	−0.44	0.23	0.39	0.38	0.33	0.26	0.19
	1.0	−18.39	−2.20	−0.06	0.39	0.46	0.42	0.34	0.27	0.19
0.7	0.2	−198.85	−42.62	−15.17	−6.31	−2.68	−1.04	−0.29	0.01	0.08
	0.3	−147.33	−29.41	−9.78	−3.77	−1.44	−0.45	−0.04	0.10	0.10
	0.4	−110.40	−21.07	−6.64	−2.36	−0.77	−0.14	0.09	0.15	0.11
	0.5	−84.67	−15.50	−4.60	−1.48	−0.36	0.05	0.17	0.17	0.11
	0.6	−66.02	−11.56	−3.19	−0.86	−0.08	0.18	0.23	0.19	0.12
	0.7	−51.97	−8.63	−2.15	−0.42	0.12	0.27	0.27	0.20	0.12
	0.8	−41.04	−6.37	−1.35	−0.08	0.27	0.34	0.29	0.21	0.12
	0.9	−32.30	−4.58	−0.72	0.19	0.39	0.39	0.32	0.22	0.12
	1.0	−25.16	−3.12	−0.21	0.40	0.49	0.43	0.33	0.23	0.13
0.8	0.2	−259.75	−55.70	−19.86	−8.29	−3.56	−1.43	−0.46	−0.06	0.03
	0.3	−192.48	−38.47	−12.84	−4.99	−1.95	−0.66	−0.12	0.05	0.05
	0.4	−144.25	−27.58	−8.74	−3.16	−1.09	−0.26	0.05	0.11	0.06
	0.5	−110.65	−20.32	−6.08	−2.00	−0.55	−0.01	0.15	0.15	0.07
	0.6	−86.30	−15.17	−4.24	−1.20	−0.19	0.15	0.22	0.17	0.08
	0.7	−67.95	−11.34	−2.88	−0.62	0.08	0.27	0.27	0.19	0.08
	0.8	−53.67	−8.40	−1.84	−0.18	0.28	0.36	0.30	0.20	0.08
	0.9	−42.26	−6.05	−1.02	0.16	0.44	0.43	0.33	0.21	0.08
	1.0	−32.93	−4.15	−0.35	0.44	0.56	0.49	0.36	0.22	0.09
0.9	0.2	−328.76	−70.51	−25.16	−10.53	−4.54	−1.84	−0.62	−0.12	0.00
	0.3	−243.63	−48.72	−16.28	−6.35	−2.50	−0.87	−0.20	0.03	0.03
	0.4	−182.60	−34.94	−11.09	−4.03	−1.41	−0.37	0.02	0.10	0.04
	0.5	−140.07	−25.75	−7.74	−2.57	−0.74	−0.06	0.15	0.14	0.05
	0.6	−109.25	−19.24	−5.40	−1.56	−0.28	0.15	0.23	0.17	0.05
	0.7	−86.04	−14.40	−3.68	−0.83	0.06	0.30	0.30	0.20	0.06
	0.8	−67.96	−10.66	−2.37	−0.27	0.31	0.41	0.34	0.21	0.06
	0.9	−53.52	−7.70	−1.33	0.17	0.51	0.50	0.38	0.22	0.06
	1.0	−41.71	−5.29	−0.49	0.52	0.67	0.57	0.41	0.23	0.07
1.0	0.2	−405.88	−87.06	−31.07	−13.01	−5.62	−2.29	−0.77	−0.16	−0.02
	0.3	−300.78	−60.15	−20.11	−7.85	−3.10	−1.09	−0.26	0.02	0.02
	0.4	−225.44	−43.14	−13.70	−4.99	−1.76	−0.47	0.01	0.11	0.04
	0.5	−172.93	−31.80	−9.56	−3.18	−0.92	−0.09	0.17	0.17	0.05
	0.6	−134.89	−23.76	−6.68	−1.94	−0.35	0.17	0.28	0.20	0.06
	0.7	−106.23	−17.78	−4.56	−1.04	0.06	0.36	0.35	0.23	0.06
	0.8	−83.92	−13.18	−2.93	−0.35	0.37	0.50	0.41	0.25	0.06
	0.9	−66.08	−9.52	−1.65	0.19	0.62	0.61	0.46	0.26	0.07
	1.0	−51.51	−6.54	−0.61	0.63	0.81	0.70	0.49	0.28	0.07

ED5-2 Wye, 45 Degree, Converging

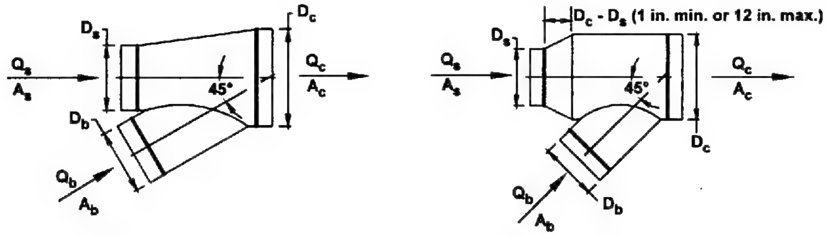

		C_b Values								
		Q_b/Q_c								
A_s/A_c	A_b/A_c	0.1	0.2	0.3	0.4	0.5	0.6	0.7	0.8	0.9
0.2	0.2	−25.19	−3.97	−0.64	0.32	0.67	0.82	0.90	0.96	1.08
	0.3	−58.03	−10.14	−2.63	−0.45	0.36	0.69	0.84	0.93	1.08
	0.4	−104.08	−18.80	−5.40	−1.51	−0.07	0.52	0.77	0.88	1.01
	0.5	−163.36	−29.97	−8.97	−2.87	−0.62	0.29	0.67	0.80	0.84
	0.6	−235.59	−43.47	−13.22	−4.44	−1.20	0.12	0.65	0.83	0.85
	0.7	−320.90	−59.38	−18.21	−6.25	−1.84	−0.04	0.68	0.91	0.93
	0.8	−419.32	−77.73	−23.95	−8.33	−2.56	−0.22	0.72	1.02	1.02
	0.9	−530.86	−98.50	−30.44	−10.66	−3.36	−0.40	0.79	1.16	1.14
	1.0	−655.51	−121.72	−37.68	−13.26	−4.25	−0.59	0.87	1.33	1.28
0.3	0.2	−14.27	−1.77	0.13	0.66	0.85	0.93	0.97	1.03	1.21
	0.3	−33.62	−5.28	−0.95	0.27	0.70	0.87	0.94	1.01	1.19
	0.4	−60.85	−10.26	−2.48	−0.30	0.47	0.77	0.88	0.93	1.04
	0.5	−95.87	−16.64	−4.44	−1.00	0.21	0.66	0.82	0.84	0.84
	0.6	−138.38	−24.26	−6.68	−1.73	0.01	0.66	0.88	0.91	0.88
	0.7	−188.60	−33.25	−9.32	−2.58	−0.20	0.68	0.98	1.02	0.95
	0.8	−246.54	−43.60	−12.34	−3.54	−0.43	0.72	1.11	1.15	1.03
	0.9	−312.21	−55.33	−15.76	−4.61	−0.68	0.78	1.26	1.31	1.13
	1.0	−385.59	−68.43	−19.56	−5.79	−0.94	0.86	1.45	1.49	1.24
0.4	0.2	−8.77	−0.64	0.54	0.85	0.95	0.99	1.03	1.09	1.31
	0.3	−21.41	−2.85	−0.10	0.63	0.87	0.96	1.00	1.06	1.26
	0.4	−39.30	−6.02	−1.05	0.28	0.72	0.87	0.91	0.92	1.00
	0.5	−62.10	−9.96	−2.16	−0.06	0.63	0.85	0.90	0.88	0.86
	0.6	−89.77	−14.65	−3.42	−0.38	0.61	0.93	0.99	0.95	0.90
	0.7	−122.46	−20.19	−4.88	−0.74	0.61	1.04	1.12	1.06	0.95
	0.8	−160.18	−26.56	−6.55	−1.15	0.62	1.18	1.29	1.19	1.01
	0.9	−202.93	−33.77	−8.44	−1.60	0.64	1.36	1.48	1.35	1.07
	1.0	−250.70	−41.83	−10.54	−2.09	0.68	1.56	1.71	1.53	1.15
0.5	0.2	−5.45	0.04	0.79	0.97	1.02	1.04	1.07	1.14	1.39
	0.3	−14.10	−1.39	0.40	0.84	0.97	1.00	1.02	1.07	1.28
	0.4	−26.48	−3.53	−0.24	0.59	0.83	0.89	0.88	0.85	0.86
	0.5	−41.84	−5.96	−0.80	0.51	0.88	0.97	0.95	0.90	0.87
	0.6	−60.61	−8.90	−1.46	0.43	0.97	1.09	1.06	0.97	0.90
	0.7	−82.80	−12.36	−2.22	0.35	1.09	1.25	1.20	1.08	0.93
	0.8	−108.39	−16.35	−3.09	0.27	1.24	1.45	1.38	1.20	0.96
	0.9	−137.41	−20.86	−4.07	0.19	1.42	1.68	1.59	1.35	0.99
	1.0	−169.84	−25.90	−5.15	0.11	1.63	1.95	1.83	1.52	1.02
0.6	0.2	−5.54	−0.08	0.70	0.91	0.98	1.01	1.05	1.14	1.42
	0.3	−14.48	−1.75	0.13	0.64	0.81	0.88	0.92	0.98	1.19
	0.4	−27.10	−4.14	−0.68	0.26	0.57	0.68	0.71	0.72	0.76
	0.5	−42.84	−6.91	−1.50	−0.02	0.47	0.64	0.68	0.69	0.70
	0.6	−62.07	−10.28	−2.48	−0.34	0.37	0.61	0.67	0.66	0.63
	0.7	−84.79	−14.26	−3.62	−0.71	0.27	0.59	0.67	0.63	0.54
	0.8	−111.02	−18.84	−4.92	−1.12	0.16	0.58	0.67	0.61	0.44
	0.9	−140.76	−24.03	−6.40	−1.57	0.04	0.58	0.68	0.59	0.31
	1.0	−174.01	−29.83	−8.04	−2.07	−0.08	0.58	0.70	0.56	0.15
0.7	0.2	−3.96	0.25	0.83	0.97	1.01	1.04	1.08	1.17	1.47
	0.3	−11.07	−1.10	0.34	0.71	0.83	0.87	0.90	0.95	1.13
	0.4	−20.92	−2.92	−0.27	0.43	0.65	0.72	0.73	0.73	0.77
	0.5	−33.20	−5.01	−0.85	0.24	0.59	0.69	0.71	0.69	0.70
	0.6	−48.21	−7.55	−1.55	0.03	0.53	0.68	0.69	0.65	0.61
	0.7	−65.95	−10.56	−2.37	−0.20	0.48	0.68	0.69	0.62	0.49
	0.8	−86.42	−14.01	−3.30	−0.46	0.43	0.68	0.69	0.58	0.35
	0.9	−109.65	−17.93	−4.35	−0.75	0.38	0.70	0.70	0.53	0.18
	1.0	−135.63	−22.32	−5.53	−1.07	0.33	0.72	0.71	0.48	−0.03

ED5-2 Wye, 45 Degree, Converging (*Continued*)

		C_b Values (*Concluded*)								
		Q_b/Q_c								
A_s/A_c	A_b/A_c	0.1	0.2	0.3	0.4	0.5	0.6	0.7	0.8	0.9
0.8	0.2	−2.78	0.50	0.91	1.01	1.03	1.05	1.09	1.18	1.49
	0.3	−8.58	−0.65	0.47	0.74	0.82	0.85	0.86	0.89	1.02
	0.4	−16.29	−2.00	0.05	0.56	0.71	0.75	0.74	0.74	0.78
	0.5	−25.98	−3.59	−0.37	0.44	0.68	0.73	0.72	0.69	0.69
	0.6	−37.82	−5.52	−0.87	0.31	0.65	0.72	0.70	0.64	0.58
	0.7	−51.83	−7.79	−1.44	0.17	0.63	0.73	0.69	0.59	0.43
	0.8	−68.01	−10.42	−2.10	0.01	0.62	0.75	0.69	0.53	0.25
	0.9	−86.37	−13.39	−2.84	−0.16	0.61	0.77	0.68	0.47	0.03
	1.0	−106.91	−16.73	−3.68	−0.35	0.61	0.79	0.68	0.38	−0.25
0.9	0.2	−1.87	0.68	0.98	1.03	1.05	1.06	1.09	1.18	1.49
	0.3	−6.70	−0.33	0.54	0.74	0.79	0.80	0.80	0.81	0.87
	0.4	−12.69	−1.29	0.29	0.66	0.76	0.77	0.75	0.74	0.78
	0.5	−20.37	−2.48	0.00	0.59	0.74	0.75	0.72	0.69	0.67
	0.6	−29.77	−3.94	−0.34	0.52	0.73	0.75	0.70	0.63	0.54
	0.7	−40.89	−5.66	−0.73	0.45	0.74	0.76	0.68	0.56	0.36
	0.8	−53.74	−7.64	−1.18	0.37	0.76	0.78	0.67	0.48	0.13
	0.9	−68.32	−9.89	−1.69	0.28	0.77	0.80	0.65	0.38	−0.15
	1.0	−84.66	−12.42	−2.27	0.18	0.80	0.83	0.62	0.26	−0.49
1.0	0.2	−1.17	0.81	1.02	1.05	1.05	1.06	1.09	1.18	1.48
	0.3	−5.09	−0.02	0.64	0.78	0.81	0.81	0.80	0.80	0.86
	0.4	−9.81	−0.72	0.48	0.74	0.79	0.78	0.76	0.74	0.77
	0.5	−15.89	−1.61	0.29	0.71	0.79	0.77	0.72	0.68	0.65
	0.6	−23.34	−2.69	0.07	0.68	0.80	0.77	0.69	0.60	0.49
	0.7	−32.15	−3.96	−0.18	0.66	0.82	0.78	0.67	0.51	0.27
	0.8	−42.35	−5.44	−0.47	0.64	0.85	0.79	0.63	0.41	0.00
	0.9	−53.94	−7.12	−0.80	0.61	0.88	0.81	0.60	0.28	−0.34
	1.0	−66.93	−9.01	−1.17	0.58	0.92	0.82	0.55	0.13	−0.75

		C_s Values								
		Q_s/Q_c								
A_s/A_c	A_b/A_c	0.1	0.2	0.3	0.4	0.5	0.6	0.7	0.8	0.9
0.2	0.2	−10.16	−2.08	−0.43	0.24	0.62	0.88	1.10	1.29	1.46
	0.3	−7.83	−1.20	0.03	0.50	0.77	0.97	1.14	1.30	1.46
	0.4	−5.62	−0.59	0.30	0.65	0.85	1.01	1.16	1.31	1.46
	0.5	−3.96	−0.18	0.48	0.74	0.90	1.04	1.18	1.32	1.47
	0.6	−2.71	0.12	0.60	0.80	0.94	1.06	1.19	1.32	1.47
	0.7	−1.75	0.34	0.70	0.85	0.96	1.07	1.19	1.32	1.47
	0.8	−0.99	0.52	0.77	0.88	0.98	1.08	1.20	1.32	1.47
	0.9	−0.38	0.66	0.82	0.91	0.99	1.09	1.20	1.33	1.47
	1.0	0.13	0.77	0.87	0.93	1.00	1.10	1.20	1.33	1.47
0.3	0.2	−23.33	−5.14	−1.67	−0.44	0.12	0.42	0.58	0.67	0.72
	0.3	−18.44	−3.44	−0.84	0.00	0.36	0.54	0.64	0.69	0.73
	0.4	−13.64	−2.22	−0.34	0.25	0.49	0.60	0.67	0.70	0.73
	0.5	−10.00	−1.37	0.00	0.41	0.57	0.64	0.69	0.71	0.73
	0.6	−7.26	−0.75	0.24	0.52	0.62	0.67	0.70	0.72	0.73
	0.7	−5.15	−0.29	0.41	0.60	0.66	0.69	0.71	0.72	0.73
	0.8	−3.48	0.07	0.55	0.66	0.69	0.70	0.71	0.72	0.73
	0.9	−2.14	0.36	0.65	0.71	0.72	0.72	0.72	0.72	0.73
	1.0	−1.03	0.60	0.74	0.75	0.73	0.73	0.72	0.72	0.73
0.4	0.2	−42.17	−9.48	−3.34	−1.23	−0.31	0.12	0.33	0.42	0.44
	0.3	−33.68	−6.60	−1.98	−0.53	0.05	0.31	0.41	0.45	0.45
	0.4	−25.24	−4.51	−1.13	−0.13	0.25	0.40	0.46	0.47	0.45
	0.5	−18.83	−3.04	−0.57	0.13	0.37	0.46	0.48	0.48	0.46
	0.6	−13.99	−1.97	−0.17	0.31	0.46	0.50	0.50	0.48	0.46
	0.7	−10.27	−1.17	0.12	0.44	0.52	0.53	0.51	0.49	0.46
	0.8	−7.32	−0.54	0.35	0.54	0.57	0.55	0.52	0.49	0.46
	0.9	−4.94	−0.04	0.53	0.62	0.61	0.57	0.53	0.49	0.46
	1.0	−2.98	0.37	0.68	0.68	0.64	0.58	0.54	0.50	0.46
0.5	0.2	−66.95	−15.18	−5.49	−2.21	−0.81	−0.16	0.14	0.26	0.28
	0.3	−53.80	−10.77	−3.45	−1.17	−0.27	0.11	0.26	0.30	0.29
	0.4	−40.66	−7.54	−2.16	−0.57	0.02	0.25	0.32	0.33	0.30
	0.5	−30.68	−5.27	−1.30	−0.18	0.21	0.33	0.36	0.34	0.30
	0.6	−23.15	−3.62	−0.69	0.09	0.33	0.39	0.38	0.35	0.30
	0.7	−17.34	−2.38	−0.24	0.29	0.42	0.43	0.40	0.35	0.30
	0.8	−12.75	−1.41	0.11	0.44	0.49	0.47	0.41	0.36	0.30
	0.9	−9.04	−0.64	0.39	0.56	0.55	0.49	0.43	0.36	0.30
	1.0	−5.99	0.00	0.61	0.65	0.59	0.51	0.43	0.36	0.30

ED5-2 Wye, 45 Degree, Converging (*Concluded*)

		C_s Values (*Concluded*)								
		Q_s/Q_c								
A_s/A_c	A_b/A_c	0.1	0.2	0.3	0.4	0.5	0.6	0.7	0.8	0.9
0.6	0.2	−97.90	−22.29	−8.18	−3.41	−1.39	−0.46	−0.03	0.13	0.16
	0.3	−79.03	−15.99	−5.28	−1.94	−0.64	−0.09	0.13	0.19	0.17
	0.4	−60.15	−11.37	−3.44	−1.09	−0.23	0.10	0.21	0.22	0.18
	0.5	−45.80	−8.13	−2.22	−0.55	0.03	0.22	0.26	0.24	0.18
	0.6	−34.97	−5.77	−1.35	−0.17	0.20	0.30	0.30	0.25	0.18
	0.7	−26.62	−3.98	−0.71	0.11	0.33	0.36	0.32	0.26	0.19
	0.8	−20.02	−2.59	−0.21	0.33	0.43	0.41	0.34	0.26	0.19
	0.9	−14.68	−1.48	0.18	0.49	0.51	0.44	0.35	0.27	0.19
	1.0	−10.29	−0.57	0.51	0.63	0.57	0.47	0.37	0.27	0.19
0.7	0.2	−135.28	−30.88	−11.42	−4.85	−2.08	−0.80	−0.21	0.02	0.06
	0.3	−109.64	−22.35	−7.50	−2.88	−1.07	−0.31	0.00	0.09	0.07
	0.4	−83.96	−16.08	−5.02	−1.73	−0.52	−0.05	0.11	0.13	0.08
	0.5	−64.44	−11.67	−3.36	−0.99	−0.17	0.11	0.18	0.15	0.09
	0.6	−49.71	−8.47	−2.19	−0.48	0.06	0.22	0.22	0.17	0.09
	0.7	−38.35	−6.04	−1.31	−0.10	0.24	0.30	0.26	0.18	0.09
	0.8	−29.37	−4.16	−0.64	0.18	0.37	0.36	0.28	0.19	0.09
	0.9	−22.12	−2.65	−0.10	0.41	0.47	0.40	0.30	0.19	0.09
	1.0	−16.14	−1.41	0.33	0.60	0.55	0.44	0.32	0.20	0.09
0.8	0.2	−179.32	−41.01	−15.25	−6.55	−2.88	−1.19	−0.41	−0.10	−0.04
	0.3	−145.86	−29.89	−10.14	−3.99	−1.58	−0.55	−0.13	0.00	−0.02
	0.4	−112.34	−21.71	−6.91	−2.50	−0.86	−0.22	0.01	0.05	−0.01
	0.5	−86.85	−15.96	−4.75	−1.54	−0.41	−0.01	0.10	0.08	0.00
	0.6	−67.62	−11.78	−3.22	−0.87	−0.10	0.13	0.16	0.10	0.00
	0.7	−52.79	−8.62	−2.08	−0.38	0.12	0.23	0.20	0.11	0.00
	0.8	−41.06	−6.16	−1.20	0.00	0.29	0.31	0.23	0.12	0.01
	0.9	−31.59	−4.19	−0.51	0.29	0.43	0.37	0.26	0.13	0.01
	1.0	−23.78	−2.58	0.06	0.53	0.54	0.42	0.28	0.14	0.01
0.9	0.2	−230.27	−52.75	−19.69	−8.53	−3.81	−1.63	−0.63	−0.22	−0.13
	0.3	−187.95	−38.69	−13.24	−5.29	−2.16	−0.83	−0.28	−0.10	−0.10
	0.4	−145.53	−28.34	−9.15	−3.41	−1.26	−0.41	−0.10	−0.04	−0.09
	0.5	−113.27	−21.07	−6.42	−2.19	−0.69	−0.15	0.01	0.00	−0.09
	0.6	−88.94	−15.78	−4.48	−1.35	−0.30	0.03	0.09	0.03	−0.08
	0.7	−70.16	−11.78	−3.04	−0.73	−0.02	0.16	0.14	0.04	−0.08
	0.8	−55.33	−8.67	−1.93	−0.25	0.20	0.26	0.18	0.06	−0.07
	0.9	−43.33	−6.18	−1.05	0.12	0.37	0.33	0.21	0.07	−0.07
	1.0	−33.46	−4.14	−0.34	0.42	0.50	0.39	0.24	0.08	−0.07
1.0	0.2	−288.39	−66.15	−24.77	−10.80	−4.88	−2.14	−0.87	−0.35	−0.22
	0.3	−236.14	−48.79	−16.81	−6.80	−2.85	−1.15	−0.44	−0.20	−0.19
	0.4	−183.77	−36.02	−11.76	−4.47	−1.73	−0.63	−0.22	−0.12	−0.18
	0.5	−143.95	−27.05	−8.39	−2.98	−1.03	−0.31	−0.08	−0.08	−0.17
	0.6	−113.91	−20.52	−6.00	−1.93	−0.55	−0.09	0.01	−0.04	−0.16
	0.7	−90.73	−15.58	−4.23	−1.17	−0.20	0.07	0.08	−0.02	−0.16
	0.8	−72.41	−11.74	−2.86	−0.58	0.06	0.19	0.13	−0.01	−0.16
	0.9	−57.61	−8.66	−1.77	−0.12	0.27	0.28	0.16	0.01	−0.15
	1.0	−45.42	−6.15	−0.88	0.25	0.44	0.36	0.20	0.02	−0.15

ED5-6 Capped Wye, Branch with 45-Degree Elbow, Branch 90 Degrees to Main, Converging

A_b/A_c	0.1	0.2	0.3	0.4	0.5	0.6	0.7	0.8	0.9	1.0
C_b	1.26	1.07	0.94	0.86	0.81	0.76	0.71	0.67	0.64	0.64

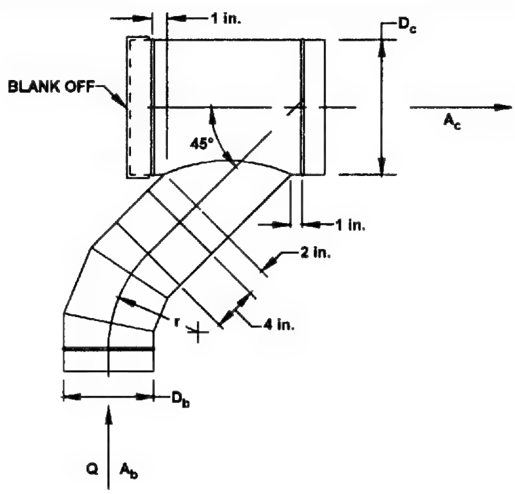

ED5-9 Symmetrical Wye, 60 Degree, $D_{b1} \geq D_{b2}$, Converging

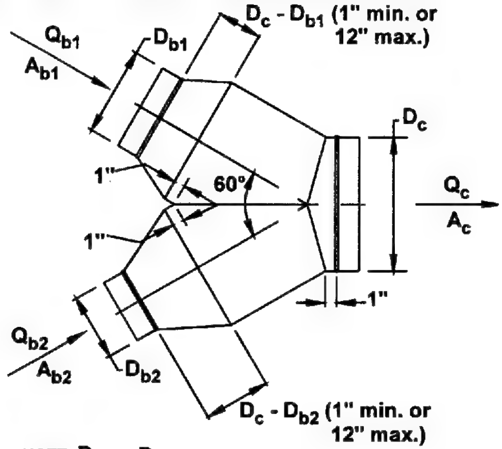

NOTE: $D_{b1} \geq D_{b2}$

		C_{b1} Values								
		Q_{b1}/Q_c								
A_{b1}/A_c	A_{b2}/A_c	0.1	0.2	0.3	0.4	0.5	0.6	0.7	0.8	0.9
0.2	0.2	−11.95	−1.89	−0.09	0.41	0.62	0.74	0.80	0.80	0.79
	0.3	−11.95	−1.89	−0.09	0.41	0.62	0.74	0.80	0.80	0.79
0.3	0.2	−45.45	−9.39	−2.44	−0.41	0.33	0.68	0.89	1.03	1.13
	0.3	−16.88	−2.92	−0.09	0.59	0.86	1.02	1.09	1.10	1.08
0.4	0.2	−72.04	−14.00	−4.26	−1.24	−0.10	0.33	0.50	0.57	0.63
	0.3	−52.95	−9.91	−2.86	−0.69	0.07	0.30	0.40	0.49	0.62
	0.4	−28.86	−6.22	−2.15	−0.57	0.19	0.55	0.72	0.79	0.85
0.5	0.2	−126.04	−23.80	−7.44	−2.64	−0.85	−0.13	0.16	0.26	0.28
	0.3	−91.07	−16.91	−5.16	−1.73	−0.46	0.04	0.23	0.29	0.28
	0.4	−56.41	−10.07	−2.90	−0.82	−0.07	0.21	0.30	0.31	0.29
	0.5	−30.58	−5.23	−1.06	0.00	0.32	0.43	0.47	0.47	0.41
0.6	0.2	−209.81	−39.31	−12.13	−4.35	−1.54	−0.40	0.06	0.22	0.23
	0.3	−147.43	−27.69	−8.75	−3.20	−1.13	−0.29	0.05	0.17	0.18
	0.4	−85.06	−16.07	−5.38	−2.04	−0.71	−0.17	0.04	0.12	0.13
	0.5	−58.22	−11.03	−3.84	−1.49	−0.50	−0.09	0.07	0.11	0.12
	0.6	−40.57	−7.86	−2.60	−0.99	−0.26	0.00	0.14	0.21	0.25
0.7	0.2	−291.57	−54.52	−17.03	−6.21	−2.27	−0.68	−0.04	0.19	0.21
	0.3	−197.37	−38.02	−12.54	−4.92	−2.01	−0.76	−0.22	0.01	0.08
	0.4	−102.97	−21.41	−8.05	−3.64	−1.75	−0.84	−0.40	−0.17	−0.05
	0.5	−65.15	−14.75	−6.16	−3.07	−1.61	−0.85	−0.44	−0.22	−0.09
	0.6	−48.24	−11.70	−4.97	−2.59	−1.40	−0.76	−0.37	−0.15	−0.03
	0.7	−73.02	−16.68	−6.90	−3.29	−1.61	−0.80	−0.29	0.02	0.22
0.8	0.2	−373.33	−69.73	−21.93	−8.08	−3.00	−0.95	−0.13	0.15	0.20
	0.3	−247.31	−48.35	−16.32	−6.65	−2.89	−1.24	−0.49	−0.15	−0.02
	0.4	−120.88	−26.76	−10.71	−5.24	−2.78	−1.52	−0.84	−0.45	−0.24
	0.5	−72.08	−18.46	−8.48	−4.65	−2.71	−1.61	−0.95	−0.55	−0.31
	0.6	−55.91	−15.54	−7.35	−4.20	−2.54	−1.53	−0.89	−0.51	−0.30
	0.7	−80.68	−20.52	−9.27	−4.90	−2.75	−1.56	−0.80	−0.34	−0.06
	0.8	−105.46	−25.49	−11.19	−5.59	−2.96	−1.60	−0.72	−0.18	0.19
0.9	0.2	−479.24	−89.56	−28.39	−10.59	−4.04	−1.41	−0.36	0.01	0.09
	0.3	−305.31	−61.27	−21.50	−9.28	−4.39	−2.16	−1.07	−0.54	−0.29
	0.4	−131.17	−32.88	−14.60	−7.98	−4.74	−2.91	−1.79	−1.10	−0.68
	0.5	−67.90	−22.76	−12.17	−7.53	−4.89	−3.19	−2.05	−1.30	−0.81
	0.6	−68.95	−23.08	−12.11	−7.45	−4.84	−3.15	−2.01	−1.26	−0.79
	0.7	−90.48	−27.35	−13.58	−7.95	−4.97	−3.16	−1.96	−1.17	−0.65
	0.8	−112.02	−31.63	−15.05	−8.44	−5.11	−3.18	−1.90	−1.07	−0.51
	0.9	−130.32	−35.19	−16.07	−8.70	−5.18	−3.19	−1.88	−1.08	−0.53
1.0	0.2	−585.16	−109.39	−34.85	−13.11	−5.09	−1.86	−0.59	−0.13	−0.01
	0.3	−363.31	−74.20	−26.68	−11.91	−5.90	−3.08	−1.66	−0.94	−0.56
	0.4	−141.46	−39.00	−18.50	−10.71	−6.71	−4.29	−2.74	−1.74	−1.12
	0.5	−63.71	−27.06	−15.85	−10.41	−7.07	−4.77	−3.16	−2.05	−1.31
	0.6	−81.99	−30.62	−16.87	−10.70	−7.13	−4.77	−3.13	−2.02	−1.28
	0.7	−100.28	−34.19	−17.89	−11.00	−7.19	−4.76	−3.11	−1.99	−1.24
	0.8	−118.58	−37.76	−18.91	−11.29	−7.26	−4.76	−3.09	−1.96	−1.20
	0.9	−136.88	−41.32	−19.93	−11.55	−7.32	−4.77	−3.07	−1.98	−1.23
	1.0	−155.18	−44.89	−20.95	−11.80	−7.39	−4.78	−3.05	−1.99	−1.25

ED5-9 Symmetrical Wye, 60 Degree, $D_{b1} \geq D_{b2}$, Converging (*Concluded*)

		C_{b2} Values								
		Q_{b2}/Q_c								
A_{b1}/A_c	A_{b2}/A_c	0.1	0.2	0.3	0.4	0.5	0.6	0.7	0.8	0.9
0.2	0.2	−11.95	−1.89	−0.09	0.41	0.62	0.74	0.80	0.80	0.79
	0.3	−11.95	−1.89	−0.09	0.41	0.62	0.74	0.80	0.80	0.79
0.3	0.2	−8.24	−1.18	0.05	0.42	0.61	0.73	0.78	0.77	0.76
	0.3	−16.88	−2.92	−0.09	0.59	0.86	1.02	1.09	1.10	1.08
0.4	0.2	−6.95	−1.00	0.16	0.53	0.67	0.71	0.72	0.72	0.71
	0.3	−16.21	−2.90	−0.44	0.40	0.79	0.98	1.05	1.06	1.05
	0.4	−28.86	−6.22	−2.15	−0.57	0.19	0.55	0.72	0.79	0.85
0.5	0.2	−4.82	−0.01	0.56	0.71	0.82	0.89	0.92	0.90	0.89
	0.3	−12.27	−1.17	0.44	0.88	1.11	1.25	1.29	1.25	1.23
	0.4	−20.76	−2.93	−0.21	0.48	0.73	0.84	0.88	0.87	0.82
	0.5	−30.58	−5.23	−1.06	0.00	0.32	0.43	0.47	0.47	0.41
0.6	0.2	−3.68	0.07	0.77	0.98	1.06	1.08	1.08	1.06	1.04
	0.3	−9.06	−0.55	0.86	1.27	1.42	1.48	1.49	1.46	1.42
	0.4	−17.62	−2.12	0.06	0.60	0.83	0.95	0.98	0.95	0.91
	0.5	−28.00	−4.26	−0.99	−0.16	0.20	0.39	0.45	0.41	0.38
	0.6	−40.57	−7.86	−2.60	−0.99	−0.26	0.00	0.14	0.21	0.25
0.7	0.2	−5.44	−0.40	0.55	0.86	0.98	1.02	1.04	1.03	1.02
	0.3	−9.36	−0.77	0.73	1.20	1.39	1.47	1.49	1.47	1.44
	0.4	−19.57	−3.09	−0.44	0.36	0.71	0.89	0.97	0.98	0.97
	0.5	−31.88	−6.02	−1.90	−0.63	−0.05	0.26	0.40	0.44	0.46
	0.6	−46.44	−9.82	−3.47	−1.41	−0.48	−0.04	0.21	0.36	0.45
	0.7	−73.02	−16.68	−6.90	−3.29	−1.61	−0.80	−0.29	0.02	0.22
0.8	0.2	−7.21	−0.87	0.33	0.73	0.90	0.97	1.00	1.00	0.99
	0.3	−9.67	−0.99	0.60	1.13	1.36	1.45	1.49	1.48	1.46
	0.4	−21.53	−4.06	−0.93	0.11	0.59	0.83	0.96	1.01	1.03
	0.5	−35.77	−7.77	−2.82	−1.09	−0.29	0.13	0.35	0.48	0.55
	0.6	−52.32	−11.78	−4.34	−1.83	−0.70	−0.09	0.28	0.51	0.65
	0.7	−78.89	−18.64	−7.76	−3.71	−1.83	−0.85	−0.22	0.16	0.42
	0.8	−105.46	−25.49	−11.19	−5.59	−2.96	−1.60	−0.72	−0.18	0.19
0.9	0.2	−4.98	−0.34	0.54	0.85	0.97	1.03	1.04	1.03	1.01
	0.3	−9.97	−1.21	0.48	1.06	1.32	1.44	1.49	1.49	1.48
	0.4	−23.54	−4.98	−1.39	−0.12	0.47	0.78	0.95	1.04	1.09
	0.5	−40.14	−9.57	−3.69	−1.56	−0.55	−0.01	0.31	0.51	0.63
	0.6	−58.25	−14.28	−5.64	−2.53	−1.08	−0.30	0.18	0.49	0.70
	0.7	−84.09	−21.02	−8.91	−4.38	−2.22	−1.04	−0.31	0.15	0.46
	0.8	−109.92	−27.77	−12.18	−6.22	−3.35	−1.79	−0.81	−0.19	0.23
	0.9	−130.32	−35.19	−16.07	−8.70	−5.18	−3.19	−1.88	−1.08	−0.53
1.0	0.2	−2.75	0.19	0.76	0.96	1.05	1.08	1.08	1.06	1.04
	0.3	−10.28	−1.43	0.35	0.99	1.29	1.43	1.49	1.50	1.50
	0.4	−25.56	−5.89	−1.86	−0.36	0.35	0.72	0.93	1.07	1.15
	0.5	−44.52	−11.37	−4.56	−2.02	−0.81	−0.14	0.27	0.54	0.72
	0.6	−64.19	−16.77	−6.94	−3.24	−1.47	−0.50	0.09	0.48	0.74
	0.7	−89.28	−23.41	−10.05	−5.05	−2.61	−1.24	−0.40	0.14	0.50
	0.8	−114.38	−30.04	−13.16	−6.86	−3.75	−1.97	−0.89	−0.20	0.27
	0.9	−134.78	−37.47	−17.06	−9.33	−5.57	−3.38	−1.97	−1.09	−0.49
	1.0	−155.18	−44.89	−20.95	−11.80	−7.39	−4.78	−3.05	−1.99	−1.25

ED7-1 Centrifugal Fan Located in Plenum or Cabinet

L/D_o	0.30	0.40	0.50	0.75
C_o	0.80	0.53	0.40	0.22

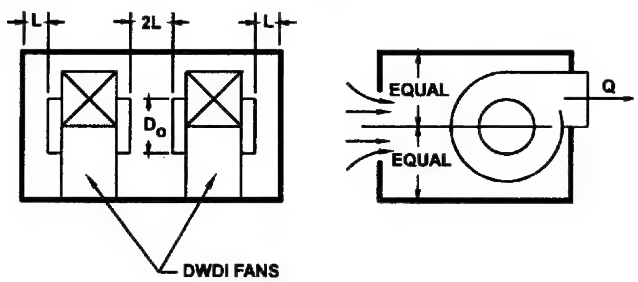

ED7-2 Fan Inlet, Centrifugal, SWSI, with 4 Gore Elbow

	C_o Values			
	L/D_o			
r/D_o	0.0	2.0	5.0	10.0
0.50	1.80	1.00	0.53	0.53
0.75	1.40	0.80	0.40	0.40
1.00	1.20	0.67	0.33	0.33
1.50	1.10	0.60	0.33	0.33
2.00	1.00	0.53	0.33	0.33
3.00	0.67	0.40	0.22	0.22

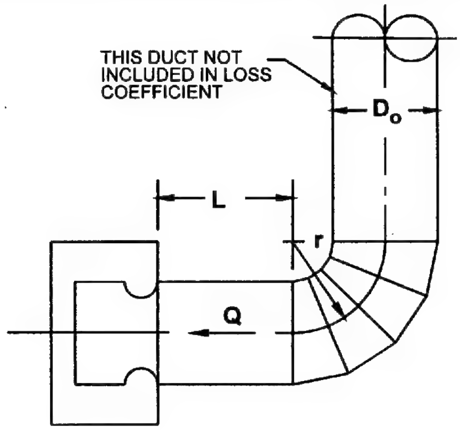

SD2-6 Stackhead

D_e/D	0.3	0.4	0.5	0.6	0.7	0.8	0.9	1.0
C_o	129	41.02	16.80	8.10	4.37	2.56	1.60	1.00

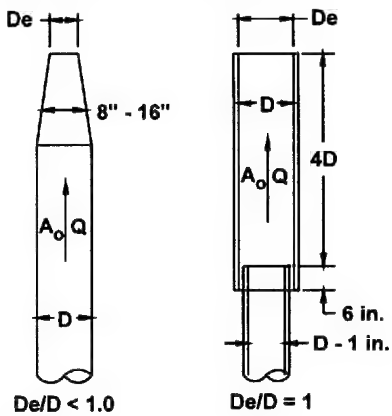

RECTANGULAR FITTINGS

CR3-1 Elbow, Smooth Radius, Without Vanes

	C_p Values										
	H/W										
r/W	0.25	0.50	0.75	1.00	1.50	2.00	3.00	4.00	5.00	6.00	8.00
0.50	1.53	1.38	1.29	1.18	1.06	1.00	1.00	1.06	1.12	1.16	1.18
0.75	0.57	0.52	0.48	0.44	0.40	0.39	0.39	0.40	0.42	0.43	0.44
1.00	0.27	0.25	0.23	0.21	0.19	0.18	0.18	0.19	0.20	0.21	0.21
1.50	0.22	0.20	0.19	0.17	0.15	0.14	0.14	0.15	0.16	0.17	0.17
2.00	0.20	0.18	0.16	0.15	0.14	0.13	0.13	0.14	0.14	0.15	0.15

Angle Factor K

θ	0	20	30	45	60	75	90	110	130	150	180
K	0.00	0.31	0.45	0.60	0.78	0.90	1.00	1.13	1.20	1.28	1.40

$C_o = KC_p$ where K = angle factor

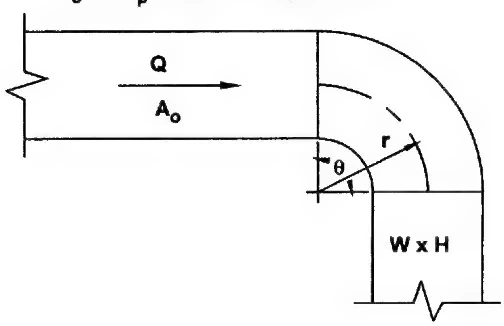

CR3-3 Elbow, Smooth Radius, One Splitter Vane

	C_p Values										
	H/W										
r*/*W	**0.25**	**0.50**	**1.00**	**1.50**	**2.00**	**3.00**	**4.00**	**5.00**	**6.00**	**7.00**	**8.00**
0.55	0.52	0.40	0.43	0.49	0.55	0.66	0.75	0.84	0.93	1.01	1.09
0.60	0.36	0.27	0.25	0.28	0.30	0.35	0.39	0.42	0.46	0.49	0.52
0.65	0.28	0.21	0.18	0.19	0.20	0.22	0.25	0.26	0.28	0.30	0.32
0.70	0.22	0.16	0.14	0.14	0.15	0.16	0.17	0.18	0.19	0.20	0.21
0.75	0.18	0.13	0.11	0.11	0.11	0.12	0.13	0.14	0.14	0.15	0.15
0.80	0.15	0.11	0.09	0.09	0.09	0.09	0.10	0.10	0.11	0.11	0.12
0.85	0.13	0.09	0.08	0.07	0.07	0.08	0.08	0.08	0.08	0.09	0.09
0.90	0.11	0.08	0.07	0.06	0.06	0.06	0.06	0.07	0.07	0.07	0.07
0.95	0.10	0.07	0.06	0.05	0.05	0.05	0.05	0.05	0.06	0.06	0.06
1.00	0.09	0.06	0.05	0.05	0.04	0.04	0.04	0.05	0.05	0.05	0.05

Angle Factor *K*

θ	**0**	**30**	**45**	**60**	**90**
K	0.00	0.45	0.60	0.78	1.00

Curve Ratio CR

r*/*W	**0.55**	**0.60**	**0.65**	**0.70**	**0.75**	**0.80**	**0.85**	**0.90**	**0.95**	**1.00**
CR	0.218	0.302	0.361	0.408	0.447	0.480	0.509	0.535	0.557	0.577

Throat Radius/Width Ratio (*R*/*W*)

r*/*W	**0.55**	**0.60**	**0.65**	**0.70**	**0.75**	**0.80**	**0.85**	**0.90**	**0.95**	**1.00**
R/*W*	0.05	0.10	0.15	0.20	0.25	0.30	0.35	0.40	0.45	0.50

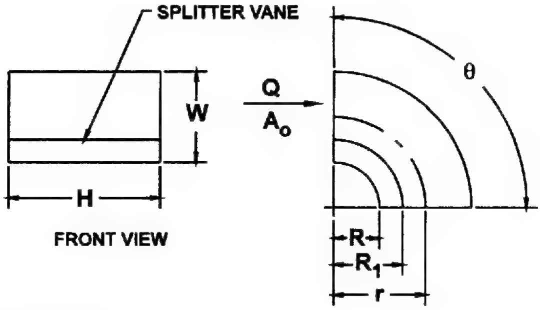

$C_o = K\,C_p$
$R_1 = R/CR$

where
R = throat radius
R_1 = splitter vane radius
CR = curve ratio
K = angle factor

CR3-6 Elbow, Mitered

	C_o Values										
	H/W										
θ	**0.25**	**0.50**	**0.75**	**1.00**	**1.50**	**2.00**	**3.00**	**4.00**	**5.00**	**6.00**	**8.00**
20	0.08	0.08	0.08	0.07	0.07	0.07	0.06	0.06	0.05	0.05	0.05
30	0.18	0.17	0.17	0.16	0.15	0.15	0.13	0.13	0.12	0.12	0.11
45	0.38	0.37	0.36	0.34	0.33	0.31	0.28	0.27	0.26	0.25	0.24
60	0.60	0.59	0.57	0.55	0.52	0.49	0.46	0.43	0.41	0.39	0.38
75	0.89	0.87	0.84	0.81	0.77	0.73	0.67	0.63	0.61	0.58	0.57
90	1.30	1.27	1.23	1.18	1.13	1.07	0.98	0.92	0.89	0.85	0.83

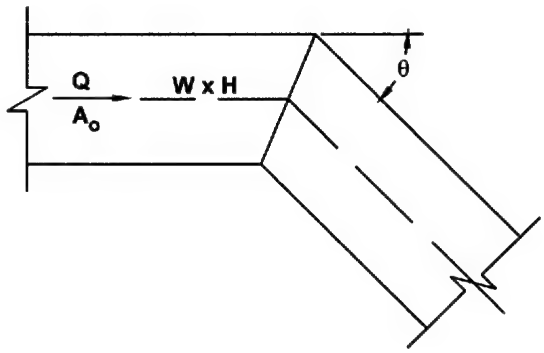

CR3-10 Elbow, Mitered, 90 Degree, Single-Thickness Vanes (Design 2)

$C_o = 0.12$

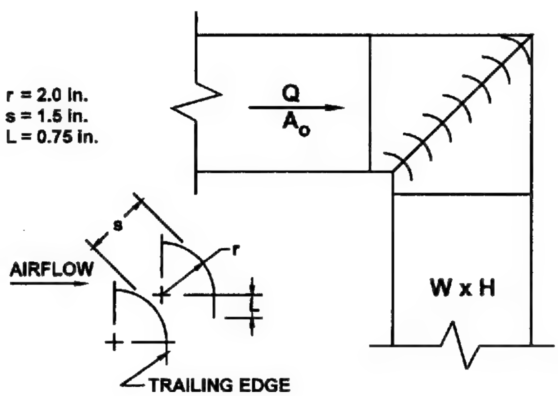

CR3-17 Elbow, Z-Shaped

	C_p Values													
	L/W													
H/W	**0.0**	**0.4**	**0.6**	**0.8**	**1.0**	**1.2**	**1.4**	**1.6**	**1.8**	**2.0**	**4.0**	**8.0**	**10.0**	**100.0**
0.25	0.00	0.68	0.99	1.77	2.89	3.97	4.41	4.60	4.64	4.60	3.39	3.03	2.70	2.53
0.50	0.00	0.66	0.96	1.72	2.81	3.86	4.29	4.47	4.52	4.47	3.30	2.94	2.62	2.46
0.75	0.00	0.64	0.94	1.67	2.74	3.75	4.17	4.35	4.39	4.35	3.20	2.86	2.55	2.39
1.00	0.00	0.62	0.90	1.61	2.63	3.61	4.01	4.18	4.22	4.18	3.08	2.75	2.45	2.30
1.50	0.00	0.59	0.86	1.53	2.50	3.43	3.81	3.97	4.01	3.97	2.93	2.61	2.33	2.19
2.00	0.00	0.56	0.81	1.45	2.37	3.25	3.61	3.76	3.80	3.76	2.77	2.48	2.21	2.07
3.00	0.00	0.51	0.75	1.34	2.18	3.00	3.33	3.47	3.50	3.47	2.56	2.28	2.03	1.91
4.00	0.00	0.48	0.70	1.26	2.05	2.82	3.13	3.26	3.29	3.26	2.40	2.15	1.91	1.79
6.00	0.00	0.45	0.65	1.16	1.89	2.60	2.89	3.01	3.04	3.01	2.22	1.98	1.76	1.66
8.00	0.00	0.43	0.63	1.13	1.84	2.53	2.81	2.93	2.95	2.93	2.16	1.93	1.72	1.61

Reynolds No. Correction Factor K_r

Re/1000	**10**	**20**	**30**	**40**	**60**	**80**	**100**	**140**	**500**
K_r	1.40	1.26	1.19	1.14	1.09	1.06	1.04	1.00	1.00

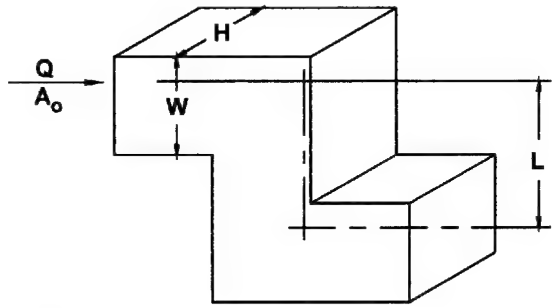

$C_o = K_r C_p$

where K_r = Reynolds no. correction factor

CR6-1 Screen (Only)

	C_o Values												
	n												
A_1/A_o	**0.30**	**0.35**	**0.40**	**0.45**	**0.50**	**0.55**	**0.60**	**0.65**	**0.70**	**0.75**	**0.80**	**0.90**	**1.00**
0.2	155.00	102.50	75.00	55.00	41.25	31.50	24.25	18.75	14.50	11.00	8.00	3.50	0.00
0.3	68.89	45.56	33.33	24.44	18.33	14.00	10.78	8.33	6.44	4.89	3.56	1.56	0.00
0.4	38.75	25.63	18.75	13.75	10.31	7.88	6.06	4.69	3.63	2.75	2.00	0.88	0.00
0.5	24.80	16.40	12.00	8.80	6.60	5.04	3.88	3.00	2.32	1.76	1.28	0.56	0.00
0.6	17.22	11.39	8.33	6.11	4.58	3.50	2.69	2.08	1.61	1.22	0.89	0.39	0.00
0.7	12.65	8.37	6.12	4.49	3.37	2.57	1.98	1.53	1.18	0.90	0.65	0.29	0.00
0.8	9.69	6.40	4.69	3.44	2.58	1.97	1.52	1.17	0.91	0.69	0.50	0.22	0.00
0.9	7.65	5.06	3.70	2.72	2.04	1.56	1.20	0.93	0.72	0.54	0.40	0.17	0.00
1.0	6.20	4.10	3.00	2.20	1.65	1.26	0.97	0.75	0.58	0.44	0.32	0.14	0.00
1.2	4.31	2.85	2.08	1.53	1.15	0.88	0.67	0.36	0.40	0.31	0.22	0.10	0.00
1.4	3.16	2.09	1.53	1.12	0.84	0.64	0.49	0.38	0.30	0.22	0.16	0.07	0.00
1.6	2.42	1.60	1.17	0.86	0.64	0.49	0.38	0.29	0.23	0.17	0.13	0.05	0.00
1.8	1.91	1.27	0.93	0.68	0.51	0.39	0.30	0.23	0.18	0.14	0.10	0.04	0.00
2.0	1.55	1.03	0.75	0.55	0.41	0.32	0.24	0.19	0.15	0.11	0.08	0.04	0.00
2.5	0.99	0.66	0.48	0.35	0.26	0.20	0.16	0.12	0.09	0.07	0.05	0.02	0.00
3.0	0.69	0.46	0.33	0.24	0.18	0.14	0.11	0.08	0.06	0.05	0.04	0.02	0.00
4.0	0.39	0.26	0.19	0.14	0.10	0.08	0.06	0.05	0.04	0.03	0.02	0.01	0.00
6.0	0.17	0.11	0.08	0.06	0.05	0.04	0.03	0.02	0.02	0.01	0.01	0.00	0.00

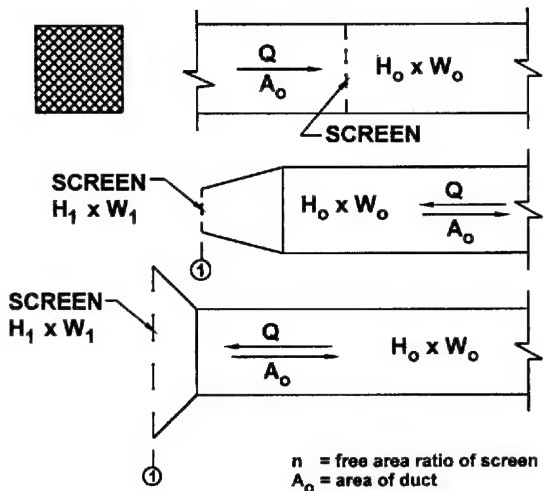

n = free area ratio of screen
A_o = area of duct
A_1 = cross-sectional area of duct or fitting where screen is located

CR6-4 Obstruction, Smooth Cylinder in Rectangular Duct

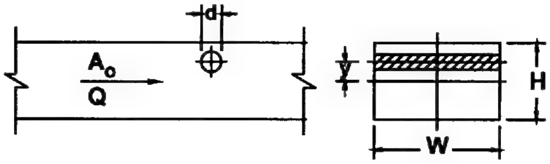

$d\,W/A_o < 0.3$
where
$S_m = d\,W$
$Re = f(d, V_o)$

		C_o Values				
		S_m/A_o				
y/H	Re/1000	0.00	0.05	0.10	0.15	0.20
0.00	0.1	0.00	0.10	0.21	0.35	0.47
	0.5	0.00	0.08	0.17	0.28	0.38
	200	0.00	0.08	0.17	0.28	0.38
	300	0.00	0.07	0.16	0.26	0.35
	400	0.00	0.05	0.11	0.19	0.25
	500	0.00	0.04	0.09	0.14	0.19
	600	0.00	0.02	0.05	0.07	0.10
	1000	0.00	0.02	0.05	0.08	0.11
0.05	0.1	0.00	0.10	0.21	0.34	0.46
	0.5	0.00	0.08	0.17	0.27	0.37
	200	0.00	0.08	0.17	0.27	0.37
	300	0.00	0.07	0.15	0.25	0.34
	400	0.00	0.05	0.11	0.18	0.24
	500	0.00	0.04	0.08	0.13	0.18
	600	0.00	0.02	0.04	0.07	0.10
	1000	0.00	0.02	0.05	0.08	0.11
0.10	0.1	0.00	0.09	0.20	0.32	0.44
	0.5	0.00	0.07	0.16	0.26	0.35
	200	0.00	0.07	0.16	0.26	0.35
	300	0.00	0.07	0.15	0.24	0.32
	400	0.00	0.05	0.11	0.17	0.23
	500	0.00	0.04	0.08	0.13	0.18
	600	0.00	0.02	0.04	0.07	0.09
	1000	0.00	0.02	0.05	0.08	0.10
0.15	0.1	0.00	0.09	0.19	0.31	0.42
	0.5	0.00	0.07	0.15	0.25	0.34
	200	0.00	0.07	0.15	0.25	0.34
	300	0.00	0.06	0.14	0.23	0.31
	400	0.00	0.05	0.10	0.17	0.22
	500	0.00	0.04	0.08	0.12	0.17
	600	0.00	0.02	0.04	0.07	0.09
	1000	0.00	0.02	0.04	0.07	0.10
0.20	0.1	0.00	0.08	0.18	0.29	0.40
	0.5	0.00	0.07	0.14	0.24	0.32
	200	0.00	0.07	0.14	0.24	0.32
	300	0.00	0.06	0.13	0.22	0.29
	400	0.00	0.04	0.10	0.16	0.21
	500	0.00	0.03	0.07	0.12	0.16
	600	0.00	0.02	0.04	0.06	0.09
	1000	0.00	0.02	0.04	0.07	0.09
0.25	0.1	0.00	0.08	0.17	0.28	0.38
	0.5	0.00	0.06	0.14	0.22	0.30
	200	0.00	0.06	0.14	0.22	0.30
	300	0.00	0.06	0.12	0.20	0.28
	400	0.00	0.04	0.09	0.15	0.20
	500	0.00	0.03	0.07	0.11	0.15
	600	0.00	0.02	0.04	0.06	0.08
	1000	0.00	0.02	0.04	0.06	0.09
0.30	0.1	0.00	0.07	0.16	0.26	0.35
	0.5	0.00	0.06	0.13	0.21	0.28
	200	0.00	0.06	0.13	0.21	0.28
	300	0.00	0.05	0.12	0.19	0.26
	400	0.00	0.04	0.08	0.14	0.19
	500	0.00	0.03	0.06	0.10	0.14
	600	0.00	0.02	0.03	0.05	0.07
	1000	0.00	0.02	0.04	0.06	0.08
0.35	0.1	0.00	0.07	0.14	0.23	0.32
	0.5	0.00	0.05	0.11	0.19	0.25
	200	0.00	0.05	0.11	0.19	0.25
	300	0.00	0.05	0.11	0.17	0.23
	400	0.00	0.04	0.08	0.12	0.17
	500	0.00	0.03	0.06	0.09	0.13
	600	0.00	0.01	0.03	0.05	0.07
	1000	0.00	0.02	0.03	0.05	0.07
0.40	0.1	0.00	0.06	0.13	0.20	0.28
	0.5	0.00	0.05	0.10	0.16	0.22
	200	0.00	0.05	0.10	0.16	0.22
	300	0.00	0.04	0.09	0.15	0.20
	400	0.00	0.03	0.07	0.11	0.15
	500	0.00	0.02	0.05	0.08	0.11
	600	0.00	0.01	0.03	0.04	0.06
	1000	0.00	0.01	0.03	0.05	0.06

CR9-1 Damper, Butterfly

	C_o Values									
	θ									
H/W	0	10	20	30	40	50	60	65	70	90
0.12	0.04	0.30	1.10	3.00	8.00	23.00	60.00	100.00	190.00	99999
0.25	0.08	0.33	1.18	3.30	9.00	26.00	70.00	128.00	210.00	99999
1.00	0.08	0.33	1.18	3.30	9.00	26.00	70.00	128.00	210.00	99999
2.00	0.13	0.35	1.25	3.60	10.00	29.00	80.00	155.00	230.00	99999

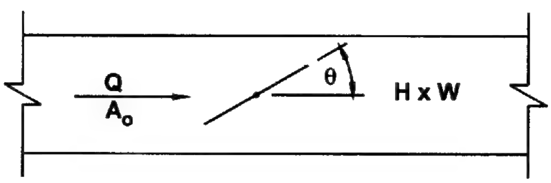

CR9-4 Damper, Opposed Blades

	C_o Values								
	θ								
L/R	0	10	20	30	40	50	60	70	80
0.3	0.52	0.79	1.91	3.77	8.55	19.46	70.12	295.21	807.23
0.4	0.52	0.85	2.07	4.61	10.42	26.73	92.90	346.25	926.34
0.5	0.52	0.93	2.25	5.44	12.29	33.99	118.91	393.36	1045.44
0.6	0.52	1.00	2.46	5.99	14.15	41.26	143.69	440.25	1163.09
0.8	0.52	1.08	2.66	6.96	18.18	56.47	193.92	520.27	1324.85
1.0	0.52	1.17	2.91	7.31	20.25	71.68	245.45	576.00	1521.00
1.5	0.52	1.38	3.16	9.51	27.56	107.41	361.00	717.05	1804.40

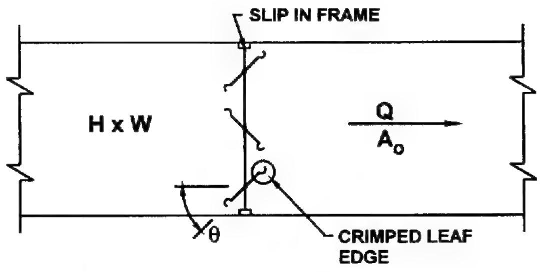

$$L/R = \frac{N\,W}{2(H+W)}$$

where
- N = number of damper blades
- W = duct dimension parallel to blade axis, in.
- H = duct height, in.
- L = sum of damper blade lengths, in.
- R = perimeter of duct, in.

CR9-6 Fire Damper, Curtain Type, Type B

$C_o = 0.19$

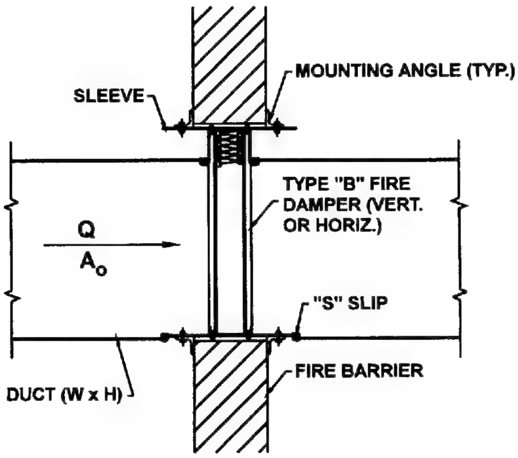

ER2-1 Bellmouth, Plenum to Round, Exhaust/Return Systems

	C_o Values												
	r/D_1												
A_o/A_1	0.00	0.01	0.02	0.03	0.04	0.05	0.06	0.08	0.10	0.12	0.16	0.20	10.00
1.5	0.22	0.20	0.15	0.14	0.12	0.10	0.09	0.07	0.05	0.04	0.03	0.01	0.01
2.0	0.13	0.11	0.08	0.08	0.07	0.06	0.05	0.04	0.03	0.02	0.02	0.01	0.01
2.5	0.08	0.07	0.05	0.05	0.04	0.04	0.03	0.02	0.02	0.01	0.01	0.00	0.00
3.0	0.06	0.05	0.04	0.03	0.03	0.02	0.02	0.02	0.01	0.01	0.01	0.00	0.00
4.0	0.03	0.03	0.02	0.02	0.02	0.01	0.01	0.01	0.01	0.01	0.00	0.00	0.00
8.0	0.01	0.01	0.01	0.00	0.00	0.00	0.00	0.00	0.00	0.00	0.00	0.00	0.00

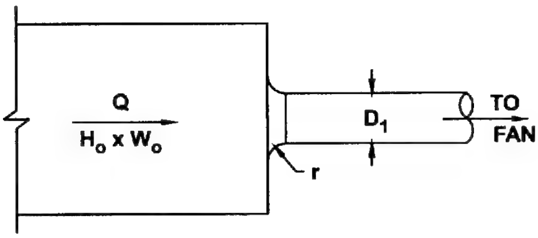

ER3-1 Elbow, 90 Degree, Variable Inlet/Outlet Areas, Exhaust/Return Systems

	C_o Values						
	W_1/W_o						
H/W_o	0.6	0.8	1.0	1.2	1.4	1.6	2.0
0.25	1.76	1.43	1.24	1.14	1.09	1.06	1.06
1.00	1.70	1.36	1.15	1.02	0.95	0.90	0.84
4.00	1.46	1.10	0.90	0.81	0.76	0.72	0.66
100.00	1.50	1.04	0.79	0.69	0.63	0.60	0.55

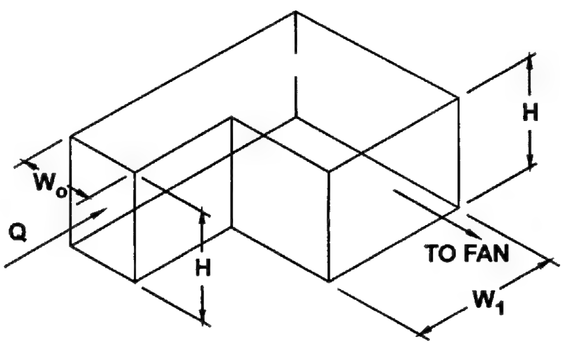

ER4-3 Transition, Rectangular to Round, Exhaust/Return Systems

	C_o Values									
	θ									
A_o/A_1	10	15	20	30	45	60	90	120	150	180
0.06	0.30	0.54	0.53	0.65	0.77	0.88	0.95	0.98	0.98	0.93
0.10	0.30	0.50	0.53	0.64	0.75	0.84	0.89	0.91	0.91	0.88
0.25	0.25	0.36	0.45	0.52	0.58	0.62	0.64	0.64	0.64	0.64
0.50	0.15	0.21	0.25	0.30	0.33	0.33	0.33	0.32	0.31	0.30
1.00	0.00	0.00	0.00	0.00	0.00	0.00	0.00	0.00	0.00	0.00
2.00	0.24	0.28	0.26	0.20	0.22	0.24	0.49	0.73	0.97	1.04
4.00	0.89	0.78	0.79	0.70	0.88	1.12	2.72	4.33	5.62	6.58
6.00	1.89	1.67	1.59	1.49	1.98	2.52	6.51	10.14	13.05	15.14
10.00	5.09	5.32	5.15	5.05	6.50	8.05	19.06	29.07	37.08	43.05

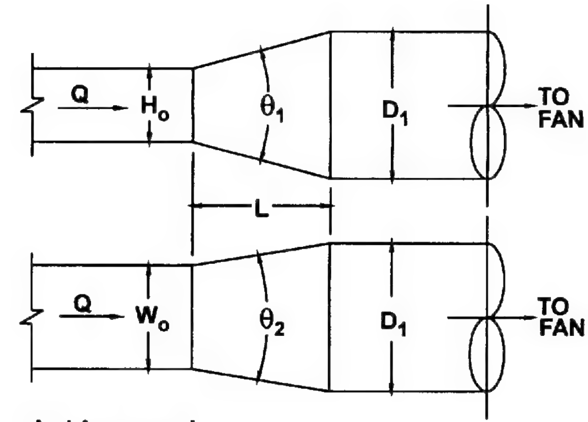

A_o / A_1 < OR > 1
θ IS LARGER OF θ_1 AND θ_2

SR2-1 Abrupt Exit

H/W	0.1	0.2	0.9	1.0	1.1	4.0	5.0	10.0
C_o	1.55	1.55	1.55	2.00	1.55	1.55	1.55	1.55

$C_o = 1.0$

Note: Table is LAMINAR flow; $C_o = 1.0$ is TURBULENT flow.

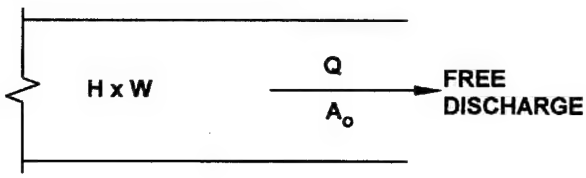

SR2-3 Plain Diffuser (Two Sides Parallel), Free Discharge

		C_o Values								
		θ								
A_1/A_o	Re/1000	8	10	14	20	30	45	60	90	120
1	50	0.00	0.00	0.00	0.00	0.00	0.00	0.00	0.00	0.00
	100	0.00	0.00	0.00	0.00	0.00	0.00	0.00	0.00	0.00
	200	0.00	0.00	0.00	0.00	0.00	0.00	0.00	0.00	0.00
	400	0.00	0.00	0.00	0.00	0.00	0.00	0.00	0.00	0.00
	2000	0.00	0.00	0.00	0.00	0.00	0.00	0.00	0.00	0.00
2	50	0.50	0.51	0.56	0.63	0.80	0.96	1.04	1.09	1.09
	100	0.48	0.50	0.56	0.63	0.80	0.96	1.04	1.09	1.09
	200	0.44	0.47	0.53	0.63	0.74	0.93	1.02	1.08	1.08
	400	0.40	0.42	0.50	0.62	0.74	0.93	1.02	1.08	1.08
	2000	0.40	0.42	0.50	0.62	0.74	0.93	1.02	1.08	1.08
4	50	0.34	0.38	0.48	0.63	0.76	0.91	1.03	1.07	1.07
	100	0.31	0.36	0.45	0.59	0.72	0.88	1.02	1.07	1.07
	200	0.26	0.31	0.41	0.53	0.67	0.83	0.96	1.06	1.06
	400	0.22	0.27	0.39	0.53	0.67	0.83	0.96	1.06	1.06
	2000	0.22	0.27	0.39	0.53	0.67	0.83	0.96	1.06	1.06
6	50	0.32	0.34	0.41	0.56	0.70	0.84	0.96	1.08	1.08
	100	0.27	0.30	0.41	0.56	0.70	0.84	0.96	1.08	1.08
	200	0.24	0.27	0.36	0.52	0.67	0.81	0.94	1.06	1.06
	400	0.20	0.24	0.36	0.52	0.67	0.81	0.94	1.06	1.06
	2000	0.18	0.24	0.34	0.50	0.67	0.81	0.94	1.05	1.05

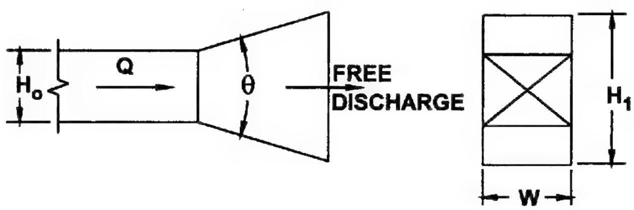

SR2-5 Pyramidal Diffuser, Free Discharge

		C_o Values								
		θ								
A_1/A_o	Re/1000	8	10	14	20	30	45	60	90	120
1	50	0.00	0.00	0.00	0.00	0.00	0.00	0.00	0.00	0.00
	100	0.00	0.00	0.00	0.00	0.00	0.00	0.00	0.00	0.00
	200	0.00	0.00	0.00	0.00	0.00	0.00	0.00	0.00	0.00
	400	0.00	0.00	0.00	0.00	0.00	0.00	0.00	0.00	0.00
	2000	0.00	0.00	0.00	0.00	0.00	0.00	0.00	0.00	0.00
2	50	0.65	0.68	0.74	0.82	0.92	1.05	1.10	1.08	1.08
	100	0.61	0.66	0.73	0.81	0.90	1.04	1.09	1.08	1.08
	200	0.57	0.61	0.70	0.79	0.89	1.04	1.09	1.08	1.08
	400	0.50	0.56	0.64	0.76	0.88	1.02	1.07	1.08	1.08
	2000	0.50	0.56	0.64	0.76	0.88	1.02	1.07	1.08	1.08
4	50	0.53	0.60	0.69	0.78	0.90	1.02	1.07	1.09	1.09
	100	0.49	0.55	0.66	0.78	0.90	1.02	1.07	1.09	1.09
	200	0.42	0.50	0.62	0.74	0.87	1.00	1.06	1.08	1.08
	400	0.36	0.44	0.56	0.70	0.84	0.99	1.06	1.08	1.08
	2000	0.36	0.44	0.56	0.70	0.84	0.99	1.06	1.08	1.08
6	50	0.50	0.57	0.66	0.77	0.91	1.02	1.07	1.08	1.08
	100	0.47	0.54	0.63	0.76	0.98	1.02	1.07	1.08	1.08
	200	0.42	0.48	0.60	0.73	0.88	1.00	1.06	1.08	1.08
	400	0.34	0.44	0.56	0.73	0.86	0.98	1.06	1.08	1.08
	2000	0.34	0.44	0.56	0.73	0.86	0.98	1.06	1.08	1.08
10	50	0.45	0.53	0.64	0.74	0.85	0.97	1.10	1.12	1.12
	100	0.40	0.48	0.62	0.73	0.85	0.97	1.10	1.12	1.12
	200	0.34	0.44	0.56	0.69	0.82	0.95	1.10	1.11	1.11
	400	0.28	0.40	0.55	0.67	0.80	0.93	1.09	1.11	1.11
	2000	0.28	0.40	0.55	0.67	0.80	0.93	1.09	1.11	1.11

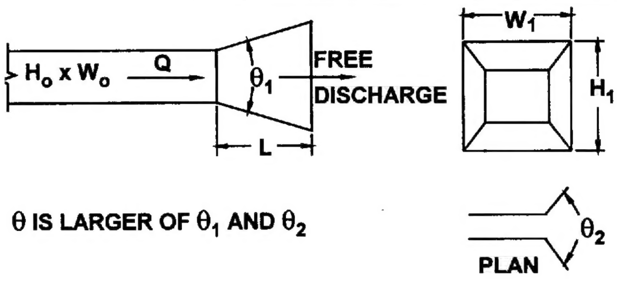

SR2-6 Pyramidal Diffuser, with Wall

L/D_h	0.5	1.0	2.0	3.0	4.0	5.0	6.0	8.0	10.0	12.0	14.0
C_o	0.49	0.40	0.30	0.26	0.23	0.21	0.19	0.17	0.16	0.15	0.14
θ	26	19	13	11	9	8	7	6	6	5	5

θ is the optimum angle.

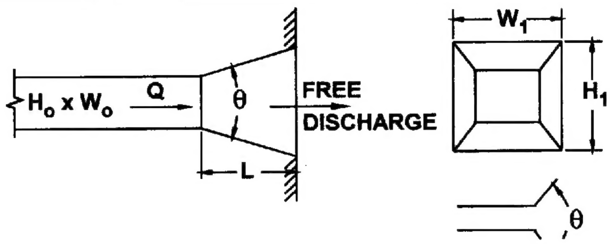

SR3-1 Elbow, 90 Degree, Variable Inlet/Outlet Areas, Supply Air Systems

	C_o Values						
	W_o/W_1						
H/W_1	0.6	0.8	1.0	1.2	1.4	1.6	2.0
0.25	0.63	0.92	1.24	1.64	2.14	2.71	4.24
1.00	0.61	0.87	1.15	1.47	1.86	2.30	3.36
4.00	0.53	0.70	0.90	1.17	1.49	1.84	2.64
100.00	0.54	0.67	0.79	0.99	1.23	1.54	2.20

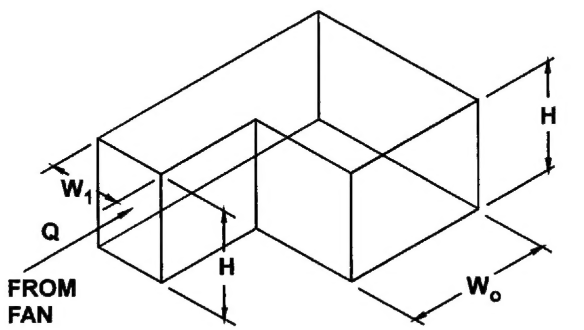

SR4-1 Transition, Rectangular, Two Sides Parallel, Symmetrical, Supply Air Systems

	C_o Values									
	θ									
A_o/A_1	10	15	20	30	45	60	90	120	150	180
0.10	0.05	0.05	0.05	0.05	0.07	0.08	0.19	0.29	0.37	0.43
0.17	0.05	0.04	0.04	0.04	0.05	0.07	0.18	0.28	0.36	0.42
0.25	0.05	0.04	0.04	0.04	0.06	0.07	0.17	0.27	0.35	0.41
0.50	0.06	0.05	0.05	0.05	0.06	0.07	0.14	0.20	0.26	0.27
1.00	0.00	0.00	0.00	0.00	0.00	0.00	0.00	0.00	0.00	1.00
2.00	0.56	0.52	0.60	0.96	1.40	1.48	1.52	1.48	1.44	1.40
4.00	2.72	3.04	3.52	6.72	9.60	10.88	11.20	11.04	10.72	10.56
10.00	24.00	26.00	36.00	53.00	69.00	82.00	93.00	93.00	92.00	91.00
16.00	66.56	69.12	102.40	143.36	181.76	220.16	256.00	253.44	250.88	250.88

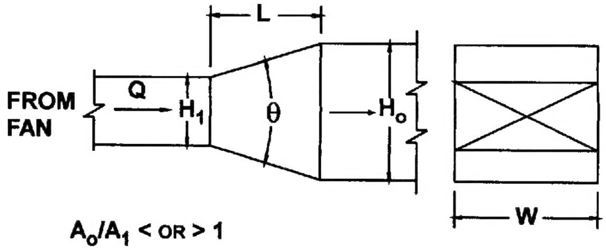

A_o/A_1 < OR > 1

SR5-1 Smooth Wye of Type $A_s + A_b \geq A_c$, Branch 90° to Main, Diverging

		C_o Values								
		Q_b/Q_c								
A_s/A_c	A_b/A_c	0.1	0.2	0.3	0.4	0.5	0.6	0.7	0.8	0.9
0.50	0.25	3.44	0.70	0.30	0.20	0.17	0.16	0.16	0.17	0.18
	0.50	11.00	2.37	1.06	0.64	0.52	0.47	0.47	0.47	0.48
	1.00	60.00	13.00	4.78	2.06	0.96	0.47	0.31	0.27	0.26
0.75	0.25	2.19	0.55	0.35	0.31	0.33	0.35	0.36	0.37	0.39
	0.50	13.00	2.50	0.89	0.47	0.34	0.31	0.32	0.36	0.43
	1.00	70.00	15.00	5.67	2.62	1.36	0.78	0.53	0.41	0.36
1.00	0.25	3.44	0.78	0.42	0.33	0.30	0.31	0.40	0.42	0.46
	0.50	15.50	3.00	1.11	0.62	0.48	0.42	0.40	0.42	0.46
	1.00	67.00	13.75	5.11	2.31	1.28	0.81	0.59	0.47	0.46

		C_s Values								
		Q_s/Q_c								
A_s/A_c	A_b/A_c	0.1	0.2	0.3	0.4	0.5	0.6	0.7	0.8	0.9
0.50	0.25	8.75	1.62	0.50	0.17	0.05	0.00	−0.02	−0.02	0.00
	0.50	7.50	1.12	0.25	0.06	0.05	0.09	0.14	0.19	0.22
	1.00	5.00	0.62	0.17	0.08	0.08	0.09	0.12	0.15	0.19
0.75	0.25	19.13	3.38	1.00	0.28	0.05	−0.02	−0.02	0.00	0.06
	0.50	20.81	3.23	0.75	0.14	−0.02	−0.05	−0.05	−0.02	0.03
	1.00	16.88	2.81	0.63	0.11	−0.02	−0.05	0.01	0.00	0.07
1.00	0.25	46.00	9.50	3.22	1.31	0.52	0.14	−0.02	−0.05	−0.01
	0.50	35.00	6.75	2.11	0.75	0.24	0.00	−0.10	−0.09	−0.04
	1.00	38.00	7.50	2.44	0.81	0.24	−0.03	−0.08	−0.06	−0.02

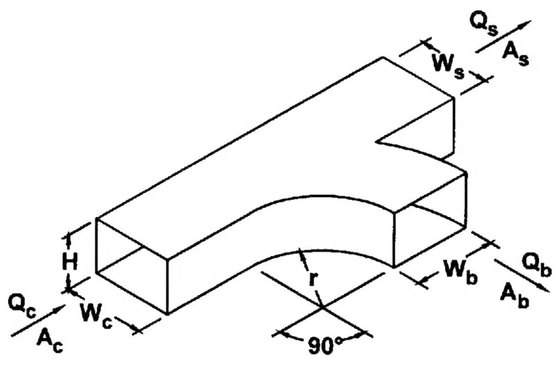

$r/W_b = 1.0$
$A_s = A_b \geq A_c$

SR5-13 Tee, 45 Degree Entry Branch, Diverging

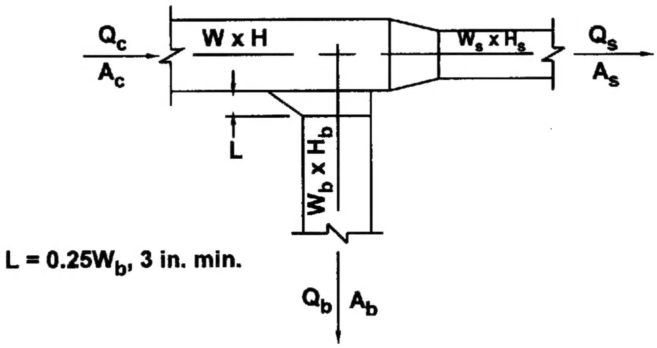

	C_b Values								
	Q_b/Q_c								
A_b/A_c	0.1	0.2	0.3	0.4	0.5	0.6	0.7	0.8	0.9
0.1	0.73	0.34	0.32	0.34	0.35	0.37	0.38	0.39	0.40
0.2	3.10	0.73	0.41	0.34	0.32	0.32	0.33	0.34	0.35
0.3	7.59	1.65	0.73	0.47	0.37	0.34	0.32	0.32	0.32
0.4	14.20	3.10	1.28	0.73	0.51	0.41	0.36	0.34	0.32
0.5	22.92	5.08	2.07	1.12	0.73	0.54	0.44	0.38	0.35
0.6	33.76	7.59	3.10	1.65	1.03	0.73	0.56	0.47	0.41
0.7	46.71	10.63	4.36	2.31	1.42	0.98	0.73	0.58	0.49
0.8	61.79	14.20	5.86	3.10	1.90	1.28	0.94	0.73	0.60
0.9	78.98	18.29	7.59	4.02	2.46	1.65	1.19	0.91	0.73

	C_s Values								
	Q_s/Q_c								
A_s/A_c	0.1	0.2	0.3	0.4	0.5	0.6	0.7	0.8	0.9
0.1	0.04								
0.2	0.98	0.04							
0.3	3.48	0.31	0.04						
0.4	7.55	0.98	0.18	0.04					
0.5	13.18	2.03	0.49	0.13	0.04				
0.6	20.38	3.48	0.98	0.31	0.10	0.04			
0.7	29.15	5.32	1.64	0.60	0.23	0.09	0.04		
0.8	39.48	7.55	2.47	0.98	0.42	0.18	0.08	0.04	
0.9	51.37	10.17	3.48	1.46	0.67	0.31	0.15	0.07	0.04

SR5-14 Wye, Symmetrical, Dovetail, $Q_b/Q_c = 0.5$, Diverging

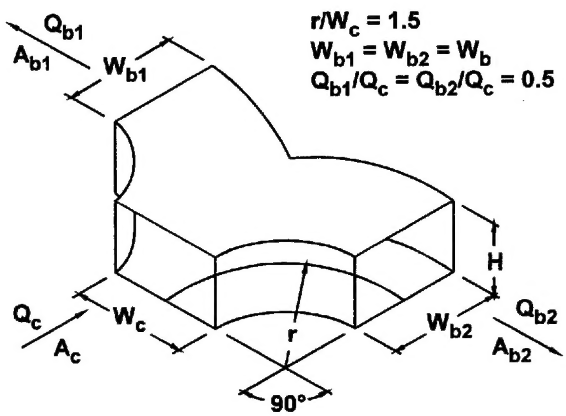

A_b/A_c	0.5	1.0
C_b	0.30	1.00

Branches are identical: $Q_{b1} = Q_{b2} = Q_b$, and $C_{b1} = C_{b2} = C_b$

SR7-1 Fan, Centrifugal, Without Outlet Diffuser, Free Discharge

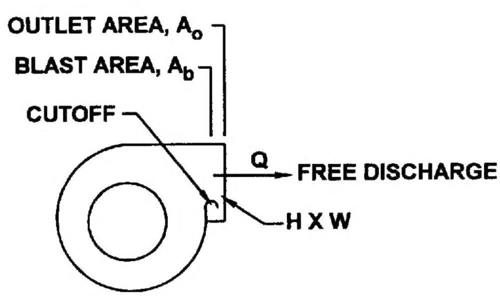

A_b/A_o	0.4	0.5	0.6	0.7	0.8	0.9	1.0
C_o	2.00	2.00	1.00	0.80	0.47	0.22	0.00